AFCRC-TR-58-239
ASTIA Document No. 152582

MASSACHUSETTS INSTITUTE OF TECHNOLOGY
DEPARTMENT OF METEOROLOGY

THE STUDY OF THE DIFFUSION OF GASES OR AEROSOLS IN THE LOWER ATMOSPHERE

H. E. CRAMER, F. A. RECORD, H. C. VAUGHAN

FINAL REPORT UNDER CONTRACT No. AF 19(604)-1058

Project Supervisor — H. G. HOUGHTON

15 MAY 1958

The research reported in this document has been sponsored by the Geophysics Research Directorate of the Air Force Cambridge Research Center, Air Research and Development Command.

TABLE OF CONTENTS

ABSTRACT

The principal objectives of the research described in this report have been to achieve improved understanding of the basic physical processes involved in the dispersal of airborne material in the lower atmosphere; and, to establish empirical relationships between basic diffusion parameters and direct meteorological indicators that permit satisfactory quantitative estimates of dispersal from continuous point sources, over travel distances of the order of 1 km, in a wide variety of general weather conditions. These objectives have been achieved largely as the result of a series of comprehensive field observations involving simultaneous measurements both of diffusion and the structure of atmospheric turbulence. The diffusion measurements comprise 10-min average concentrations of sulfur-dioxide gas emitted from a continuous point source near ground level, at travel distances from 50 to 800 m from the release-point for the tracer. The meteorological observations include mean wind speeds, frequency distributions of azimuth wind direction, vertical profiles of wind speed and air temperature, and measurements of the fluctuations in wind velocity obtained from bivanes and heated-thermocouple anemometers. Over one hundred individual experiments of this type were carried out at Round Hill and at a field site near O'Neill, Nebraska during Project Prairie Grass, an extensive series of diffusion measurements sponsored by the Air Force Cambridge Research Center during the summer of 1956. These data comprise the most comprehensive set of small-scale diffusion and meteorological observations currently available. They provide a fairly complete picture of the probable variations in basic diffusion parameters over travel distances of the order of 1 km in all conditions of thermal stratification.

Analysis of these measurements indicates that the prediction of dispersal for small-scale processes is a relatively simple manner. Satisfactory estimates of diffusion from a continuous point source near ground level are provided by a knowledge of source strength, mean wind speed, and the frequency distribution of azimuth wind direction. In the presence of temperature inversions, the estimates for a particular site are somewhat improved by the inclusion of a measure of thermal stratification, such as Richardson's number or the Stability Ratio. The distribution of azimuth wind direction appears to contain implicit information on site roughness and other factors affecting dispersal, and the standard deviation of azimuth wind direction shows promise of serving as a universal diffusion indicator; measures of thermal stratification, on the other hand, appear to be largely independent of site characteristics. The experimental results suggest a simple theoretical diffusion model that is utilized in the derivation of a complete set of small-scale diffusion equations applicable to elevated as well as ground-level sources. The equations are closely similar in form to those of O. G. Sutton and differ principally in the substitution of direct meteorological indicators, the standard deviations of azimuth and elevation angle, for generalized coefficients derived from the vertical profile of mean wind wpeed; and, in the absence of restriction on the value of the power-law exponent on travel distance. Quantitative estimates of maximum ground-level concentrations associated with effluent emission from tall stacks are obtained, for a wide range of thermal stratification (near-neutral to extreme instability), from the equations and the experimental data. The results scatter about Sutton's estimates of maximum ground-level concentration which appear to be reliable first approximations; however, the distances from the base of the stack at which these concentrations occur are significantly smaller than Sutton's estimate.

Fast-response data, obtained during Project Prairie Grass from five bivanes and heated-thermocouple anemometers aligned either parallel or normal to the prevailing wind direction, have been analyzed by high-speed computational techniques to provide estimates of power spectra and the Eulerian scales of turbulence within the frequency range from about 0.5 to 0.01 cycles sec^{-1}. Analysis of scale estimates for the eddy velocities, based on the results from twelve experiments, indicate the following tentative conclusions: Fluctuations in the w-component are smaller than the minimum separation distance of 6 m used in the experiments analysed to date and no detailed scale estimates are possible. During the daytime, and at night in the presence of thermal instability, there is a continuous spectrum of eddy sizes for both the u- and v-components within the frequency range embraced by the measurements. Only slight differences are noted between the relative dimensions of the u- and v-components and between transverse and longitudinal orientations; at low frequencies, scales for the v-component appear to be larger than those for the u-component and there is a tendency for the fluctuations in both components to be elongated in the direction of the mean flow. At night, the transverse scales are considerably smaller than the longitudinal scales and the fluctuations in the v-component tend to be larger than those in the u-component. The spectrum of eddy sizes found during the night-time observations is not continuous over the whole frequency range; low frequency fluctuations are present only in about half the cases studied. When the scale estimates for various frequency bands are plotted against inverse wave number, a close linear relationship between the variates is indicated. Further examination of the experimental data shows that space and time correlations in the direction of mean flow are equivalent and are related by the usual substitution $\underline{x} = \underline{u}\ \underline{t}$. It appears that the daytime scale estimates will be of limited use in explaining the 10-min diffusion measurements since the major features of the time-mean plume principally reflect the influence of fluctuations with frequencies below 0.01 cycles sec^{-1}.

The variation in basic diffusion parameters as a function of the period of sampling was investigated in a series of field experiments conducted at Round Hill during the fall of 1957; sulfur-dioxide gas from a continuous point source located near ground level was again used as a tracer. The sampling array comprised three independently-operated, overlapping networks located at a height of 1.5 m at travel distances of 50, 100, and 200 m; limited concentration data were also available along the vertical coordinate for the layer from 0.5 to 2.5 m. The experiments were based on sampling intervals of 0.5, 3, and 10 min. Results of the data analysis show that, at night, average peak concentrations for the 0.5- and 3-min periods are about 1.3 times larger than the observed 10-min values. During the daytime, average peak concentrations for the 0.5- and 3-min sampling periods exceed the 10-min values by factors of about 2.4 and 1.5, respectively. The shorter-period variations in basic plume characteristics are highly correlated with 10-min standard deviations of azimuth wind direction; these relationships are utilized in obtaining estimates of the probable variations, at the three travel distances, in peak concentration for sampling periods from 0.5 to 10 min over a range of thermal stratification extending from near-neutral to extreme instability.

New developments in meteorological instrumentation include low-inertia anemometers which utilize small aluminum cups and a chopper that permits a beam of light to fall on a photo diode once during each rotation of the cup wheel. These instruments are particularly useful in obtaining representative measurements of the mean wind speed in the presence of stable thermal stratification. Considerable effort has been devoted to the design and construction of a system for the automatic collection and presentation of data from the fast-response meteorological instruments. The present recording system requires a major data abstraction and reduction effort before the measurements are in a form suitable for high-speed computations. The system that has evolved performs four major functions: encoding of analog information (shaft rotation, voltage, etc.) from sensing elements in the form of binary numbers; storage of these numbers in a relay memory until they can be placed on perforated paper tape; decoding of the paper tape; and, presentation of the data either in the form of sequences printed on an IBM electric typewriter or as entries on punch cards. Construction of the system is about two-thirds completed. Use of the system requires substitution of analog to binary converters for the microtorque potentiometers now used in the bivanes; a number of satisfactory types are available.

LIST OF FIGURES

LIST OF FIGURES (cont.)

LIST OF FIGURES (cont.)

LIST OF TABLES

APPENDIX A

I. INTRODUCTION

The diffusion of airborne material in the lower atmosphere is of particular interest to meteorologists for at least two reasons. First, there are many practical problems, such as smoke screening, emission of contaminants from tall stacks, etc., which require dependable quantitative estimates of dispersal in a wide variety of weather conditions. Second, many of the unsolved problems in the physics of the earth's boundary layer depend for solution upon improved knowledge of the eddy transfer processes responsible for the vertical diffusion of characteristic air properties, such as heat, momentum, and water vapor. All these phenomena occur as a consequence of turbulent mixing and it appears likely that the same basic mechanisms are involved in each instance. Diffusion studies, therefore, serve a dual purpose; they contribute not only to the solution of basic problems in meteorological physics, but also lead to the resolution of many practical problems.

There have been two principal lines of attack followed in atmospheric diffusion studies. The older approach, identified with the well-known work of Sir Graham Sutton and other British investigators (1; 2; 3; 4), utilizes the vertical gradient of mean wind speed as the primary meteorological factor in predicting dispersal. The diffusion theories thus derived apply strictly to small-scale diffusion over a relatively smooth surface in the presence of near-neutral thermal stratification. Extension of the theories to the more-frequently encountered thermal stratifications of temperature lapse and inversion, to rough surfaces, and to travel distances in excess of 1 km has been questioned. Recent diffusion measurements (5; 6; 7) appear to confirm these limitations. However, in view of the complexity of atmospheric diffusion and the limited empirical data available at the time the above theories were formulated, the work of Sir Graham Sutton and his collaborators represents an outstanding achievement.

Within the past decade, investigations of atmospheric diffusion have been guided by a different point of view which holds that improved understanding of dispersal processes, and consequent simplification of prediction techniques, depends upon increased knowledge of the structure of turbulence, i.e., fluctuations in wind velocity. This has been the view of investigators at the Round Hill Field Station of the Massachusetts Institute of Technology. In the initial research programs, attention was focused principally on the development of measurement techniques suitable for studying fluctuations in wind velocity and on the utilisation of these techniques to provide basic information on turbulent structure (8; 9; 10; 11). During the period covered by this report, the research program has had two principal objectives: (1) To obtain simultaneous, comprehensive measurements both of diffusion, downwind from a continuous point source located near ground level, and of the structure of turbulence in a wide variety of general weather conditions. (2) To establish, from these data, empirical relationships between dispersal and simple meteorological parameters useful in formulating techniques for providing satisfactory quantitative dispersal estimates. Achievement of these objectives has in part depended upon an extensive series of diffusion experiments in which sulfur-dioxide gas was used as a tracer. Midget impingers containing 10 ml of dilute hydrogen-peroxide solution were located at various distances downwind from a continuous point source. During the experiments, the impingers were aerated at a known, constant rate; sulfur dioxide present in the air samples reacted with the hydrogen peroxide to form sulfuric acid, thus increasing the electrical conductivity of the solutions. Time-mean concentrations for the 10-min sampling periods were determined from laboratory analyses of the conductance of the aerated solutions. This technique, which proved very reliable, is capable of detecting concentrations of one part sulfur dioxide in one hundred million parts of air. During 1954 and 1955, twenty-nine diffusion experiments were conducted over a 200-m range at the Round Hill Field Station. In the summer of 1956, approximately seventy similar experiments were conducted over a maximum range of 800 m during Project Prairie Grass, an extensive series of diffusion experiments sponsored by the Air Force Cambridge Research Center at a field site near O'Neill, Nebraska. The Project Prairie Grass experiments also included an extensive series of measurements of fluctuations in wind velocity, utilizing five bivanes equipped with heated-thermocouple anemometers; these instruments were mounted at a height of 2 m above the ground and placed either parallel or normal to the mean wind direction. Analysis of these data to provide information on power spectra and the scales of turbulence is proceeding. During the fall of 1957, a new series of diffusion experiments was initiated at Round Hill to investigate variations in time-mean concentration as a function of the duration of the period of sampling. Three independently-operated sampling networks at travel distances of 50, 100, and 200 m were utilized in measuring average concentrations for sampling periods of 30 sec, 3 min, and 10 min. In the course of the diffusion experiments, certain improvements were made in existing meteorological instrumentation and some progress achieved in the development of a data-recording system designed to facilitate the handling of both fast- and slow-response meteorological observations.

Much of the research mentioned above has already been described in detail in various published papers (12; 13; 14) or in a Geophysical Research Paper to be issued in the near future by the Air Force Cambridge Research Center. The general plan of this report is to summarize briefly the material that is available elsewhere and to devote principal attention to those aspects of the research program that have not previously been described.

II. DIFFUSION MEASUREMENTS AT ROUND HILL AND O'NEILL, NEBRASKA DURING 1954-1956

A. Brief summary of experimental techniques

Approximately one hundred field experiments, utilizing sulfur-dioxide gas as a tracer, were conducted during the period from 1954 through 1956 at two sites: Round Hill and O'Neill, Nebraska. About half the experiments at each site were carried out in the presence of unstable thermal stratification and half in the presence of temperature inversions. Twenty-nine sets of diffusion measurements, comprising 10-min average gas concentrations determined at selected points downwind from a continuous point source located near ground level, were obtained at Round Hill during 1954 and 1955. The sampling network consisted of 183 midget impingers mounted at a height of 2 m along three semi-circular arcs at travel distances of 50, 100, and 200 m; an angular separation of 3 deg between individual impingers was used at all travel distances. The impingers were aspirated at the rate of 1.5 l min^{-1} by means of vacuum sources positioned at the mid-points of the arcs. The sulfur-dioxide generator utilized a 100-lb cylinder of liquid sulfur dioxide immersed in a constant-temperature water bath. Heat of vaporization required for the change of state of the tracer was largely supplied by the water; this facilitated maintenance of a constant emission rate (5 to 10 g sec^{-1}) throughout the 10-min sampling period. The total amount of gas released during each experiment registered on the dials of a large gas meter. After passage through the meter, the tracer was conducted through a 100-ft length of copper tubing and released vertically at a height of 30 cm above ground level. Prior to the start of the 10-min sampling period, the tracer was permitted to traverse the entire sampling network; source operation continued for a short time after the sampling period had ended. Meteorological instrumentation included: cup anemometers and ventilated thermocouples, installed at four levels on a portable tower, for measuring vertical gradients of mean wind speed and air temperature; a cup anemometer and wind-direction vane, located at a height of 2 m near the release point, for determining mean wind speeds and frequency distributions of azimuth wind direction; four bivanes equipped with heated-thermocouple anemometers for measurements of the structure of turbulence. A schematic diagram of the field installation is presented in fig. 1. Tabular summaries of the concentration measurements and meteorological observations obtained during all of the experiments are presented in Appendix A. Descriptions of the experimental techniques and discussions of the results of data analysis may be found elsewhere (13; 14).

Seventy sets of similar concentration data were obtained at a field site near O'Neill, Nebraska in the summer of 1956 during Project Prairie Grass. The sampling network comprised 599 midget impingers; of these, 545 were mounted at a height of 1.5 m along five concentric semicircular arcs located at travel distances of 50, 100, 200, 400, and 800 m. An angular separation of 2-deg was used along the four inner arcs while a 1-deg separation was used at 800 m. The remaining 54 impingers were mounted at nine levels on each of six lightweight towers erected along the 100-m arc. Aspiration was provided by eleven vacuum units suitably positioned within the sampling network. The sulfur-

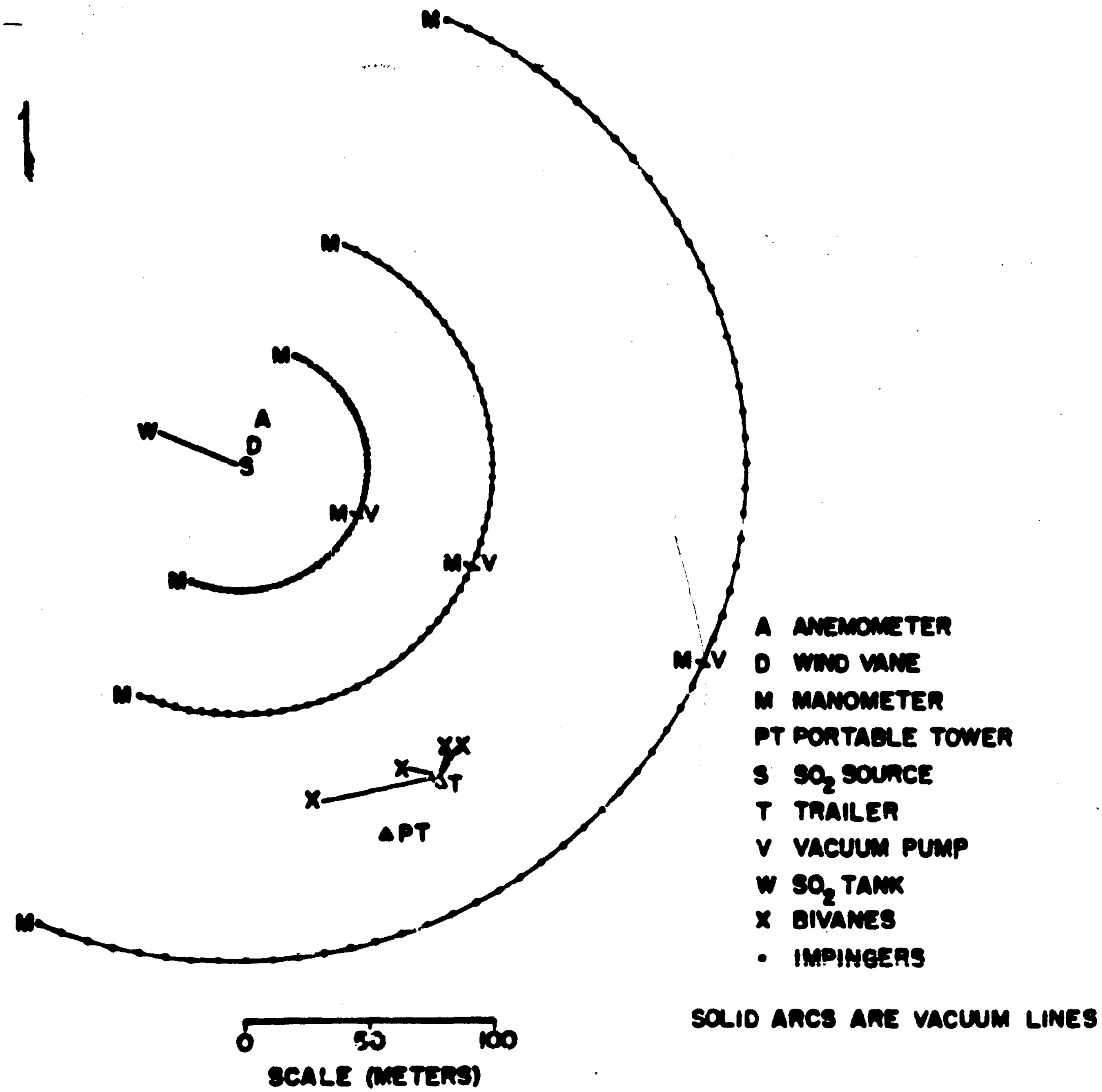

Fig. 1. Schematic diagram of field installation for 1954-1955 diffusion experiments at Round Hill.

dioxide generating apparatus was basically similar to that previously used at Round Hill but, due to the longer travel distances involved, capable of maintaining source strengths within the range from 50 to 100 g sec^{-1}. To minimize the disturbance of the natural air flow in the vicinity of release point for the tracer, the generating apparatus was set in a shallow trench and the gas conducted through a 50-m length of buried plastic pipe before being released horizontally at a height of 46 cm above ground level (see fig. 4). A contour map of the Prairie Grass field site showing the location of the arcs of the sampling network and other installations appears in fig. 2. A schematic diagram of the sulfur-dioxide generator is presented in fig. 3 and photographs of various components of the field installation are shown in fig. 4. Meteorological instrumentation included: cup anemometers and wind-direction vanes mounted at a height of 2 m both near the release point for the tracer and at a distance of 450 m directly downwind (north) of the release point; five bivanes, outfitted with heated-thermocouple anemometers, mounted at a height of 2 m at the northern boundary of the field site. Measurements of vertical profiles of mean wind speed and air temperature were made by Texas A & M. Meteorological observations were made over a 20-min sampling period centered at the mid-point of the 10-min gas release. The diffusion network was placed in operation immediately prior to the start of the gas release and continued in operation for several minutes after the end of the release, until the tracer had cleared the 800-m arc. Detailed descriptions of the conduct of the experiments, discussion of the reliability of the measurements, and complete tabular summaries of concentration data and meteorological observations are available in a Geophysical Research Paper currently

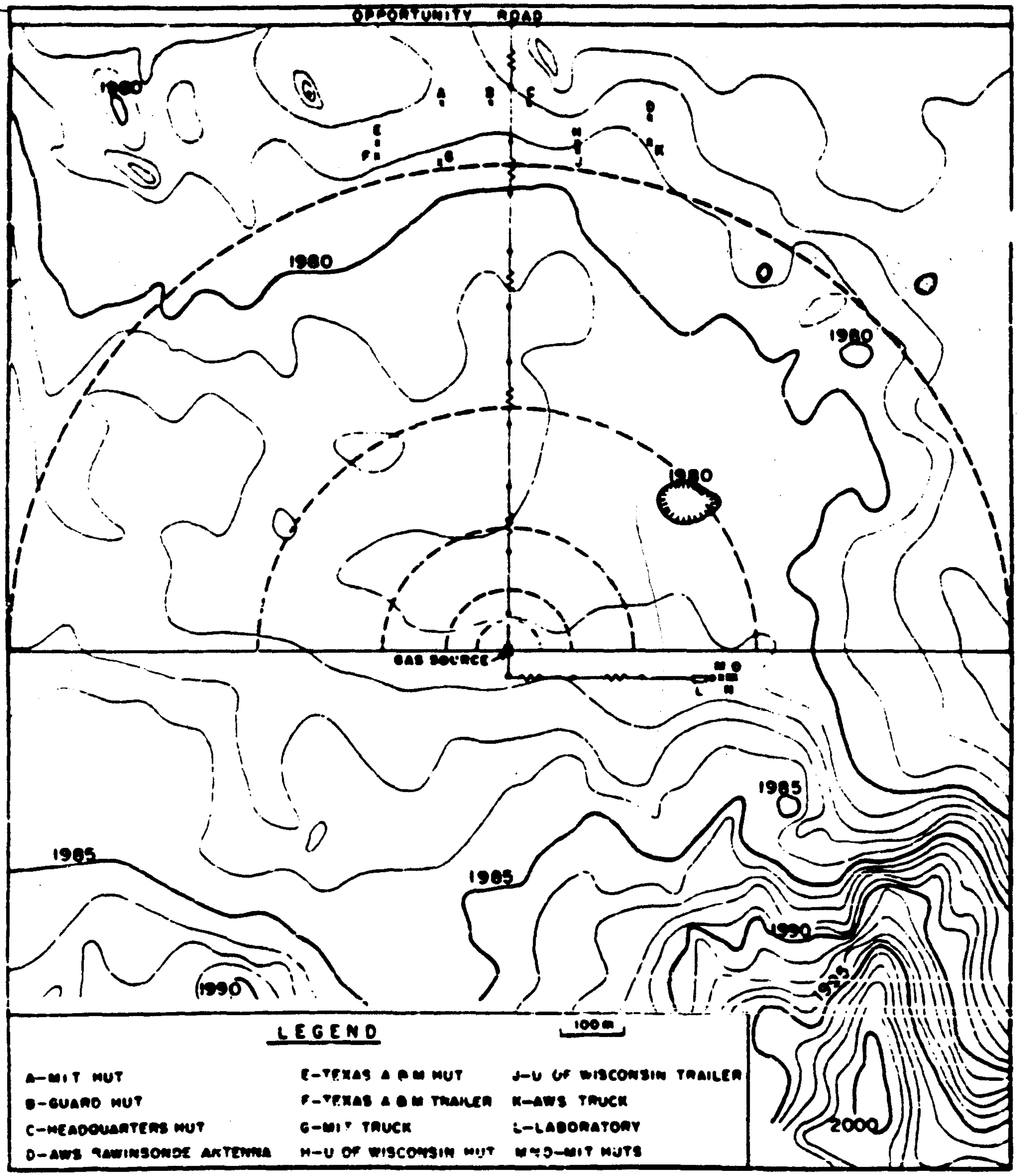

Fig. 2. Contour map of field site for Project Prairie Grass showing location of sampling arcs in diffusion network (dashed lines) and other installations.

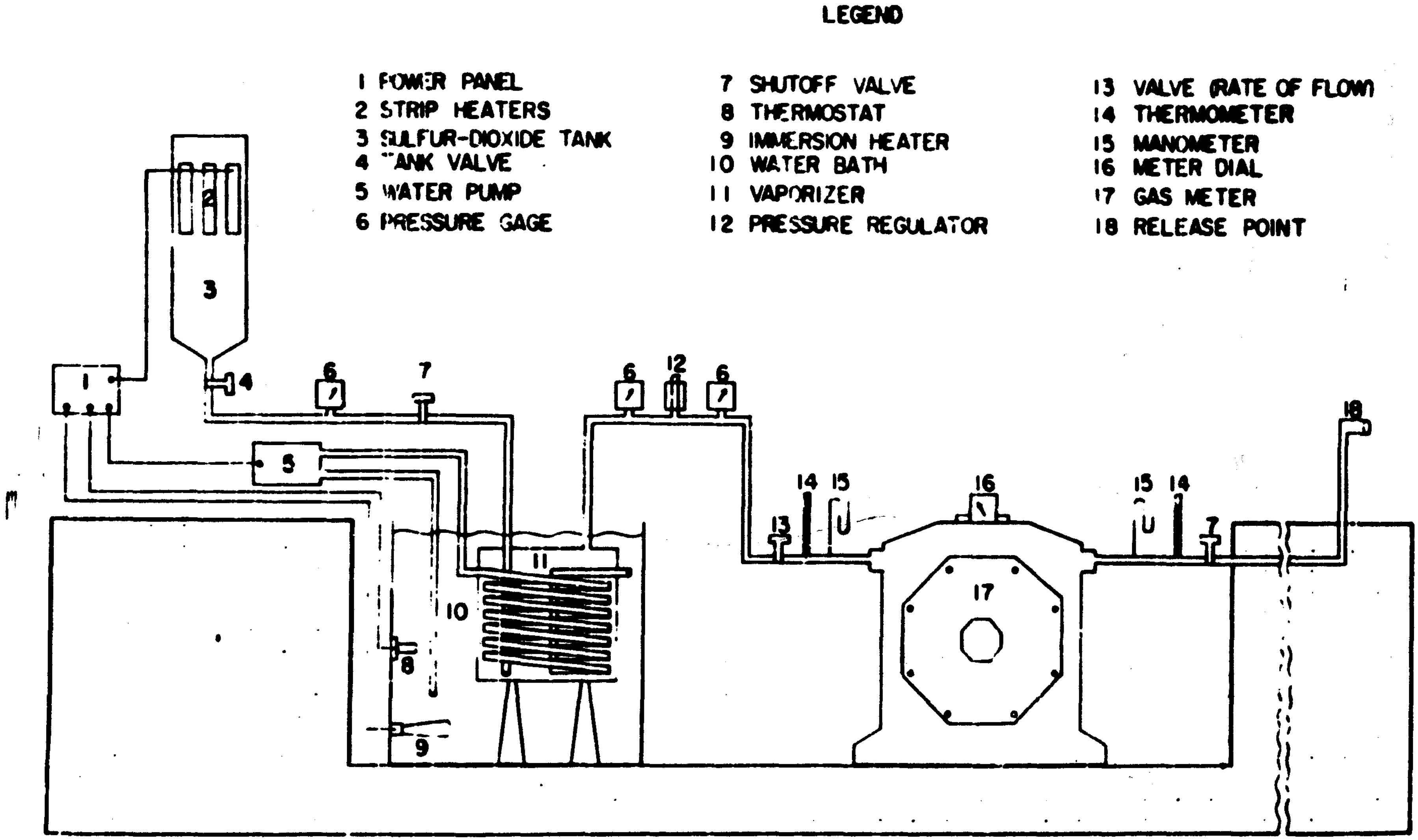

Fig. 3. Schematic diagram of sulfur-dioxide generator used in Project Prairie Grass diffusion experiments.

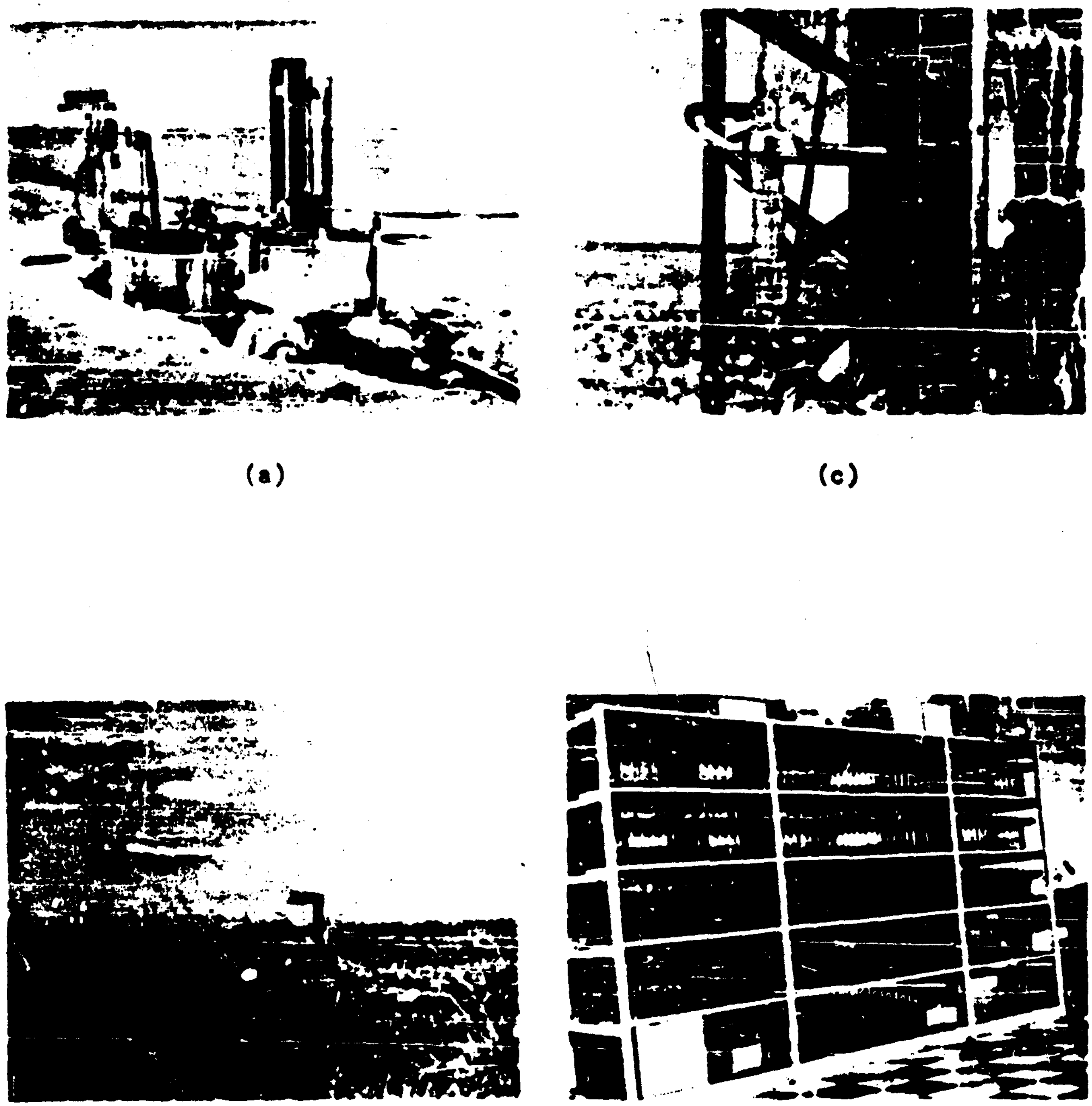

(a) (c)

(b) (d)

Fig. 4. Photographs of Project Prairie Grass diffusion installations: (a) sulfur-dioxide generating apparatus; (b) release-point for tracer; (c) midget impinger installed on one of the 60-ft towers; (d) interior of laboratory building showing storage shelves for impinger baskets.

being prepared for distribution by the Air Force Cambridge Research Center. Other descriptions of the diffusion measurements and the results of data analysis may be found elsewhere (12; 14).

It should be pointed out that surface roughness characteristics at the two sites are quite different. The O'Neill, Nebraska site is unusually smooth ($z_0 < 1$ cm) with an unobstructed upwind fetch of at least 1 km. The Round Hill site is unusually rough ($z_0 > 10$ cm); trees, houses, small buildings, and differences in elevation of the order of 100 ft are found within a distance of 0.5 to 1 km immediately upwind from the test area.

B. Results of data analysis

1. Basic relationships

Horizontal and vertical cross-sections for several time-mean gas plumes obtained during the Project Prairie Grass diffusion experiments are presented in figs. 5, 6. These examples indicate the variations in characteristic plume features (width, height, axial concentration, form of the concentration profile, etc.) observed over a wide range of general weather conditions. The fundamental problem is that of relating these observed variations in diffusion parameters to meteorological quantities which may then be used as useful indices of dispersal.

All the diffusion experiments reveal a very close relationship between the structure of the time-mean gas plume and fluctuations in azimuth wind direction. The downwind axis of the plume is found approximately

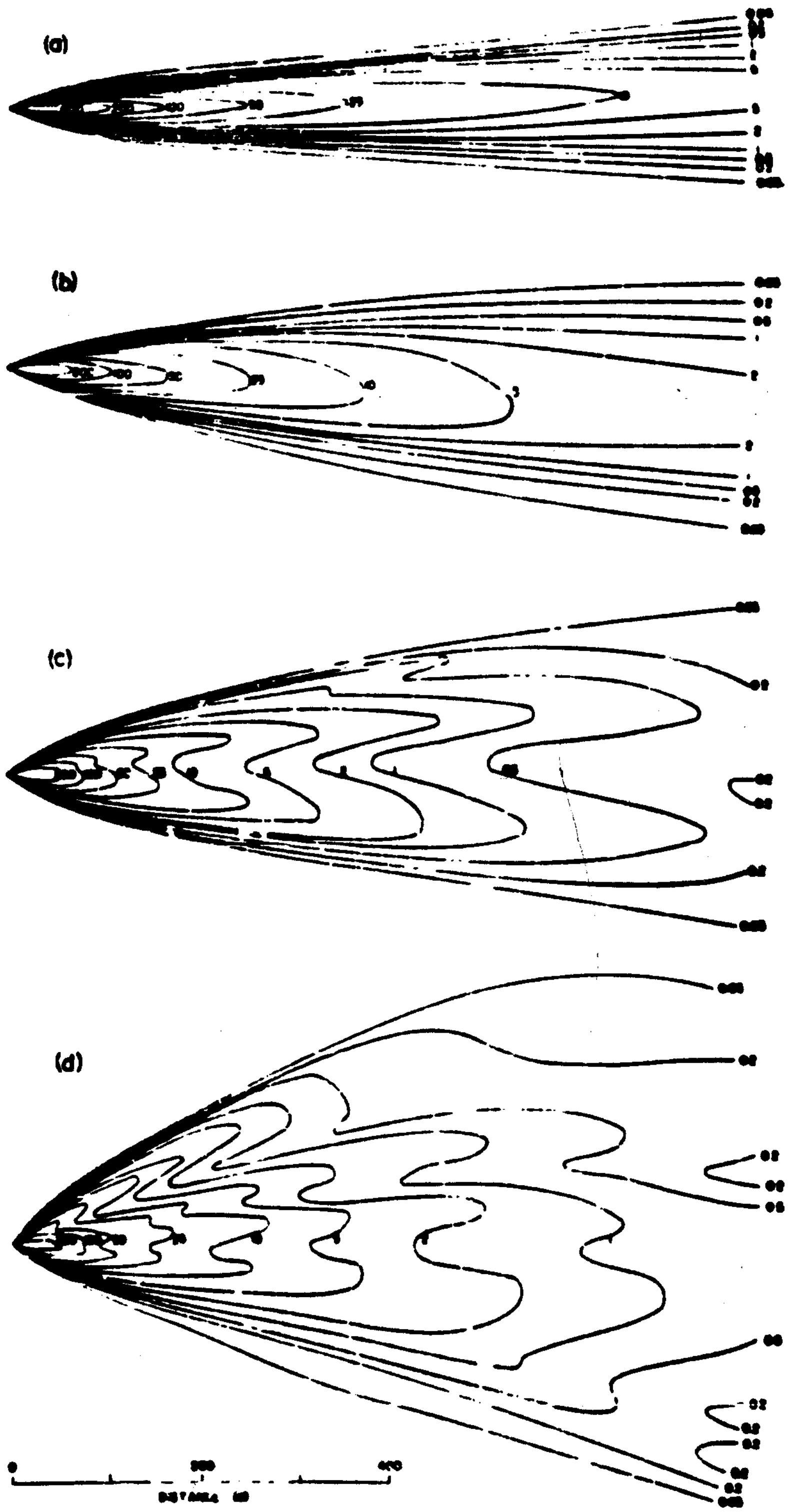

Fig. 5. Horizontal cross-sections for selected Prairie Grass diffusion experiments: concentration isopleths are in mg m^{-3} for standard source strength of 100 g sec^{-1} and mean wind speed of 5 m sec^{-1}: (a) narrow, symmetrical plume characteristic of stable thermal stratification; (b) exceptionally narrow, symmetrical daytime plume associated with high wind speeds; (c) daytime plume in which the shape of the concentration profile changes significantly with travel distance; (d) wide, irregular plume characteristic of strong midday convection.

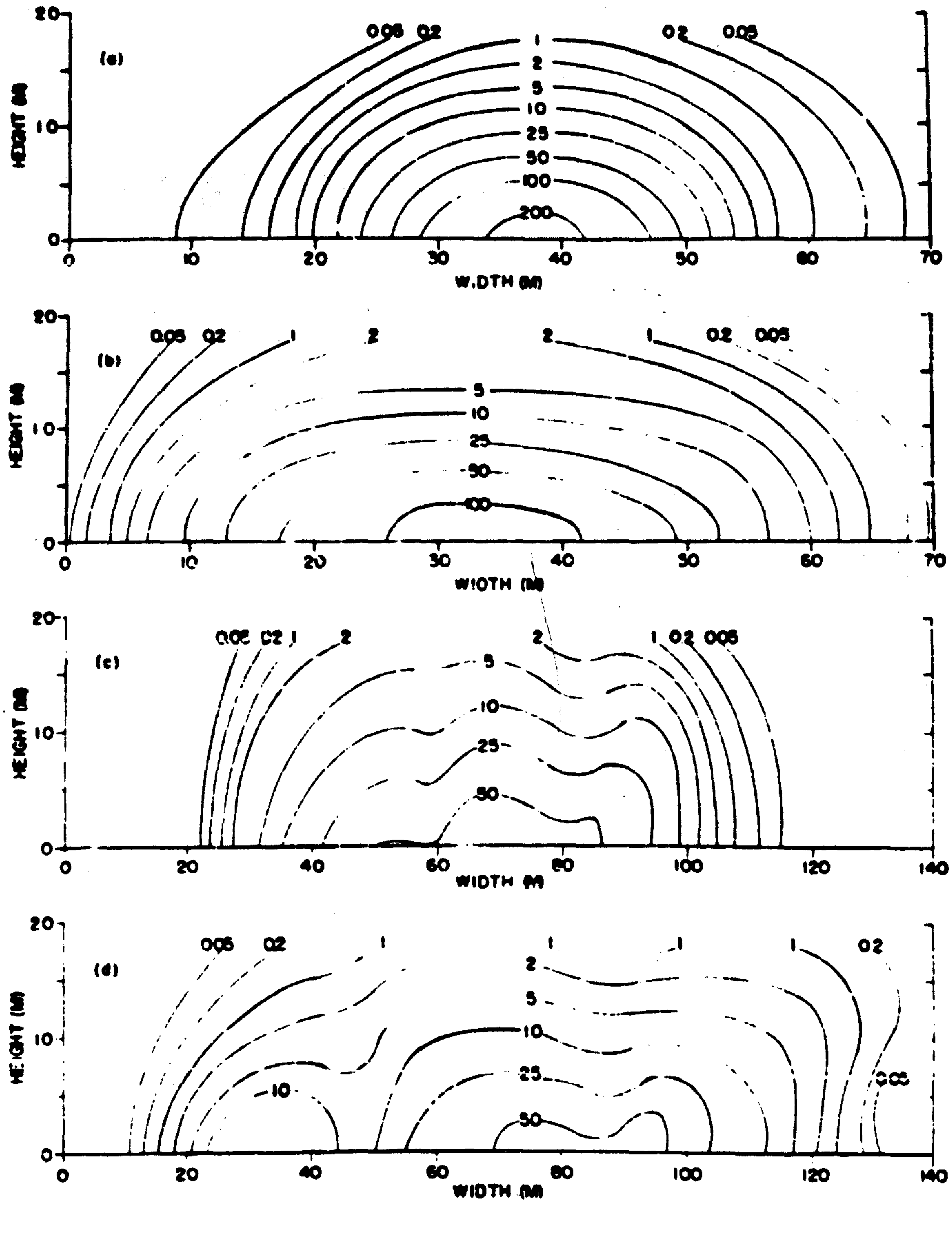

Fig. 6. Vertical cross-sections for selected Prairie Grass diffusion experiments at travel distance of 100 m; concentration isopleths are in mg m^{-3} and are adjusted for standard source strength of 100 g sec^{-1} and mean wind speed of 2 m sec^{-1}; individual examples correspond to the horizontal cross-sections shown in fig. 5.

along the direction of the mean wind and the lateral distribution of concentration at all travel distances corresponds closely to the frequency distribution of azimuth wind direction. This correspondence is best at short travel distances and tends to decrease with increasing travel distance due to enhanced dilution at the edges of the plume. Concentration profiles at three travel distances and frequency distributions of azimuth wind direction for one of the O'Neill, Nebraska nighttime experiments are presented in fig. 7. Over travel distances of the order of 1 km, the time-mean gas plume thus appears to be composed of elementary filaments that have traveled downwind from the source along lines of constant azimuth bearing. Recent experiments in England (15) and in this country (16) indicate that vertical diffusion may be described similarly. Basic features of plume structure (peak concentration χ_p, integrated-crosswind concentration χ_{CIC}, plume width W, etc.) are consequently highly correlated with the standard deviation of azimuth wind direction σ_A. In the presence of thermal instability, correlation coefficients between σ_A and the variates mentioned above are approximately 0.9 at all travel distances; during stable thermal stratification, the correlations are about 0.8. Features of plume structure, particularly χ_{CIC}, are also significantly related to measures of thermal stratification such as Richardson's Number Ri or the Stability Ratio SR. Results of multiple correlation studies show that an index combining both σ_A and either Ri or SR is of advantage in predicting nighttime peak concentrations and daytime integrated-crosswind concentrations; daytime peak concentrations and plume width in all stability stratifications are best predicted by σ_A alone; nighttime χ_{CIC} values are best predicted by SR or Ri alone.

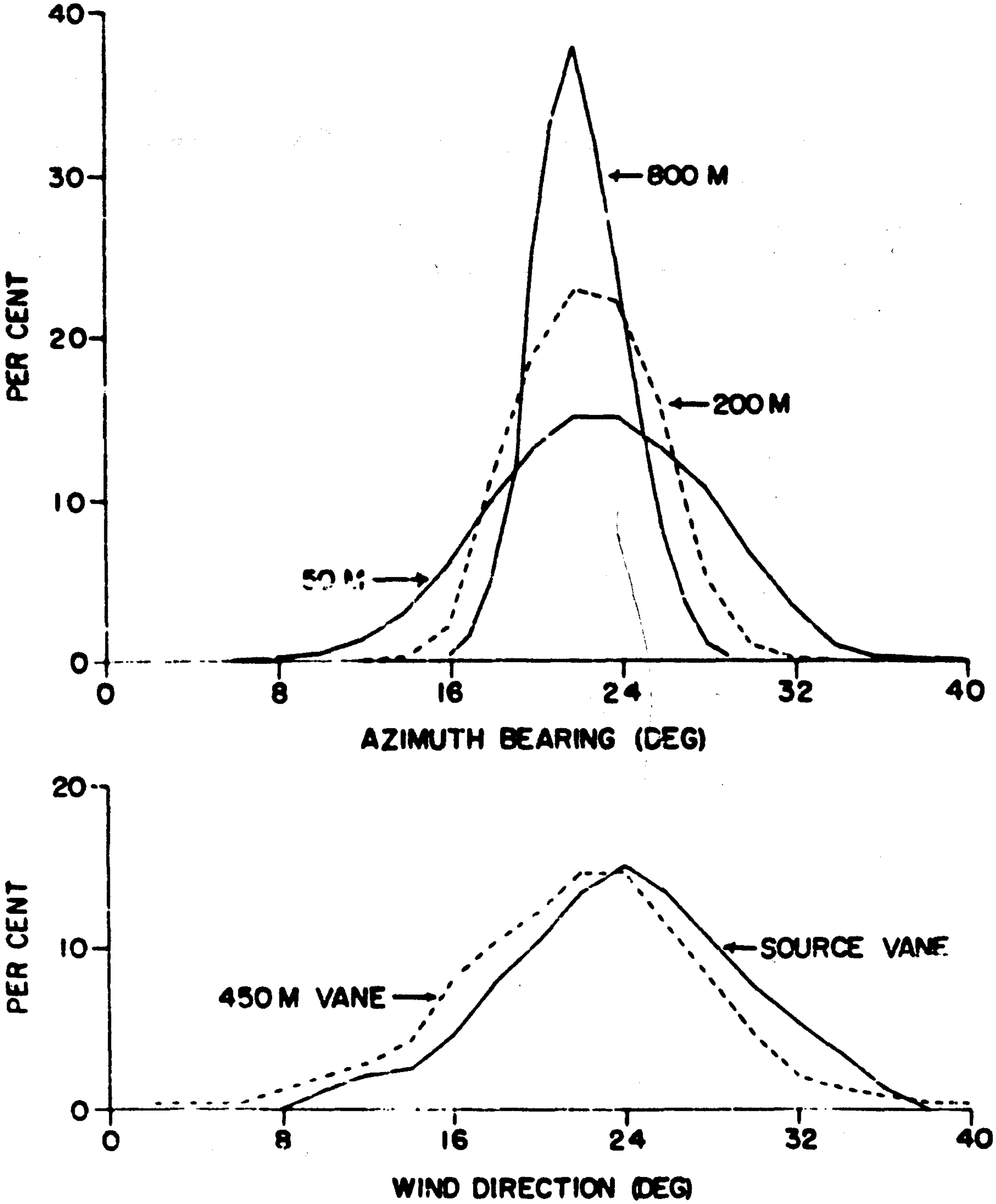

Fig. 7. Horizontal concentration profiles at three travel distances (above) and frequency distributions of azimuth wind direction (below) measured at height of 2 m at two locations. Data refer to nighttime Prairie Grass experiment conducted in presence of very stable thermal stratification.

When the Round Hill and O'Neill, Nebraska diffusion measurements for the same travel distance are plotted against σ_A, the least-squares regression lines for both sets of data are almost identical. Peak concentrations at 100 m from both sites are shown in fig. 8;[1] no adjustment has been made for the slight difference in sampling height between Round Hill (2 m) and O'Neill (1.5 m). If similar diffusion data are plotted against Ri or SP, the Round Hill and O'Neill data cannot easily be reconciled. The discrepancy is principally explained by the difference in roughness of the two sites: at Round Hill, neutral stratification corresponds to σ_A values of about 13 deg; at O'Neill, neutral stratification is identified with σ_A 7 deg. The evidence is quite conclusive that the standard deviation of azimuth wind direction contains implicit information on site roughness and other factors (such as air mass) that determine diffusion; further investigation may establish it as a universal diffusion index. It is also apparent from close inspection of the data from the two sites that lateral and vertical diffusion are not completely independent (as frequently assumed in theoretical treatments) but must be at least quasi-dependent. This point is further discussed below.

For reasons indicated above, the results of the small-scale diffusion measurements are most conveniently summarized in terms of the standard deviation of azimuth wind direction.[2] Estimates of the variation in both σ_A and the standard deviation of elevation angle σ_E with thermal stratification and site roughness are presented in table 1; entries in the table are

---

[1] Concentration data not corrected for evaporational loss of tracer solution.

[2] Except for nighttime values of integrated-crosswind concentration.

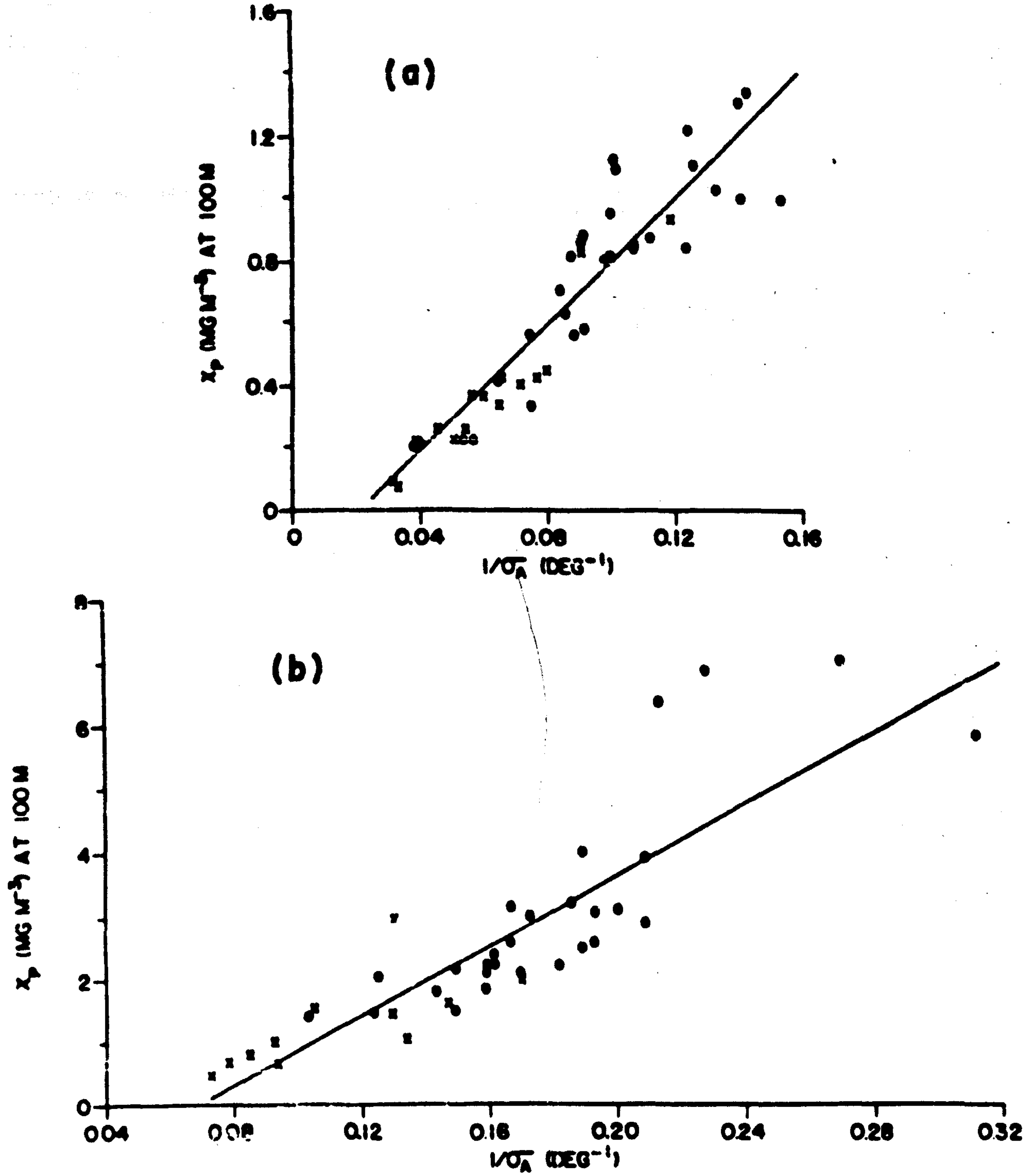

Fig. 8. Peak concentration at 100 m versus inverse standard deviation of azimuth wind direction for (a) daytime and (b) nighttime diffusion experiments. Concentrations are adjusted to standard source strength of 1 g sec^{-1} and mean wind speed of 5 m sec^{-1}. Round Hill data are indicated by symbol x and O'Neill, Nebraska data by open circles. Solid lines are least-squares regression lines.

based upon bivane measurements made at O'Neill (17) during the Great Plains Program and other data. The values apply generally within the layer from ground level to a height of 100 m; both σ_A and σ_E tend to increase with height during thermal instability and to decrease with height during thermal stability. For stable stratification, the larger values of both parameters apply near ground level and the smaller values apply at higher levels; the situation is reversed in the case of unstable thermal stratification.

Table 1. Estimated range in standard deviations of azimuth wind direction σ_A and elevation angle σ_E for various stability stratifications.

Stratification	Smooth site		Rough Site	
	σ_A (deg)	σ_E (deg)	σ_A (deg)	σ_E (deg)
Extremely stable	2-4	0-2	2-6	0-3
Moderately stable	4-8	2-4	7-15	3-5
Near-neutral	6-8	3-5	10-15	4-6
Moderately unstable	10-15	4-6	15-20	6-8
Extremely unstable	20-25	7-9	25-30	9-11

Basic diffusion parameters for twenty-two daytime and twenty nighttime[1] Prairie Grass experiments (selected on the basis of complete concentration data and meteorological observations) have been correlated with meteorological parameters (σ_A or SR); results of the regression analysis are presented in figs. 9 to 14. Concentration data, corrected for evaporational loss of impinger solution during the experiments, are adjusted to a standard source strength of 100 g sec^{-1} and a mean wind speed of 5 m sec^{-1}. The analysis technique involved determination of least-squares regression lines, for the logarithms of the variates, at each travel distance. Estimates of the diffusion parameters for selected values of the meteorological quantities were then obtained, at each travel distance, from the regression equations and the appropriate pointe connected by straight lines. A detailed account of the analysis technique and tabulated values of correlation coefficients and standard errors of estimate are available elsewhere (14). It should be mentioned that the concentrations shown in figs. 9, 10, 11, 12 refer to measurements made at a height of 1.5 m associated with continuous emission of the tracer from a point source at a height of about 0.5 m. At short travel distances (50, 100 m), the plume axis tends to be located below the height of the sampling network; thus, the measured concentrations are somewhat lower than the axial concentrations. Studies of vertical concentration profiles obtained at a travel distance of 100 m during the O'Neill experiments indicate that the measured concentrations, at a height of 1.5 m, should be increased by 10 per cent, on the average, for both daytime and nighttime gas releases to secure reasonable estimates of axial concentration (12).

---

[1] Concentrations for daytime experiments were smoothed by a weighted three-term moving average at all travel distances.

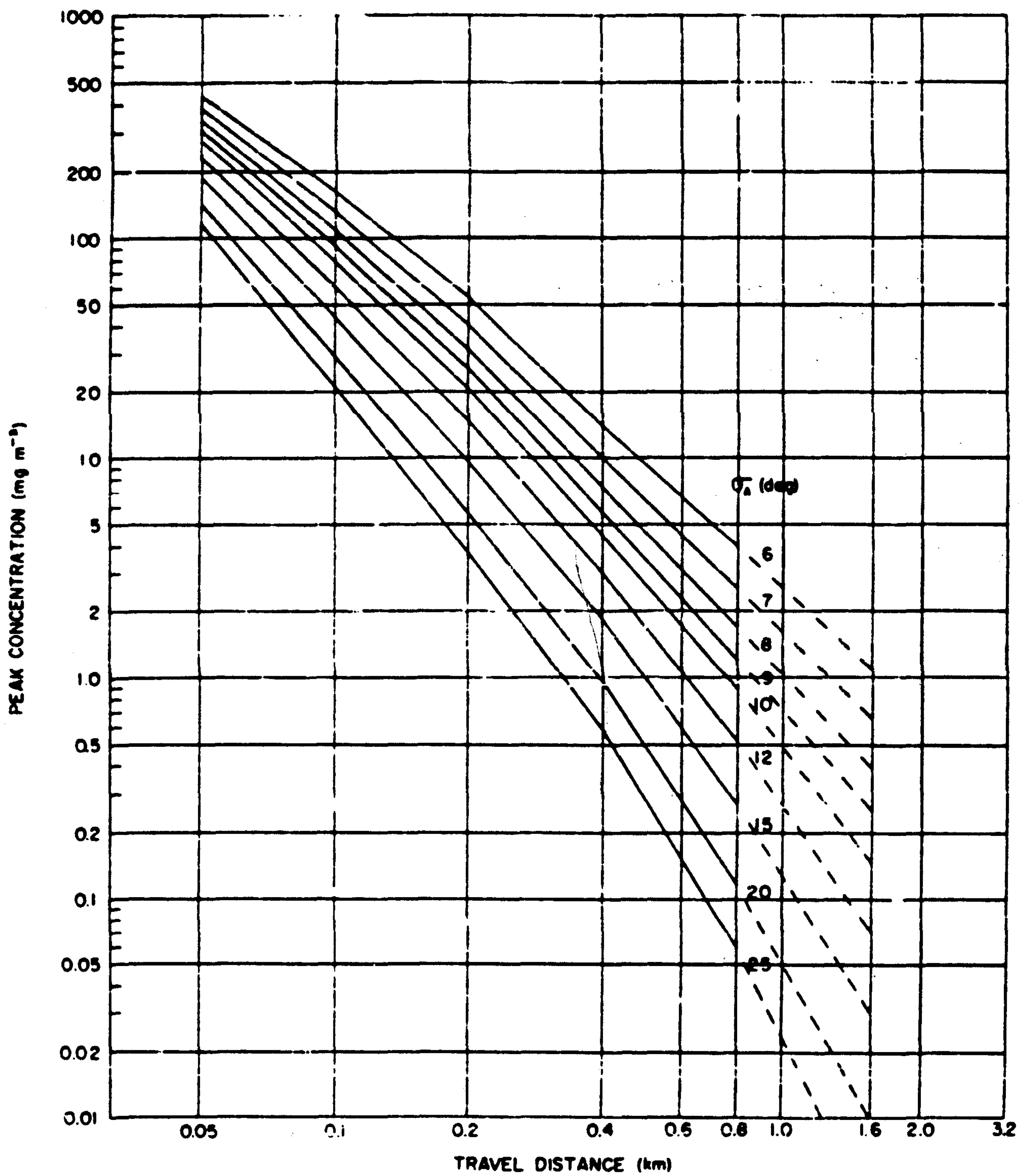

Fig. 9. Peak concentrations at height of 1.5 m expressed in terms of σ_A; data based on O'Neill daytime diffusion experiments. Values are adjusted to a source strength of 100 g sec^{-1} and a mean wind speed of 5 m sec^{-1}. Dashed lines are suggested extrapolations.

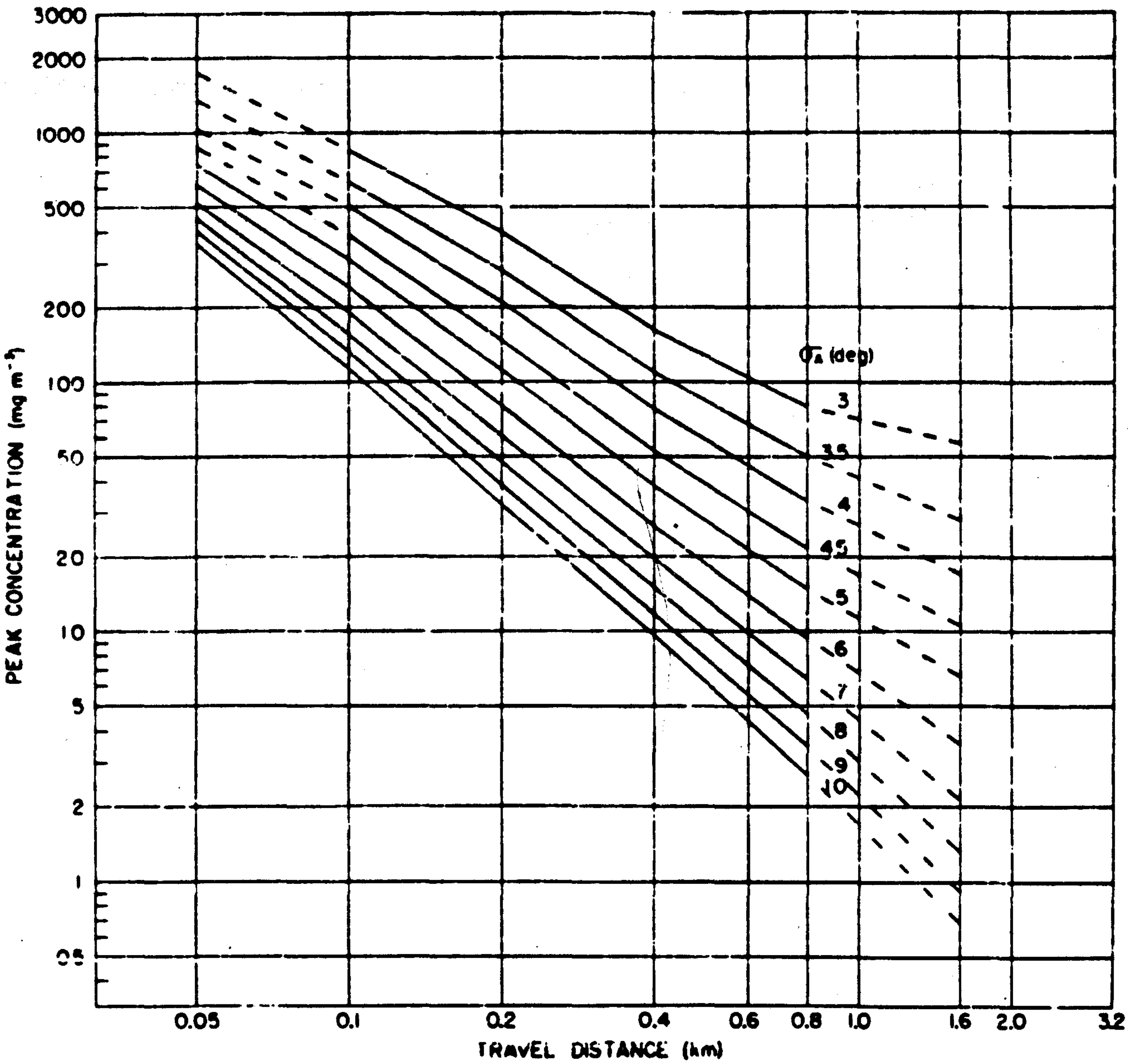

Fig. 10. Peak concentrations at height of 1.5 m expressed in terms of σ_A; data based on O'Neill nighttime diffusion experiments. Values are adjusted to a source strength of 100 g sec^{-1} and a mean wind speed of 5 m sec^{-1}. Dashed lines are suggested extrapolations.

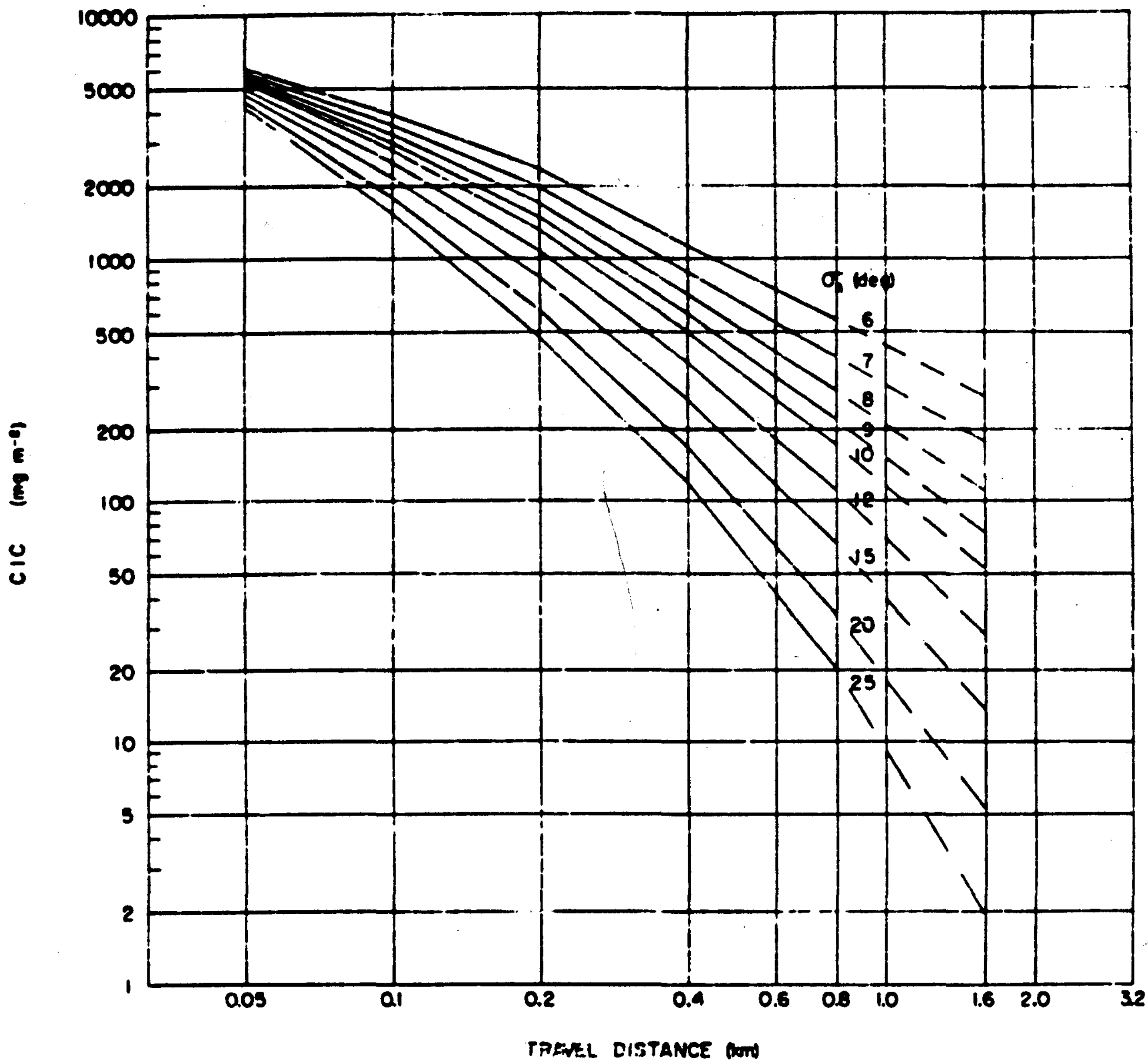

Fig. 11. Integrated-crosswind concentrations at height of 1.5 m expressed in terms of σ_A; data based on O'Neill daytime experiments. Values are adjusted to a source strength of 100 g sec^{-1} and a mean wind speed of 5 m sec^{-1}; dashed lines are suggested extrapolations.

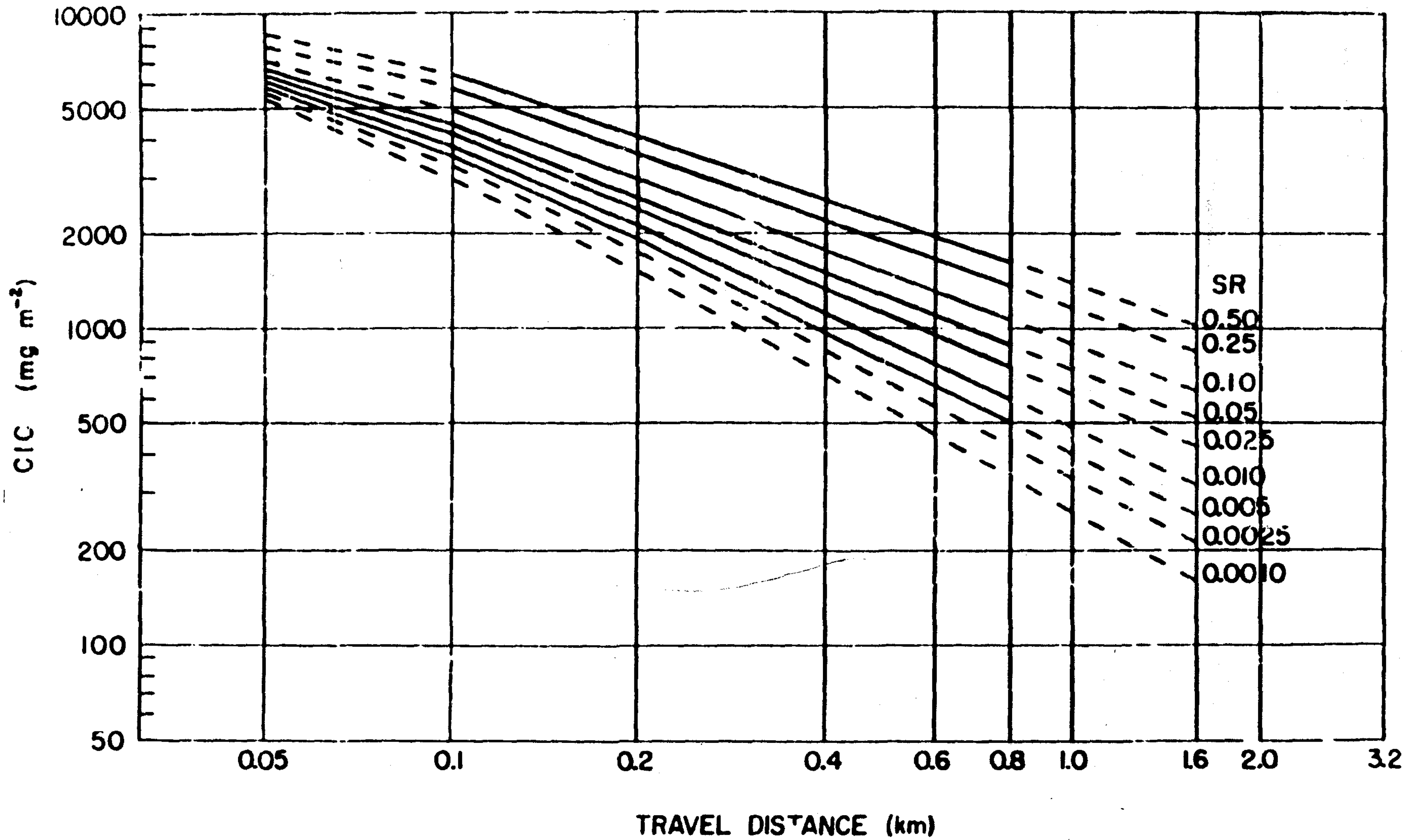

Fig. 12. Integrated-crosswind concentrations at height of 1.5 m expressed in terms of the stability ratio; data based on O'Neill nighttime diffusion experiments. Concentrations are adjusted to source strength of 100 g sec^{-1} and mean wind speed of 5 m sec^{-1}. Dashed lines represent reasonable extrapolations.

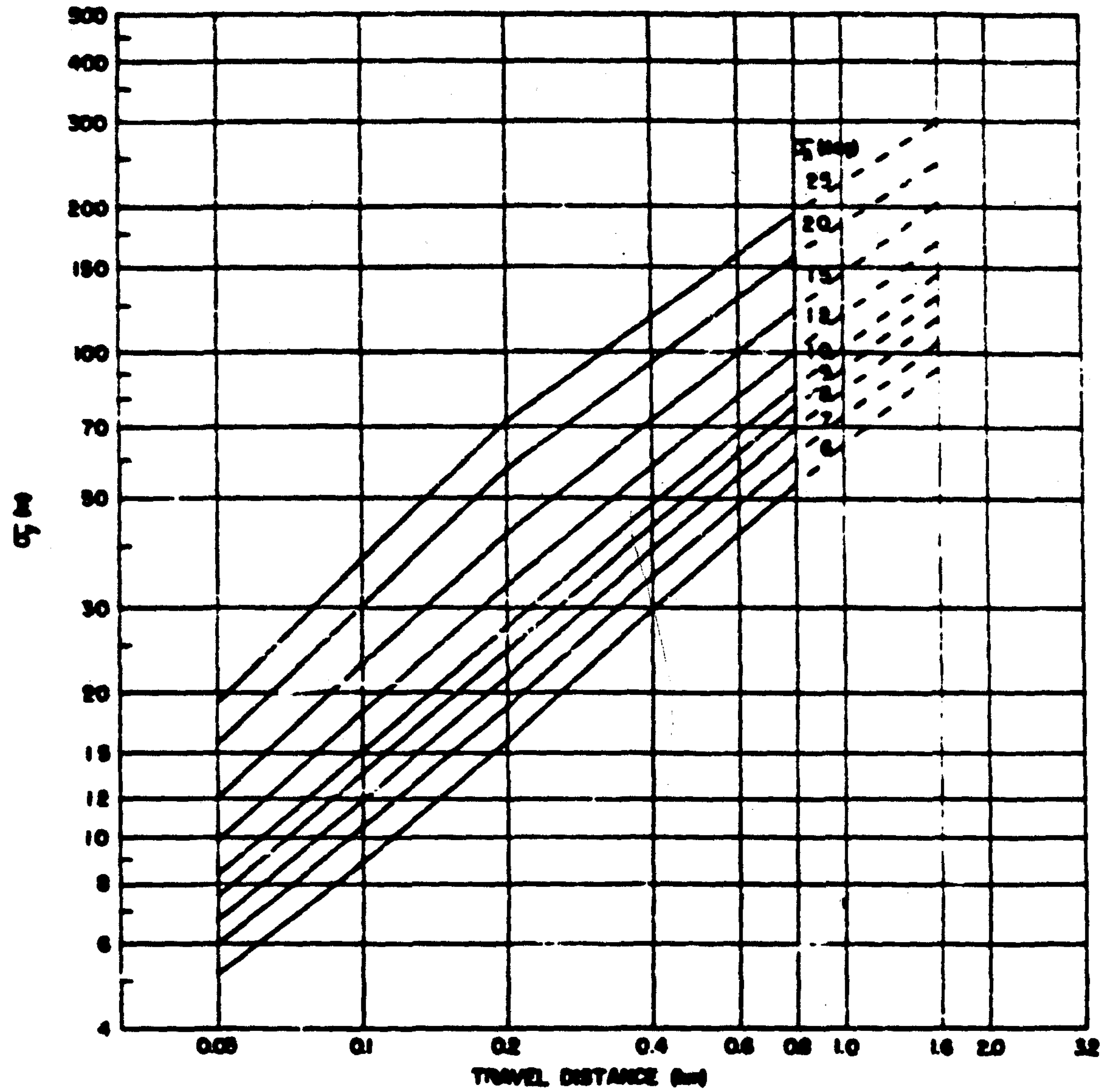

Fig. 13. Standard deviations of concentration along the lateral coordinate for O'Neill, Nebraska daytime experiments; values are expressed in terms of arc distance and dashed lines are suggested extrapolations.

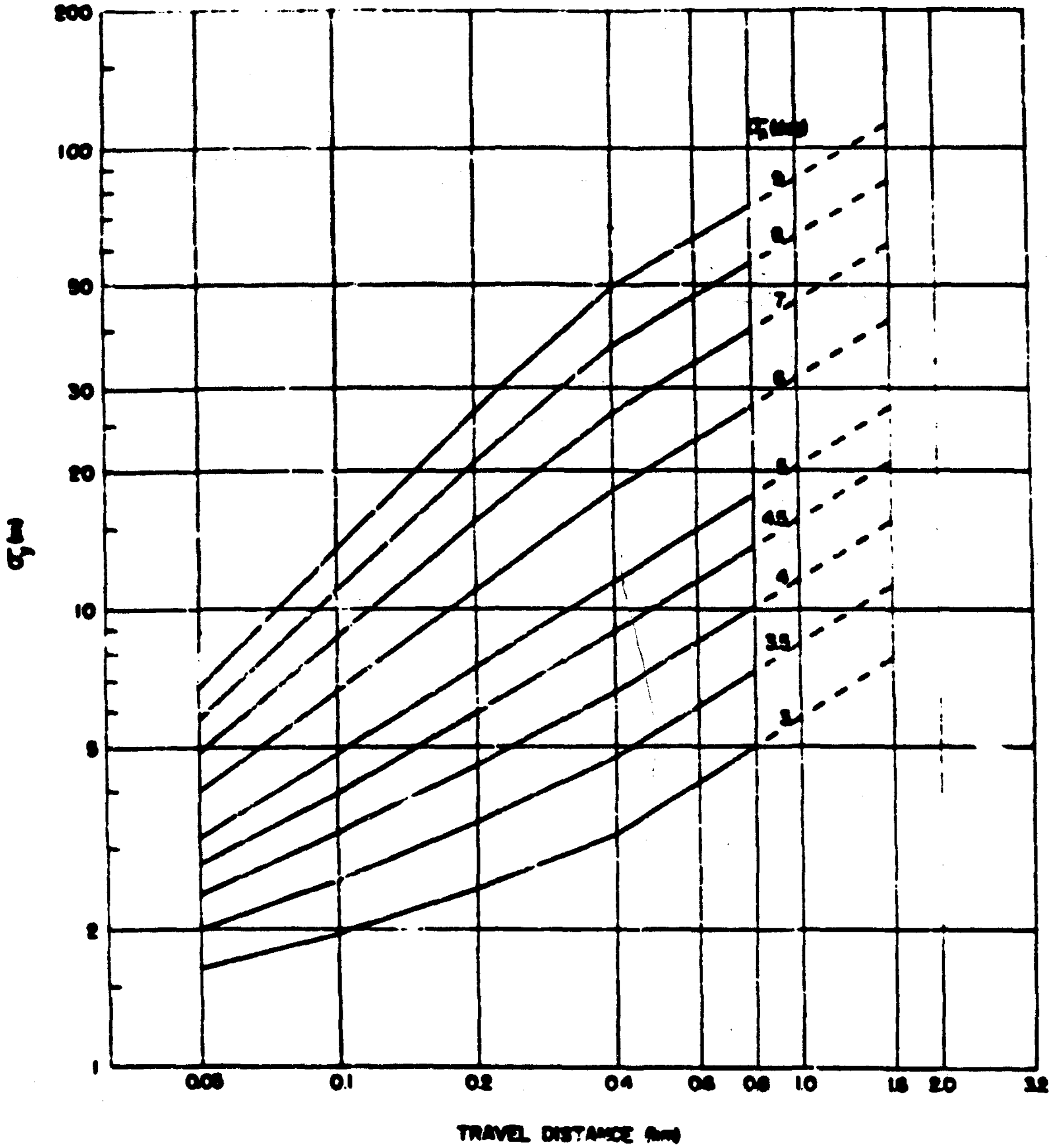

Fig. 14. Standard deviations of concentration along the lateral coordinate for O'Neill, Nebraska nighttime experiments; values are expressed in terms of arc distance and dashed lines are suggested extrapolations.

The correction at 50 m is estimated to be about 25 per cent. At travel distances greater than 200 m, it appears that the 1.5 m measurements adequately represent axial concentration except in the presence of extremely stable thermal stratification. The concentration measurements are also affected by reflection from the ground; this factor is judged insignificant at travel distances greater than 100 m in comparison with the standard errors of estimate of the regression technique and estimates of the reliability of the basic measurements. Nighttime integrated-crosswind concentrations have been presented as functions of the Stability Ratio since, for the selected cases (which represent moderate stability), χ_{CIC} is almost invariant with σ_A. If the whole range of stable thermal stratification is considered, the prediction value of σ_A increases; however, since variations in χ_{CIC} occur almost entirely as a result of the vertical spread of the plume, SR is the most likely indicator. Values of SR used in the analysis were obtained from the ratio of the temperature difference between the 4- and 1-m levels and the square of the wind speed at a height of 2 m.

Variations in basic diffusion parameters with travel distance may be expressed in terms of simple power laws of the general form

$$\chi_{P},\ \sigma_y \propto (x)^b ,$$

where x is the travel distance and b is a constant. The power-law exponent b has been evaluated for four intervals of travel distance (50-100, 100-200, 200-400, 400-800 m) with respect to peak concentration, and the standard deviations of concentration along the lateral and vertical coordinates. Estimates of the value of the exponent on σ_z were obtained by taking the difference $\underline{b}(\chi_p) - \underline{b}(\sigma_y)$. Results of these computations may be summarized as follows:

> <u>In near neutral stratification</u>, the power-law exponent on all three diffusion parameters tends to be invariant with distance. The average value of $\underline{b}$ on axial concentration is about 1.8, $\underline{b}$ on σ_y is about 0.8, and $\underline{b}$ on σ_z is thus about 1.0. These values are in substantial agreement with those obtained by Sutton (1) in the Porton experiments.
>
> <u>In unstable thermal stratification</u>, the exponent on axial concentration increases markedly with distance from about 2.0 to values in excess of 3.0 (extreme instability). The exponent on σ_y tends to be invariant with distance (0.8 to 0.9). The exponent on σ_z increases from about 1.0 to values in excess of 2.0 (extreme instability). This behavior of the power-law exponents on axial concentration and on σ_z is not explained by existing diffusion theories which do not permit a value in excess of 2.0 for $\underline{b}(\chi_p)$.
>
> <u>In stable thermal stratification</u>, the exponent on axial concentration tends to decrease with distance from about 1.6 to 1.0 (extreme stability). The exponent on σ_y is probably invariant with distance and is about 0.6. The power-law exponent on σ_z, therefore, must decrease with increasing travel distance from about 1.0 to 0.4. Although there is serious question about the absolute value of these estimates for extremely stable stratification, the results are at least in qualitative agreement with measurements made by Hilst (7) using an elevated source.

The above results indicate that simple power laws adequately explain dispersal from continuous point sources, located near ground level, only in the presence of near-neutral thermal stratification. As the stratification becomes increasingly stable or unstable, simple power laws become increasingly less effective in describing the distance variation in basic plume parameters.

The power-law analysis described above emphasizes the importance of vertical diffusion in determining the rate of decrease in axial concentration with increasing travel distance. The only direct measurements of vertical diffusion made during the Prairie Grass experiments were at a travel distance of 100 m. Estimates of σ_z at other travel distances were obtained by two indirect methods: (1) Results of the regression analysis of observed values of σ_A and σ_z at 100 m were extrapolated to other travel distances under the assumption that the vertical spread of the plume was rectilinear. (2) Values for peak concentrations (adjusted to axial) and σ_y shown in figs. 9, 10, 13, 14 were used to calculate σ_z at all travel distances; the procedure follows from equation (2) on page 18 and involves the assumption that the distributions of concentration along the lateral and vertical coordinates of the plume are approximately Gaussian. There is good agreement at 100 m between the results obtained from the latter method and the estimates derived from the regression analysis of measured values of σ_z. The estimates presented in fig. 15 were derived as follows: At 100 m, the σ_z values were obtained from the regression analysis of actual measurements; the estimates at 50 m were obtained by extrapolation of the results at 100 m, assuming rectilinear vertical spread of the plume. Daytime values for σ_z at travel distances beyond 100 m were calculated from the diffusion equation. Nighttime estimates at similar travel distances were calculated by both methods and the smaller values selected for use in the figure. The results show very clearly the remarkable vertical growth of the plume in the presence of unstable thermal stratification and the suppression of vertical growth during stable thermal stratification.

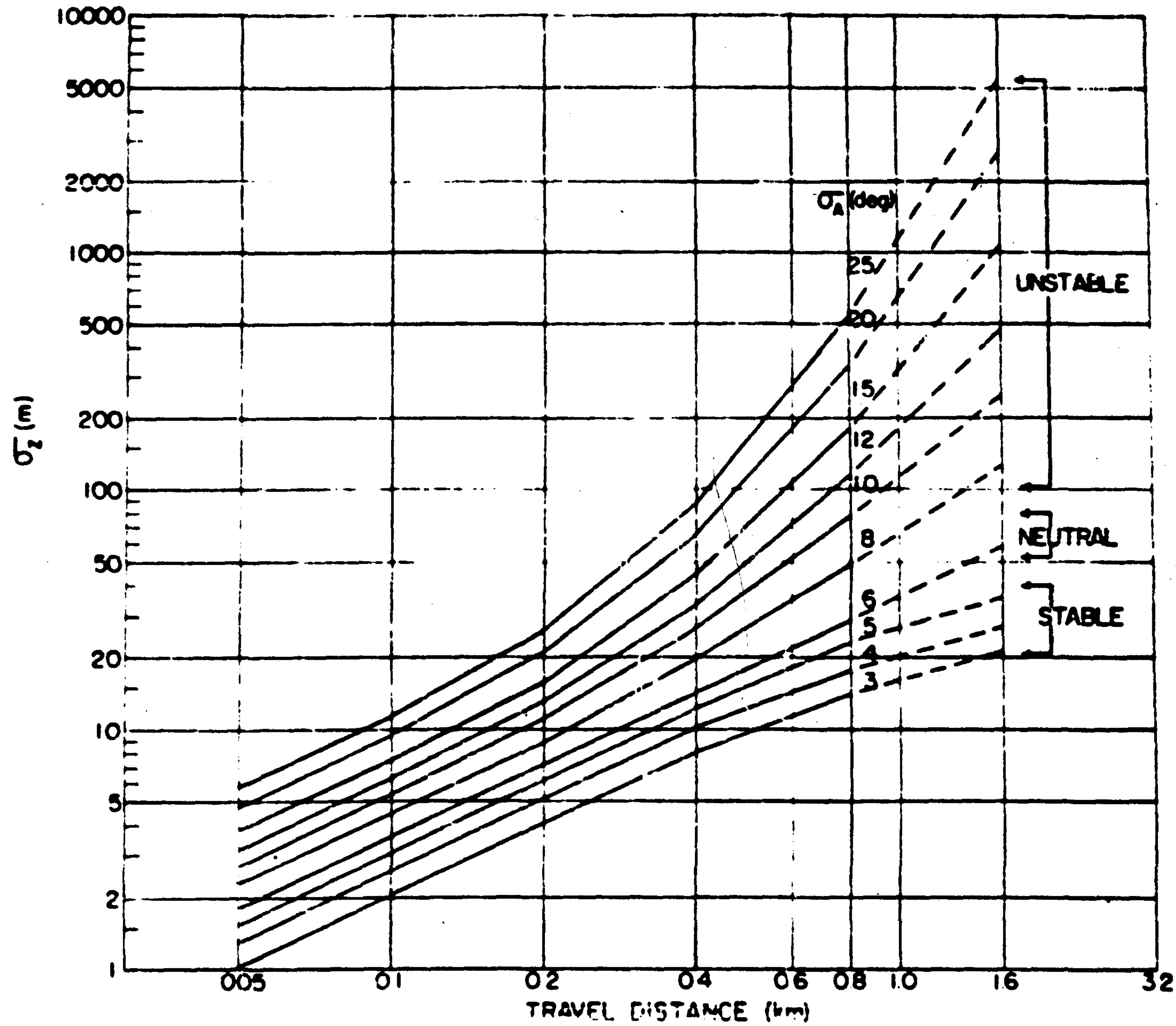

Fig. 15. Estimates of standard deviation of concentration along vertical coordinate; values are expressed in terms of arc distance. Estimates for nighttime values of $\sigma_A > 5$ deg are not shown. Dashed lines are suggested extrapolations.

2. Application of results of data analysis to diffusion theory.

Results of the analysis of the diffusion measurements reported in the previous section support the simple diffusion model shown schematically in fig. 16. The model is referred to a curvilinear coordinate system with the continuous point source at the origin; $\underline{X}$ ($y = 0$, $z = 0$) is along the mean wind; $\underline{y}$ and $\underline{z}$ are directed along arcs in the horizontal and vertical planes, respectively, at distance $\underline{r}$ from the source. The effluent travels downwind and spreads laterally over an arc segment defined by the angle Θ_A which is given by the extremes of the frequency distribution of azimuth wind direction measured at the source. Lateral boundaries of the plume are indicated by the (solid) straight lines in fig. 16a; plume width, defined on the basis of the customary 1/10 limits, is shown by the dashed lines and is assumed equal to $4.3\ \sigma_y$, where σ_y is the standard deviation of concentration in the $\underline{y}$-direction. This relationship is well supported by the O'Neill measurements. The diffusion measurements indicate that the angular plume width decreases with travel distance; near the source, $\sigma_A = \sigma_y$ but at longer travel distance $\sigma_A > \sigma_y$. Vertical spread of the plume is confined within the straight lines defined by the angle Θ_E identified with the extremes of the frequency distribution of elevation angle measured at the source; dashed lines denote the 1/10 limits used to define the vertical extent of the plume. If the vertical spread is rectilinear, $\sigma_E = \sigma_z$ at all travel distances; otherwise; the equality exists only in the immediate vicinity of the source. Experiments

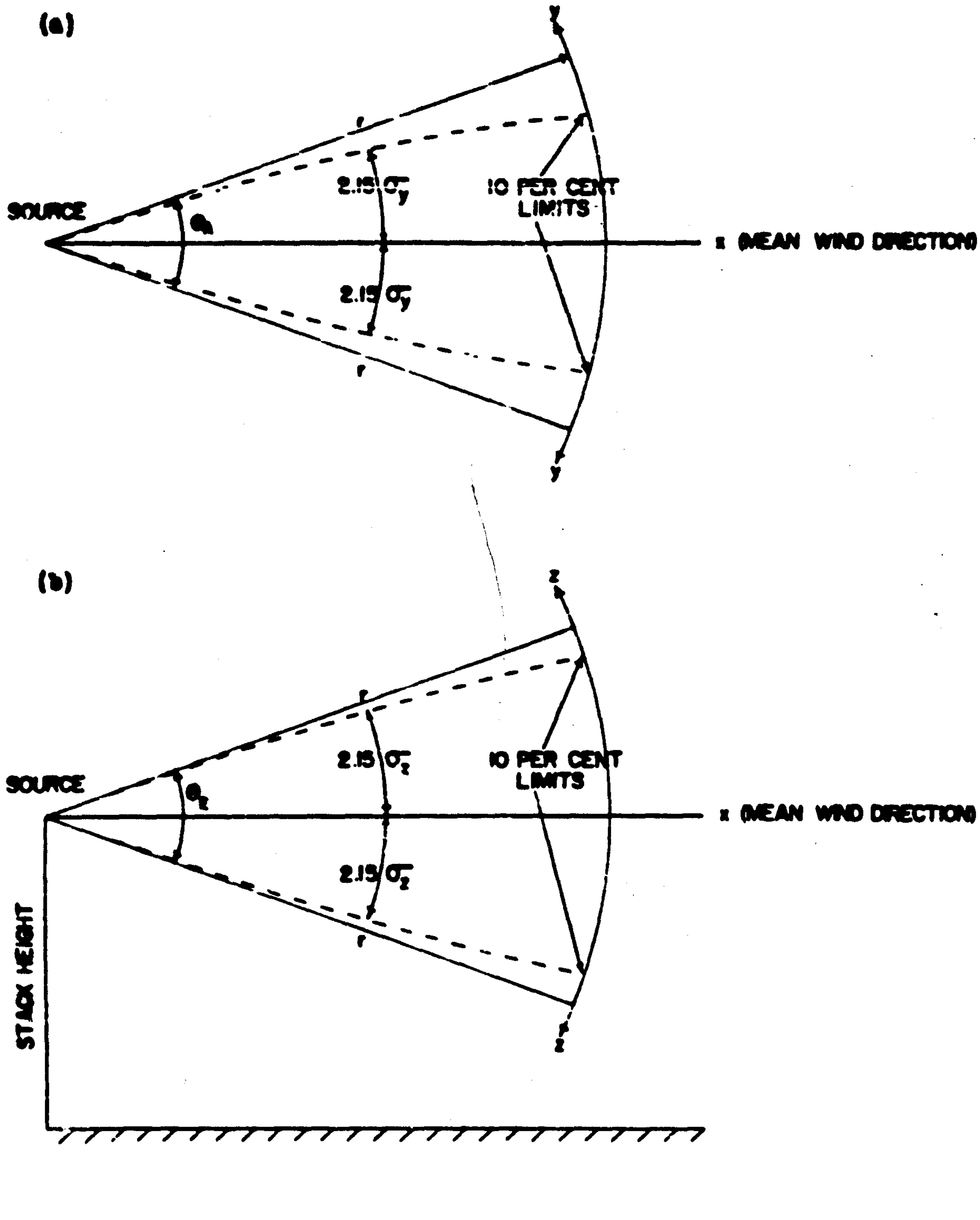

Fig. 16. Simple diffusion model for representing (a) lateral and (b) vertical dispersal of effluents emitted from an elevated source.

in England (15) indicate that the vertical spread is approximately rectilinear for travel distances of the order of 500 m in moderately-stable, near-neutral, and moderately-unstable stratification. The O'Neill experiments, on the other hand, indicate that the vertical spread is rectilinear only in near-neutral stratification: in the presence of thermal instability, the plume expands vertically, the rate of expansion increasing markedly with travel distance for extreme instability; in stable stratification, the O'Neill data indicate a suppression of the vertical growth of the plume, the rate of suppression increasing with travel distance. Measurements based on photographs of smoke plumes in very stable atmosphere indicate negligible vertical growth at travel distances in excess of about 0.5 km (7). It should be pointed out that some differences are to be expected in diffusion patterns from ground-level and elevated sources due to such factors as wind shear, variations in the power spectrum of the vertical velocity component, etc.

If the concentration in mg m^{-3} is given by $\chi_{y,z}$, then at all distances r

$$(1) \quad \int_{-\infty}^{\infty}\int_{-\infty}^{\infty} \chi_{y,z} \; r^2 \; dy \; dz = \frac{Q}{\bar{u}} = \text{const.}$$

where $\underline{Q}$ is the source strength in g sec^{-1}, $\bar{u}$ is the mean wind speed in m sec^{-1}, and $\underline{y}$, $\underline{z}$ are in radians. It can be shown that the differences between the curvilinear coordinate system and a conventional rectangular system are generally negligible. Thus, the limits of integration for equation (1) are effectively $\pm \infty$. Assuming that the effluent is normally distributed along the y- and z- coordinates, it follows from the geometry that

$$(2) \quad \chi_{y,z} = \frac{Q}{2\pi \bar{u} r^2 \sigma_y \sigma_z} \exp\left[-\frac{1}{2}\left\{\frac{y^2}{(\sigma_y)^2} + \frac{z^2}{(\sigma_z)^2}\right\}\right].$$

where σ_y, σ_z, y, z are expressed in radians. For rectilinear spread:

$$\sigma_A = \sigma_y ; \quad \sigma_E = \sigma_z ;$$

and, equation (2) becomes

$$(3) \quad \chi_{y,z} = \frac{Q}{2\pi \bar{u} r^2 \sigma_A \sigma_E} \exp\left[-\frac{1}{2}\left\{\frac{y^2}{(\sigma_A)^2} + \frac{z^2}{(\sigma_E)^2}\right\}\right].$$

If the spread of the plume along the lateral and vertical coordinates is not rectilinear but follows simple power laws of the form

$$r\,\sigma_y \propto (r)^q, \quad r\,\sigma_z \propto (r)^p \quad ;$$

then,

$$r\,\sigma_y = \sigma_A (r)^q ; \quad r\,\sigma_z = \sigma_E (r)^p \quad .$$

when the above relationships are substituted in equation (2), we obtain

$$(4) \quad \chi_{y,z} = \frac{Q}{2\pi \bar{u} r^b \sigma_A \sigma_E} \exp\left[-\frac{1}{2}\left\{\frac{y^2}{(\sigma_A)^2 r^{2q-2}} + \frac{z^2}{(\sigma_E)^2 r^{2p-2}}\right\}\right],$$

where $b = p + q$.

If σ_y, σ_z vary with distance in a more complex manner, equation (2) may be evaluated at selected values of r for which estimates of σ_y, σ_z are available.

The above diffusion equations are of the same general form as those of Sutton (1) and differ principally in the use of direct meteorological indicators (σ_E , σ_A) in place of generalized diffusion coefficients derived from the vertical profile of mean wind speed; and, in the greater freedom of variation in the exponent on distance r. Following Sutton's argument of reflection, the source strength Q in equations (2), (3), (4) is doubled for a source located at ground level or in the case of a plume from an elevated source that reaches the ground.

The equations have been tested against the O'Neill measurements of peak concentration at 100 m (see figs. 9, 10). Axial ground-level concentrations were calculated on the basis of equation (2) using values of σ_y (figs. 13, 14) and of σ_z (fig. 15) at 100 m obtained from regression analysis. The calculated axial concentrations agree closely with the measured values in near-neutral stratification. For unstable thermal stratification, the calculated values are from 10 to 25 per cent lower than the measurements; this is hardly surprising in view of uncertainties in the estimates of σ_z for extreme instability and probable deviations from normal distributions. In moderately stable stratification, calculated axial concentrations are approximately equal to the (adjusted) measured values; for extreme stability, the calculated axial concentrations are about twice as large as the measured (peak) values. This does not appear unreasonable in view of the height of the sampling network (1.5 m).

Expressions for ground-level concentration profiles associated with the operation of the model shown in fig. 16 are derived on the basis of equation (4) which describes distance variations in the diffusion parameters σ_y, σ_z in terms of simple power laws. At a given distance x from the base of the stack, the angle θ_E is approximately given by

$$(5) \qquad \theta_E = \frac{h}{x} = N \sigma_z \quad ,$$

where h is the height of the stack and N is a positive number. It follows that[1]

$$(6) \qquad N = \frac{h}{\sigma_z x} = \frac{h}{\sigma_E r^p} \quad .$$

The ratio between ground-level concentration χ_g at $x = r$ and χ_a is, allowing for reflection,

$$(7) \qquad \frac{\chi_g}{\chi_a} = 2 \exp \left[- \frac{h^2}{2(\sigma_E)^2 r^{2p}} \right] \quad .$$

Thus, the ground level concentration is given by

$$(8) \qquad \chi_g = \frac{Q}{\pi \bar{u} \; r^b \sigma_A \sigma_E} \exp \left[- \frac{h^2}{2(\sigma_E)^2 \; r^{2p}} \right] \quad .$$

If the above equation is maximised, we obtain the following expression for the distance from the base of the stack x_m at which the maximum ground-level will be found:

---

[1]In the following discussion, it is assumed that $x = r$.

$$x_m = \left[\frac{h^2 \, p}{(\sigma_E)^2 \; b} \right]^{\frac{1}{2p}} \tag{9}$$

For near-neutral stratification ($b \approx 1.80$; $p = 1.0$), the estimate for x_m reduces to

$$x_m = \frac{h}{1.35 \, \sigma_E} \quad . \tag{10}$$

The general expression for maximum ground-level concentration $\chi_{g\,(max)}$ obtained by combining equations (9), (10) is

$$\chi_{g\,(max)} = \frac{Q \left(\frac{b}{p}\right)^{b/2p} (\sigma_E)^{b/p - 1}}{\pi \bar{u} \;\; h^{b/p} \;\; \sigma_A} \exp\left[- \frac{b}{2p} \right] . \tag{11}$$

For $b = 2.0$, $p = 1.0$ this reduces to

$$\chi_{g\,(max)} = \frac{2Q \quad \sigma_E}{e \pi \bar{u} \, h^2 \quad \sigma_A} \quad . \tag{12}$$

Sutton's (13) expressions for x_m and $\chi_{g\,(max)}$ are practically identical in form with equations (10), (12):

$$\chi_{g(max)} = \frac{2Q}{e \pi \bar{u} \, h^2} \left(\frac{C_z}{C_y} \right) ;$$

$$x_m = \left(\frac{h^2}{C_z^{\,2}} \right)^{\frac{1}{2-n}} \approx \frac{h}{C_z} \; .$$

3. Quantitative estimates of dispersal from an elevated source.

The diffusion equations of the previous section provide quantitative estimates of dispersal when appropriate values for the various meteorological and diffusion parameters are inserted. Estimates of σ_A, σ_E are found in table 1 and estimates for the other diffusion parameters are given above. It should be emphasized that the diffusion data are based on measurements extending only to a distance of 800 m from the source. Extrapolation of the results to appreciably longer travel distances appears safe in near-neutral stratification. In the presence of moderate thermal stability or instability, extrapolation is less certain; for extreme stability or instability, the uncertainty is greatly increased. In other words, the suggested technique provides fairly reliable quantitative dispersal estimates for travel distances of the order of 1 km except in the presence of near-neutral stratification when extrapolation to appreciably longer distances seems justified. As noted previously, one aspect of plume structure has not been definitely established empirically - the question of whether the vertical spread of the plume is rectilinear for a wide range of thermal stratification (15); or whether, as indicated by the O'Neill estimates, the spread is rectilinear only in near-neutral stratification. In view of this uncertainty, it seems advisable to consider both possibilities in making dispersal estimates.

Profiles of axial ground-level concentration for three stability stratifications are presented in fig. 17; a stack height of 100 m is assumed and concentrations are adjusted to a standard source strength of 100 g sec^{-1}

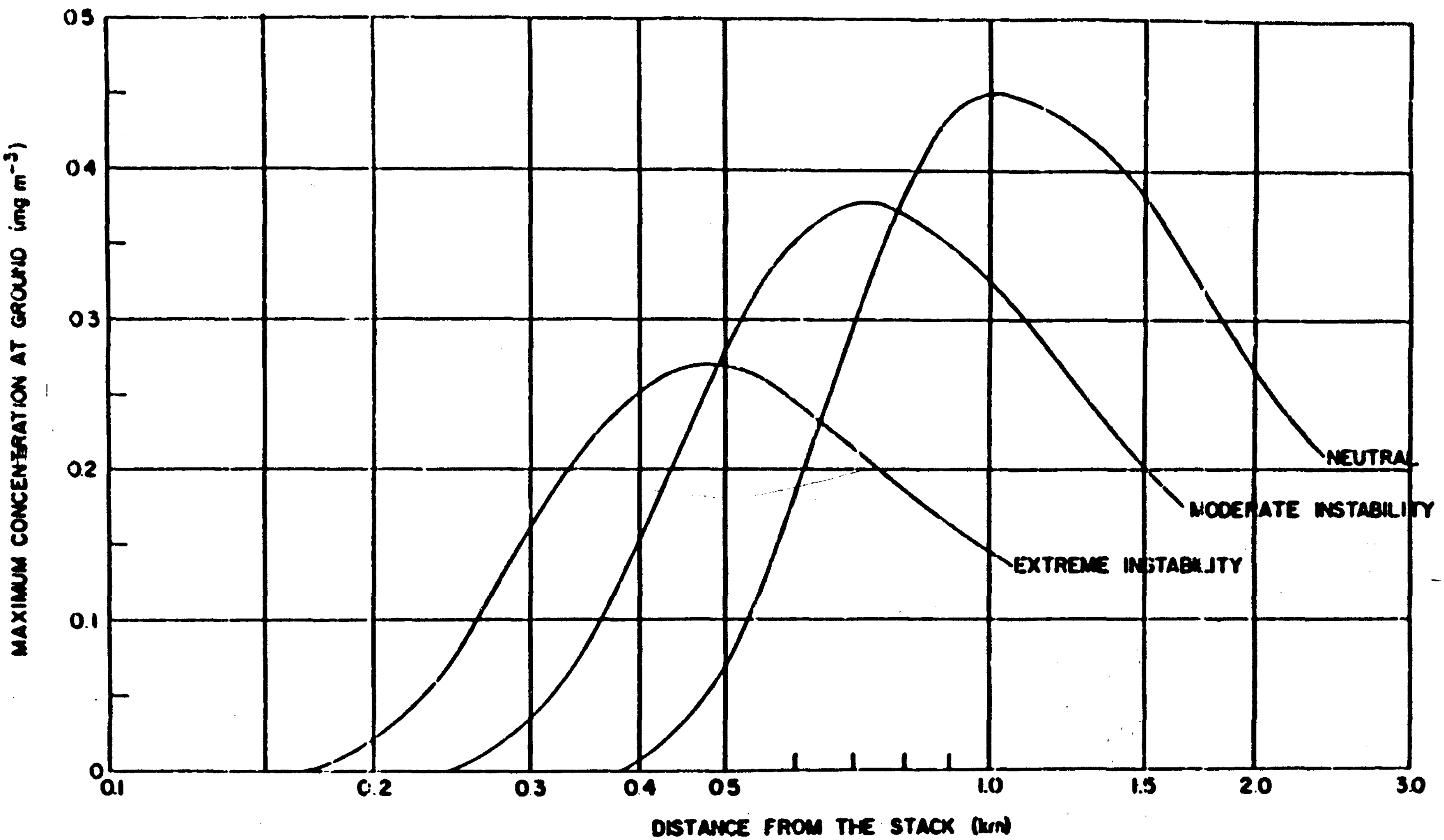

Fig. 17. Profiles of axial ground-level concentration for stack height of 100 m for three stability stratifications.

and a mean wind speed of 5 m sec^{-1}. Axial concentrations for the elevated-source plume were calculated from the σ_y values in fig. 13, assuming rectilinear vertical spread (p = 1.0). Values assumed for σ_A, σ_E (deg) are: neutral (σ_A = 7; σ_E = 4); moderate instability (σ_A = 12; σ_E = 6); extreme instability (σ_A = 25; σ_E = 9). The ~~maximum~~ concentrations in the figure may be compared with Sutton's value of 0.46 mg m^{-3} which is invariant with thermal stratification. The results show that, as might be expected, the point of maximum concentration moves closer to the stack as the instability increases. Sutton's estimates for $\underline{x}_m$ are considerably larger than those in the figure. This may be partly explained by the fact that the values selected for σ_E apply generally to a rough site.

The data presented in the preceding section of the paper clearly indicate that there are a variety of assumptions that may be made in obtaining quantitative dispersal estimates within the framework of the above diffusion model. The results in table 3 are intended to show the probable extreme range of estimates for maximum ground-level concentrations that might be expected for various stability stratifications. It has been assumed that the plume does not reach the ground in the presence of stable thermal stratification. Axial concentrations for the elevated-source plume were obtained by calculating initial concentrations at $\underline{r}$ = 100 m from σ_y in figs. 13, 14 and from σ_z based on rectilinear vertical spread from the source to 100 m. These initial estimates were then decreased with distance according to the tabulated values of $\underline{b}$. Entries for $\underline{X}$ and χ_g not enclosed by parenthesis refer to rectilinear vertical spread ($\underline{p}$ = 1.0); entries enclosed by parenthesis refer to vertical spread governed by the power-law exponent $\underline{p}$.

These computations show that in near-neutral stratification, the maximum axial ground-level concentration occurs within a distance of 1.5 km from the stack; in unstable thermal stratification, x_m is generally less than 1 km. This means that the O'Neil concentration measurements constitute a reliable basis for estimating maximum ground-level concentrations; the data in figs. 9, 10 are merely multiplied by the factor $e^{-\frac{b}{2p}} \approx 0.4$ at the appropriate distance given by equation (9). Estimates for χ_g in table 3 scatter about Sutton's value of 0.46 mg m^{-3}, and it appears that the latter may safely be used as a first approximation to maximum ground-level concentration in all stability classifications (for $\underline{h}$ = 100 m).

According to equation (11), the variation of maximum ground-level concentration with stack height, is given by the expression

$$\chi_{g(max)} \propto \frac{1}{h^{b/p}} .$$

In general, therefore, the variation follows the usual inverse-square law. However, in stable thermal stratification, the variation with height is somewhat less than that indicated by the inverse-square law; in unstable thermal stratification, the height variation is somewhat greater.

Table 2. Maximum ground-level concentrations for effective stack height of 100 m. Concentrations are adjusted to standard source strength of 100 g sec^{-1} and mean wind speed of 5 m sec^{-1}. Estimates enclosed by parentheses ( ) refer to computations using values of p ≠ 1.0.

Stability stratification	σ_A(deg)	σ_E(deg)	b	p	x_m(km)		χ_g(mg m^{-3})	
	6	3.0	1.70	1.0	1.46	-----	0.6	-----
Near neutral	10	4.0	1.85	1.0	1.05	-----	0.3	-----
	14	5.0	2.00	1.0	0.81	-----	0.2	-----
	10	4.0	2.00	1.0	1.01	-----	0.2	(0.2)
Moderately unstable	15	5.5	2.15	1.1	0.71	(0.42)	0.2	(1.3)
	20	7.0	2.30	1.2	0.54	(0.21)	0.1	(0.6)
	20	7.0	2.20	1.2	0.54	(0.21)	0.1	(1.2)
Extremely unstable	25	8.5	2.20	1.2	0.46	(0.18)	0.1	(1.0)
	30	10.0	2.20	1.2	0.39	(0.16)	0.1	(1.0)

III. MEASUREMENTS OF THE STRUCTURE OF TURBULENCE AT O'NEILL, NEBRASKA

A. Description of fast-response meteorological instrumentation

Instrumentation for investigating characteristic features of the structure of turbulence has been under continuous development for many years at the Round Hill Field Station in connection with empirical studies of diffusion and atmospheric turbulence. The fast-response instruments used during Project Prairie Grass comprised five lightweight bivanes and heated-thermocouple anemometers. Prototypes of these instruments have been described previously (8; 9; 10; 17). A photograph of one of the field assemblies used during the Prairie Grass experiments is shown in fig. 18. The vane is constructed of optical lens cleaning tissue cemented to a fine wire framework; the total surface area is about 300 cm^2 and the weight of the entire tail assembly, including the thin-wall aluminum alloy shaft, is 2 g. Movements of the vane in both the plane of the horizon and vertically are transmitted to two Giannini microtorque potentiometers mounted in the base of the instrument; the azimuth shaft of the bivane is coupled to one of the potentiometers by a pair of 1:1 precision aluminum gears. Vertical movements of the vane are transmitted by means of a fine metal chain that passes over two identical aluminum pulleys (located at the top and bottom of the vertical shaft); the second potentiometer is connected to the shaft of the lower pulley by a flexible coupling. The bivane is supported on three legs, one of which is 180 deg from the electrical zero of the azimuth potentiometer and serves as a reference for orienting the bivane with respect to the mean wind direction.

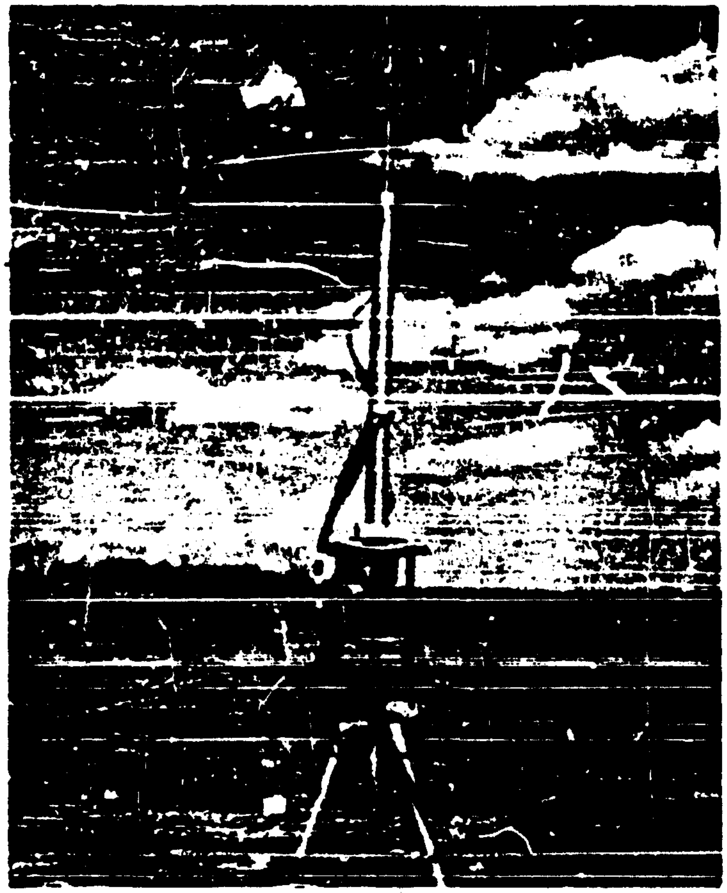

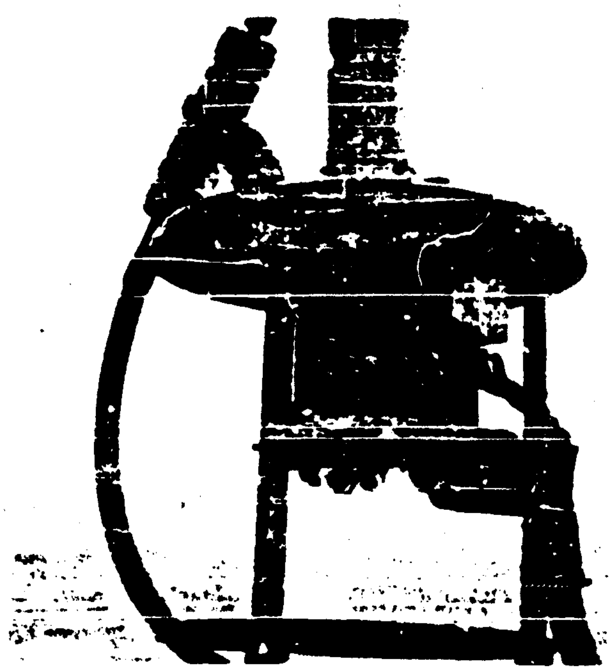

Fig. 18. Photograph of bivane and heated-thermocouple anemometer mounted on tripod (above), and (below) closeup of the base of the bivane showing micro-torque potentiometers and other components.

III. MEASUREMENTS OF THE STRUCTURE OF TURBULENCE AT O'NEILL, NEBRASKA

A. Description of fast-response meteorological instrumentation

Instrumentation for investigating characteristic features of the structure of turbulence has been under continuous development for many years at the Round Hill Field Station in connection with empirical studies of diffusion and atmospheric turbulence. The fast-response instruments used during Project Prairie Grass comprised five lightweight bivanes and heated-thermocouple anemometers. Prototypes of these instruments have been described previously (8; 9; 10; 17). A photograph of one of the field assemblies used during the Prairie Grass experiments is shown in fig. 18. The vane is constructed of optical lens cleaning tissue cemented to a fine wire framework; the total surface area is about 300 cm^2 and the weight of the entire tail assembly, including the thin-wall aluminum alloy shaft, is 2 g. Movements of the vane in both the plane of the horizon and vertically are transmitted to two Giannini microtorque potentiometers mounted in the base of the instrument; the azimuth shaft of the bivane is coupled to one of the potentiometers by a pair of 1:1 precision aluminum gears. Vertical movements of the vane are transmitted by means of a fine metal chain that passes over two identical aluminum pulleys (located at the top and bottom of the vertical shaft); the second potentiometer is connected to the shaft of the lower pulley by a flexible coupling. The bivane is supported on three legs, one of which is 180 deg from the electrical zero of the azimuth potentiometer and serves as a reference for orienting the bivane with respect to the mean wind direction.

Sensing elements of the heated-thermocouple anemometers comprise thermojunctions made from chromel-P and constantan wires measuring 0.005 cm in diameter; the wires are butt-welded by a spark-discharge technique in the field of a low power binocular microscope. This technique facilitates production of junctions of uniform physical dimensions, a condition requisite for the use of a single calibration curve for several probes. The thermojunctions are incorporated in an electrical circuit first developed by Hastings (18; 19). The probe consists of four copper studs, arranged in a t-shaped pattern, that support the thermocouple wires; two junctions are heated to a temperature of about 300 C by a constant-current a.c. power supply; the third junction is unheated and assumes ambient air temperature. Passage of air over the heated junctions produces a cooling that results in a reduced thermal e.m.f.; fluctuations in ambient air temperature are compensated by the output of the unheated junction which opposes that of the other two. Satisfactory operation of the probes depends on the maintenance of a closely-controlled (constant) heater current. In preparation for the Prairie Grass observations, the r.f. thermocouple meters previously used to monitor the current to individual probes were replaced by a single Weston a.c. milliammeter (Model 433) which has a frequency range of 25 to 500 cycles sec^{-1} and an accuracy of about 0.75 per cent. This meter and an equivalent inductance are switched from one heated-thermocouple power supply to another to determine the proper current settings. When the meter is switched out of a probe circuit, it is replaced by an equivalent d.c. resistance. This procedure eliminates the necessity for considering the characteristics of individual monitor meters in determining the proper heater currents. As an additional precaution, a Sorensen voltage regulator (Type 100 A), capable of maintaining the line voltage within 0.5 per cent, was placed in the primary of the heater-current supply circuit. As shown in fig. 18, the probes are mounted on the azimuth shafts of the bivanes so that they will be headed into the wind by the action of the vane. The response of the probes is essentially nondirectional since the heated thermojunctions are oriented parallel to the plane of the horizon and are thus insensitive to the angle of attack of the wind vector. The response in the azimuth plane varies as the cosine of the angle between the horizontal wind vector and the heading of the azimuth vane; this is normally a small angle.

The calibration curve for the heated-thermocouple anemometers used in the Prairie Grass experiments is presented in fig. 19. The curve is a composite based on the results of a series of calibrations in the Project wind tunnel at O'Neill, Nebraska prior to the start of the field program. Scatter of points about the composite curve varies from an average deviation of about 10 per cent, at both extremes of the wind-speed range, to about 5 per cent within the 3 to 10 m sec^{-1} interval; this is in part due to uncertainties in determining wind-tunnel air speeds, particularly at low draft velocities. The absolute calibration of the heated-thermocouple probes is sensitive to large differences in ambient air temperature; the O'Neill calibration curve is significantly displaced from that obtained at Round Hill which refers to an ambient air temperature of about 18 C (as contrasted with a value of about 30 C for O'Neill). Numerous other factors, such as dust collected on the thermojunctions, uncertainties in the recording apparatus,

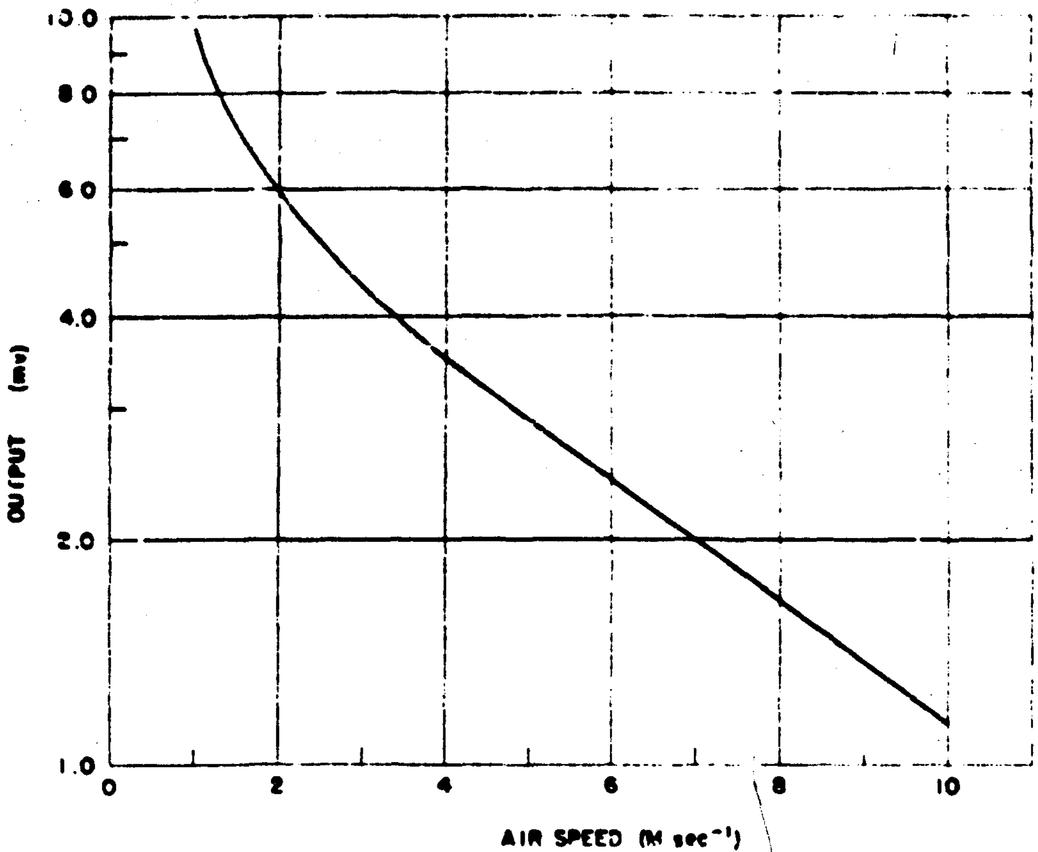

Fig. 19. Calibration curve for heated-thermocouple anemometer. Measurements obtained during Project Prairie Grass.

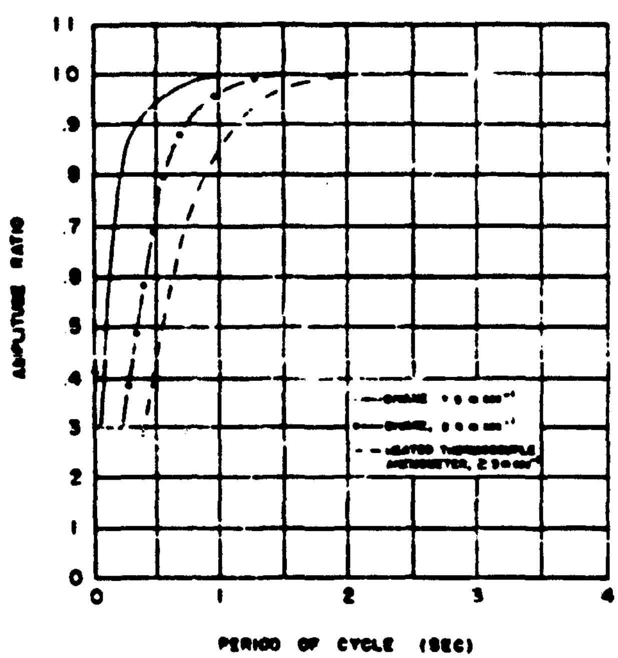

Fig. 20. Response of bivane and heated-thermocouple anemometer to simple sine waves of varying frequency.

etc., also contribute to errors in absolute calibration. In practice, therefore, absolute values of the wind speed measured by individual probes are frequently not representative. In statistical tests to determine the homogeneity of the data, for example, absolute values should be normalized with respect to the (measured) mean wind speed. As shown in fig. 19, there is a contraction of the calibration curve at high wind speeds which makes it difficult to resolve wind speeds in excess of 11 m sec^{-1}; expansion of the high wind-speed section of the calibration curve has so far been achieved only at the expense of eliminating important low wind-speed ranges.

Response characteristics of the bivanes and heated-thermocouple anemometers are shown in fig. 20. Due to the nature of the sensing elements, the response of the bivane is a function of the wind speed, particularly for speeds below 5 m sec^{-1}. The limiting factor in the speed of response of the bivane, except for very low wind speeds, is in the recording system. Critical damping of the azimuth and elevation motion of the vane is achieved by use of appropriate electrical resistances in series with the recorders. The response of the recorders to fluctuations in azimuth and elevation angle is speeded up by means of r-c networks. Since data from the bivanes and heated-thermocouple anemometers are combined to determine the vector wind components, it is important that the characteristic times of both instruments be closely matched. The curves in fig. 20 indicate that this condition is satisfied for wind speeds in excess of about 3 m sec^{-1}, and that both instruments faithfully resolve fluctuations with frequencies less than 1 to 0.5 cycles sec^{-1}.

Preparations for the Prairie Grass experiments involved the relocation of the recording equipment and auxilliary apparatus for the fast-response instrumentation in the interior of the International truck shown in fig. 21a. Power supplies for both the bivanes and heated-thermocouple anemometers were rebuilt and provision made for handling information from six instrument assemblies. Data from the sensing elements are relayed to the junction box, located on the lower left side of the truck (see fig. 21b), by insulated cables. The interior of the truck is fitted with six standard relay racks. The racks on the left side contain the power supplies for the heated-thermocouple anemometers and bivanes, Weston inductronic amplifiers for the anemometers, voltage regulator, heater-current monitor, and a master timer for automatic sequence operation of all the equipment (see fig. 21c). The racks on the right side of the truck contain eight Esterline-Angus dual recorders (0 to 1 ma), switches, and other auxilliary apparatus for the operation of the recorders (see fig. 21d). A tie point between the amplifiers, power supplies, and recorders is provided by a row of terminal strips in the interior of a 6-ft section of square duct mounted behind the relay racks. All of the wiring from the recorders to the amplifiers and power supplies is enclosed in water-tight, flexible tubing that passes through the walls and beneath the truck floor. A 200-watt, 400-cycle generator, driven by an 0.5 hp electric motor, is mounted on the lower right side of the truck; this a.c. source may be used for the anemometer heater circuits. Illumination in the truck interior is provided by two 40-watt fluorescent lamps mounted on the truck walls behind the relay racks.

(a)

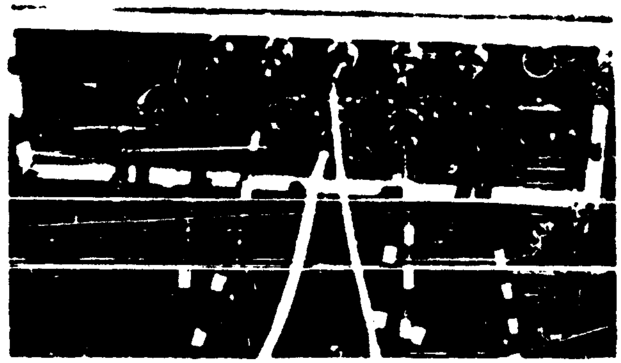

(b)

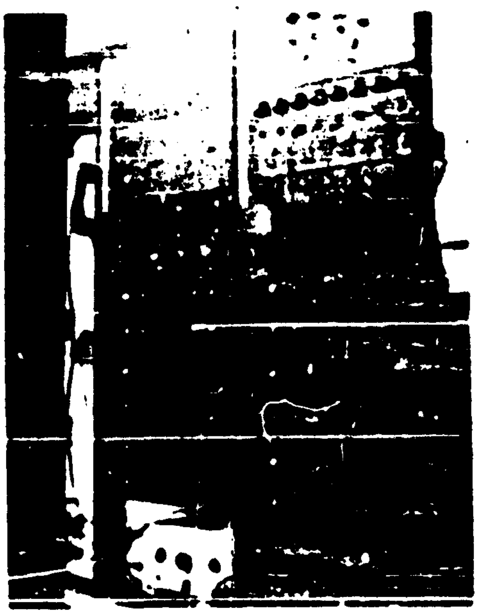

(c)

(d)

Fig. 21. Photographs of various components of fast-response meteorological instrumentation system used during Project Prairie Grass: (a) Instrument truck; (b) connector box mounted on truck for bivane and heated-thermocouple anemometer cables; (c) amplifiers and power supplies for fast-response instrumentation and (d) high-speed recorders mounted in truck interior.

B. Experimental procedures and data abstraction

Investigations of the structure of atmospheric turbulence are principally based on selective analyses of the mean square amplitudes (power spectra) and characteristic lengths (scales) of fluctuations in wind velocity. Due to the broad spectrum of eddy sizes normally present in atmospheric flow, techniques that have been successfully applied in wind-tunnel studies of turbulence (20) are only of very limited use. Within the past decade, precise methods have been developed by Tukey (21) and others for the spectral and cospectral analysis of turbulent fluctuations of the type found in the lower atmosphere. These techniques utilize Fourier transforms of autocorrelation and cross-correlation functions obtained from stationary or quasi-stationary time series. Numerous investigators have determined power spectra of the wind velocity or of its components (11; 22; 23; 24; and others); however, except for preliminary studies at Round Hill (8; 25), practically no measurements of the Eulerian scales of atmospheric turbulence are available.

The Prairie Grass experiments were designed to provide information on the Eulerian scales of turbulence of the orthogonal components of the wind velocity within the frequency band extending from about 0.5 to 0.01 cycles sec^{-1}. Five bivanes equipped with heated-thermocouple anemometers were arranged either parallel or normal to the prevailing wind direction as shown in fig. 22; the sensing elements were at a height of 2 m. Precise orientation of the azimuth scales of the bivanes with respect to the axes of the arrays was accomplished in the following manner: A small transit was mounted on the tripods used to support the bivanes and the tripod head

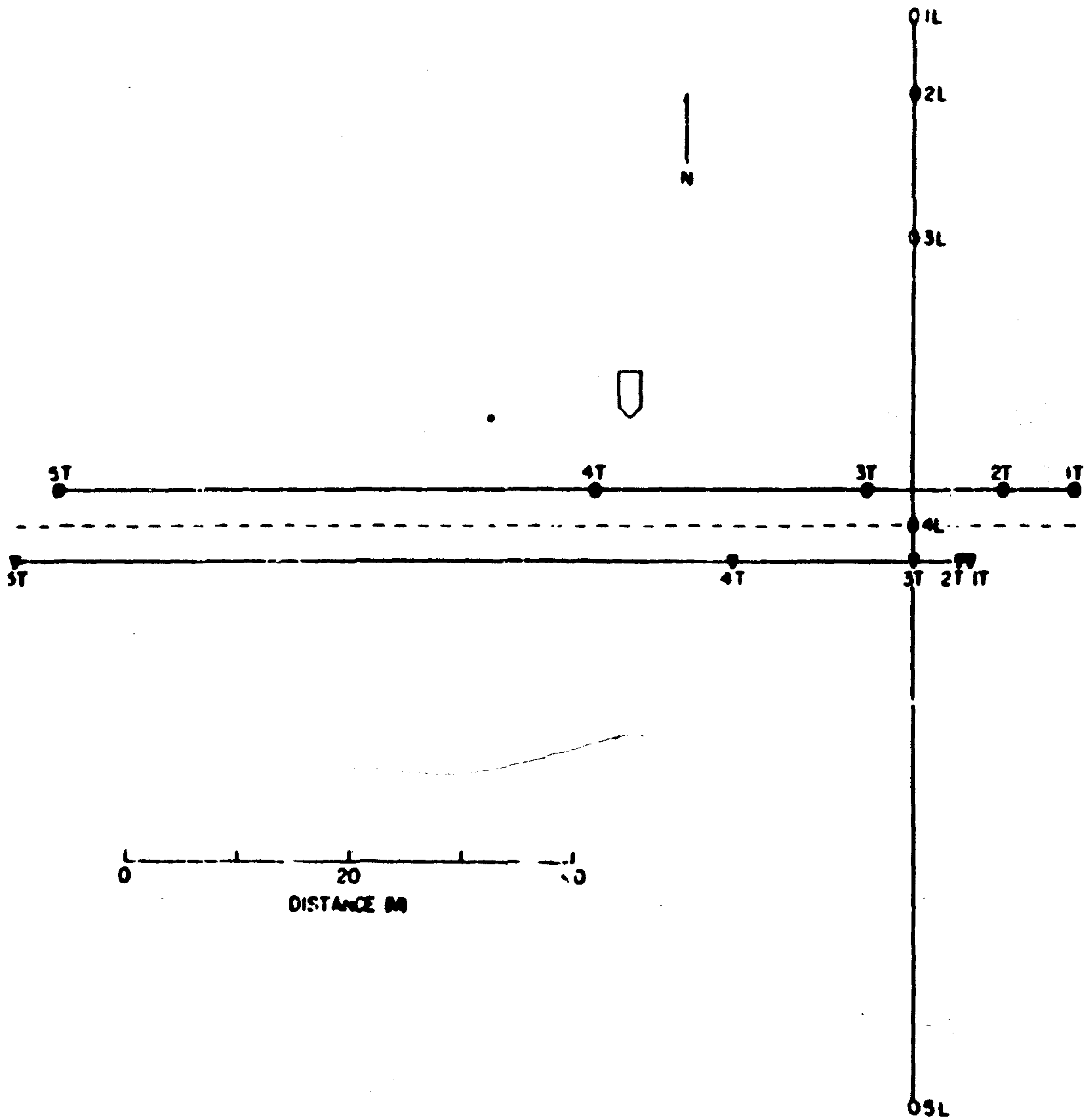

Fig. 22. Schematic diagram showing longitudinal and transverse spacings of fast-response instrumentation during Project Prairie Grass experiments. Dashed line denotes actual location of transverse array.

rotated until the position of the reference leg of the bivane, mentioned previously, was exactly (± 0.3 deg) in line with the axis of the array. To facilitate rapid changes from transverse to longitudinal orientation, two sets of tripods and two complete sets of insulated electrical cables were utilized; the tripods were left permanently in position (except for changes in transverse separation distances) and only the bivanes needed to be moved. Due to the length of time required to prepare for an experiment (1 to 2 hr), there did not appear to be any satisfactory alternative method for improving the orientation of the bivanes with respect to the mean wind direction actually observed during the experiments; experience demonstrated that forecasts of the wind direction were not sufficiently accurate to justify the additional effort required.

Data were obtained for approximately 60 experiments in which the 20-min sampling period was centered on the mid-point of the gas release for the diffusion measurments (see p. 8). The experiments are approximately equally divided between longitudinal and transverse orientations. Separation distances of 6, 12, 24, and 48 m (see fig. 22) were used for all longitudinal orientations and for about half the transverse orientations; the remaining transverse experiments utilized separations of 1, 4, 16, and 64 m. The observations comprise chart records (continuous pen traces) of fluctuations in azimuth angle, elevation angle, and total wind speed at each instrument position. Data were abstracted from the original chart records at intervals of 1.067 sec and entered on IBM punch cards at Iowa State College under the direction of Professor R. M. Stewart, Jr.; this was accomplished by means of automatic equipment that included a photoelectric scanning device for reading the chart records. Detailed descriptions of the data abstraction techniques and the apparatus will soon be available in a Scientific Report issued by Iowa State College.

C. Brief description of data processing techniques

Before spectral analyses may be performed, the raw data must first be converted into velocity components by means of a trigonometric program. The various steps involved in this program are outlined below. The following information is available on punch cards for each instrument position for each experiment: Azimuth angle (deg) A_i; Elevation angle (deg) E_i; Wind speed (m sec^{-1}) V_i. There are approximately 1130 consecutive values of each of the above quantities (N=1130) in view of the total length of record (20 min) and the time interval (1.067 sec) between individual samples. By definition, the algebraic summations of the individual velocity components taken over the complete sampling period are set equal to zero. The virtual mean azimuth A^* and elevation E^* angles required to satisfy this condition may be written in the form

$$A^* = \tan^{-1} \frac{\sum_{i=1}^{N} V_i \cos(E_i - E^*) \sin A_i}{\sum_{i=1}^{N} V_i \cos(E_i - E^*) \cos A_i} ;$$

and,

$$E^* = \tan^{-1} \frac{\sum_{i=1}^{N} V_i \sin E_i}{\sum_{i=1}^{N} V_i \cos E_i} .$$

The expressions for the component velocities referred to a Cartesian coordinate system with the $\underline{x}$-axis in the direction of the mean wind then become

$$u_i = U_i - \overline{U} \quad ;$$
$$v_i = V_i \cos (E_i - E^*) \sin (A_i - A^*);$$
$$w_i = V_i \sin (E_i - E^*);$$

where

$$\overline{U} = \frac{1}{N} \sum_{i=1}^{N} U_i \quad ; \qquad U_i = V_i \cos (E_i - E^*) \cos (A_i - A^*) \quad ;$$

and

$$\overline{u}, \ \overline{v}, \ \overline{w} = 0 \quad .$$

The spectral analysis program utilizes the auto-correlation function

$$R_p = \frac{1}{N-p} \sum_{i=1}^{N-p} x_i \quad x_{i+p} \qquad (0 \leq p \leq 60) \quad ;$$

where x_i ($1 \leq i \leq N$) is one set of u_i , v_i , or w_i to obtain smoothed spectral densities UN_k ($1 \leq k \leq 59$) for each velocity component at each sampling station. Cospectral analysis utilizes the covariance functions

$$S_p^+ = \frac{1}{N-p} \sum_{i=1}^{N-p} x_i \quad y_{i+p} \qquad (0 \leq p \leq 60) \quad ;$$

$$S_p^- = \frac{1}{N-p} \sum_{i=1}^{N-p} x_{i+p} \, y_i \qquad (0 \leq p \leq 60) \quad ;$$

where y_i $(1 \leq i \leq N)$ is another set of the same velocity component represented by x_i for another instrument position during the same experiment. From these functions, smoothed cospectral estimates UCN_k $(1 \leq k \leq 59)$ and smoothed quadrature spectral estimates UQN_k $(1 \leq k \leq 59)$ are obtained for each velocity component at 10 separation distances in each experiment.

According to Tukey (21), the UN_k , UCN_k , UQN_k estimates are averages for frequency bands centered at

$$f_c = \frac{\pi k}{\Delta t m} ;$$

the frequency limits for each band are given by

$$f_l = \frac{\pi (k \pm \frac{1}{2})}{\Delta t m} .$$

In the present case, $\Delta t = 1.067$ sec and m, the number of lags, is 60. The estimates therefore refer to a gross frequency range extending from about 0.5 to 0.008 cycles sec^{-1}.

The programming of the punch cards for high-speed computations of velocity components, spectral and cospectral analysis was performed by the General Electric Company in Lynn, Mass. under the supervision of Lt. R. P. Ely and Mr. D. A. Haugen of the Air Force Cambridge Research Center. Detailed descriptions of the procedures are available in a Geophysical Research paper.[1] The actual computations were carried out on the General Electric IBM 704 machine.

---

[1]Panofsky and Deland (23) also present a detailed discussion of the computational procedures for determining spectra and cospectra.

D. Results of preliminary scale analysis

The Eulerian scales of turbulence are usually defined in terms of the correlation coefficient R(s) between fluctuations at two points separated by a distance s. The average eddy diameter or scale L is given by the integral

$$L = \int_0^\infty R(s)\, ds \quad .$$

In practice, the upper limit of the integral is given by the separation distance at which the spatial correlation function becomes insignificant. In studying the scales of turbulence associated with a broad spectrum of eddy sizes, it is necessary to filter the data so that correlation functions may be determined for relatively narrow frequency bands; otherwise, the results will primarily reflect the influence of the longest period fluctuations present in the sample. Two quantities are derived from the autocovariance and covariance functions defined above that are analagous to the squares of linear correlation coefficients between two time series but are, also, functions of frequency k. The coherence (COH) is given by

$$COH_k = \left[(R_{COH})_k\right]^2 = (UCN_k)^2 + (UQN_k)^2 \;/\; (UN_{k,1}\;\; UN_{k,2}) \qquad (1 \le k \le 59);$$

where the subscripts 1, 2 refer to instrument positions. Inclusion of the quadrature term (UQN) permits consideration of fluctuations that are 90 deg out of phase; if these fluctuations are neglected, or are insignificant, the expression simplifies to

$$COH_k = \left[(R_{COS})_k\right]^2 = (UCN_k)^2 \;/\; (UN_{k,1}\;\; UN_{k,2}) \qquad (1 \le k \le 59).$$

Sample plots of the correlation coefficients R_{COH}, R_{COS} as functions of frequency are presented in fig. 23; data refer to fluctuations in the v-component of wind velocity at two separation distances during a daytime experiment. By definition, R_{COH} is always positive and can never be less in absolute magnitude than R_{COS}. Although R_{COS} is also, by definition, positive it has been given the sign of the covariance term UCN according to the usual convention. There are no accepted statistical tests for the significance of cospectral estimates. An approximate value for the significance level of the correlation coefficients shown in the above figure may be obtained by considering the confidence limits for linear correlation coefficients (95 per cent level), using the number of degrees of freedom established for the spectral estimates UN_k. According to Tukey (21), the number of degrees of freedom $\underline{f}$ for individual estimates of UN_k is given by

$$f = \frac{N - \frac{1}{4} m}{\frac{1}{2} m} \approx 40.$$

This indicates a significance level of about 0.30 for the R_{COH}, R_{COS}. It appears from the curves shown in fig. 23 that there is no appreciable difference in the behavior of the two correlation functions so far as scale computations are concerned; the inclusion of the quadrature estimates essentially results in random fluctuations that are statistically insignificant. The results of numerous scale computations utilizing both correlation functions support this conclusion. In the scale diagrams presented below, only the R_{COS} values have been considered.

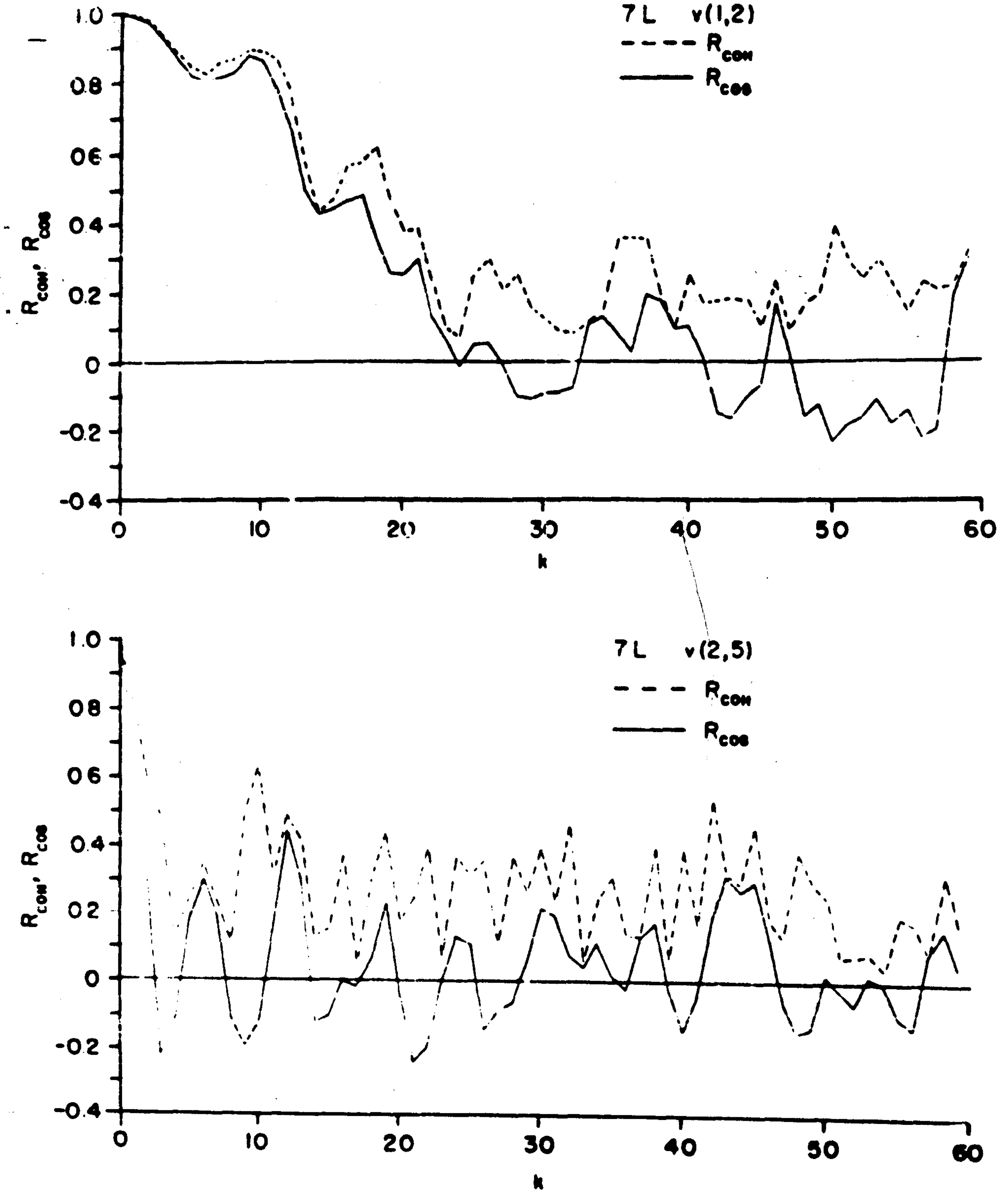

Fig. 23. Plots of the coherence and cospectral correlation coefficients for the v-component of wind velocity during a daytime experiment; data in upper diagram refer to longitudinal separation distance of 6 m while lower diagram refers to a longitudinal separation of 24 m.

Data for 12 experiments have been analyzed to obtain scale estimates for the u- and v- components of wind velocity for selected frequency bands. The minimum separation distance of 6 m used in these experiments exceeded the dimensions of the fluctuations in the w-component and no scale estimates are possible. As mentioned above, approximately half the transverse experiments utilized a minimum separation distance of 1m; when spectral and co-spectral estimates for these experiments become available, it should be possible to obtain scale estimates for the w-component. Mean wind speeds, wind directions, and standard deviations of azimuth wind direction for the Prairie Grass experiments in which scale estimates have been obtained are presented in table 3. The experiments comprise five daytime and seven nighttime cases.

Table 3. Mean wind speeds $\bar{V}$, mean wind directions $\bar{A}$, and standard deviations of azimuth wind direction σ_A for the Prairie Grass experiments used in determining Eulerian scales of turbulence.[1]

Run No.	Time (CST)	$\bar{V}$ (m sec^{-1})	$\bar{A}$ (deg)	σ_A (deg)
6 L	1655-1715	6.65	176	9.0
7 L	1355-1415	4.37	203	22.0
8 T	1655-1715	4.75	180	16.3
10 L	1155-1215	4.58	207	17.3
43 L	1155-1215	5.00	167	14.2
17 L	1955-2015	3.40	172	5.7
21 L	2155-2215	5.63	171	6.4
23 T	2055-2115	6.17	126	6.2
24 L	2255-2315	5.86	140	6.0
32 L	1955-2015	2.22	171	3.9
35 T	2257-2317	3.95	139	5.5
39 L	2225-2245	2.78	126	10.1

[1] The letter L denotes longitudinal (alongwind) orientation of the instruments and T signifies transverse (crosswind) orientation. The mean wind directions and standard deviations of azimuth angle are averages obtained from individual bivane records. Mean wind speeds are based on data from cup anemometers installed at a height of 2 m near the sulfur-dioxide source and at 450 m.

The difference between the observed mean wind direction and the expected direction (180 deg) is less than 30 deg for all the daytime experiments; however, this difference exceeds 40 deg in four of the nighttime cases. As pointed out below, these large deviations make it difficult to specify the effective orientation of the instrument arrays and result in scale estimates that are composites of longitudinal and transverse factors.

Sample scale diagrams of the u- and v- components for several experiments are presented in figs. 24 to 27. The scale curves are based on calculations of R_{COS} for selected values of the frequency $\underline{k}$; due to the large amount of information available at high frequencies, no attempt has been made to compute the correlations for all possible $\underline{k}$ values. In drawing the scale curves, the 10 values of R_{COS} for each $\underline{k}$ were plotted at the appropriate separation distances and the resulting points connected by straight lines; values of $R_{COS} < 0.30$ were considered insignificant and arbitrarily set equal to zero. For convenience in interpreting the results, the central frequencies and band widths[1] of the frequency intervals identified with the selected $\underline{k}$ values have been expressed in terms of period (inverse frequency) and are entered in table 4. The scale diagrams presented in fig. 24 are typical of the daytime cases thus far analyzed. These data indicate the presence of a continuous spectrum of eddy sizes within the period range from about 2 sec to 2 min; although the scale curves for both components are generally similar, the scales for the v-component appear to be somewhat larger than those for the u-component at all frequencies. The scale diagrams pre-

---

[1] See page 35 for the appropriate formulas.

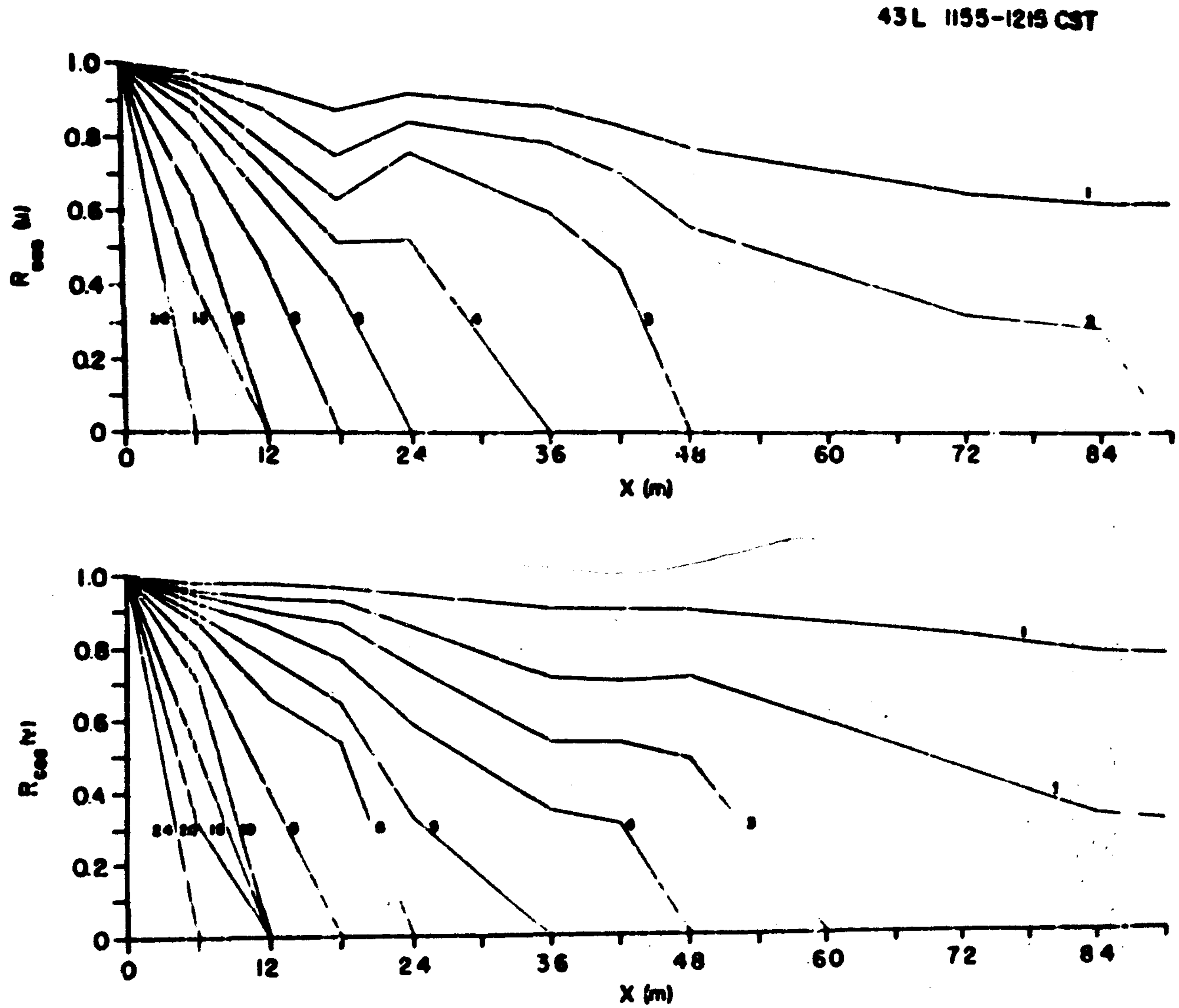

Fig. 24. Scale diagrams for the u- and v-velocity components during a daytime experiment: instruments spaced along the mean wind direction.

sented in fig. 25 refer to a nighttime experiment conducted in the presence of convective activity (as indicated by intermittent light rain showers at the field site and thunderstorm activity within the general area). The general appearance of the diagrams in fig. 25 is very similar to that of the scale diagrams in fig. 24 which are representative of strong daytime (thermal) convection. There is a marked absence of long-period fluctuations indicated in the scale diagrams of fig. 26 which are representative of a nighttime experiment conducted in the presence of moderate wind speeds and a slight temperature inversion. Also, as noted in fig. 24, the fluctuations in the v-component appear to be somewhat larger than those for the u-component. The scale diagrams presented in fig. 27 reveal the presence of long-period fluctuations; inspection of azimuth vane records show a gradual turning of the wind in the azimuth plane during the observation period; this gradual shift in wind direction is also apparent in the diffusion measurements obtained for the same experiment. These data also indicate that the shorter-period fluctuations in the v-component are somewhat larger than those for the u-component.

Scale estimates for the u- and v-components of the wind velocity have been obtained for the 12 experiments listed in table 3 by calculating the areas beneath the scale curves. In order to have a basis for comparing the results from the various experiments, the scale estimates thus obtained have been plotted as functions of inverse wave number. The daytime results, presented in fig. 28, show that the longitudinal scale estimates for both u and v are linearly related to the inverse wave number. The solid lines in the figure were fitted to the longitudinal data by the method of least squares.

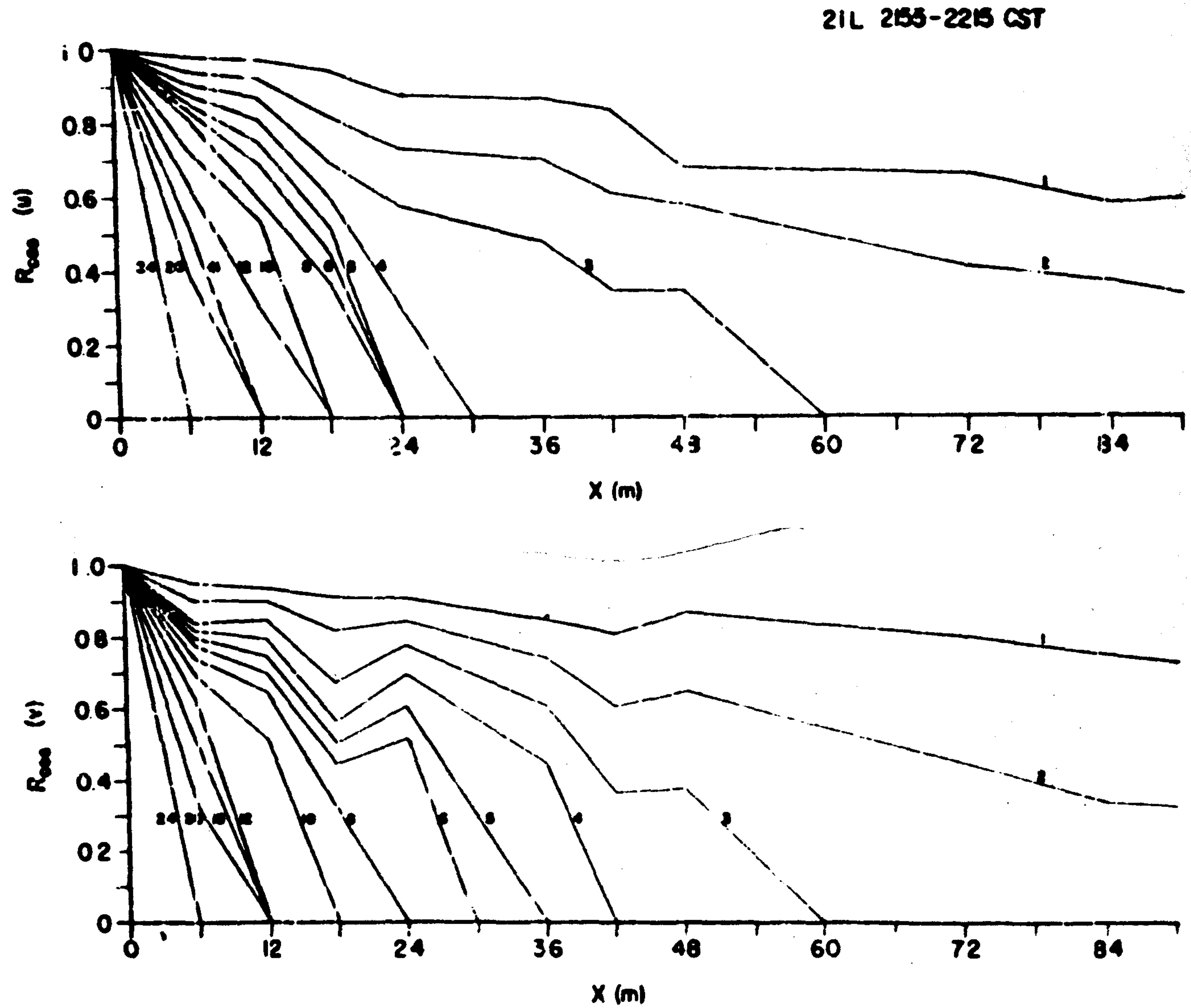

Fig. 25. Scale diagrams for the u- and v-velocity components during a nighttime experiment marked by convective instability; longitudinal orientation of instruments.

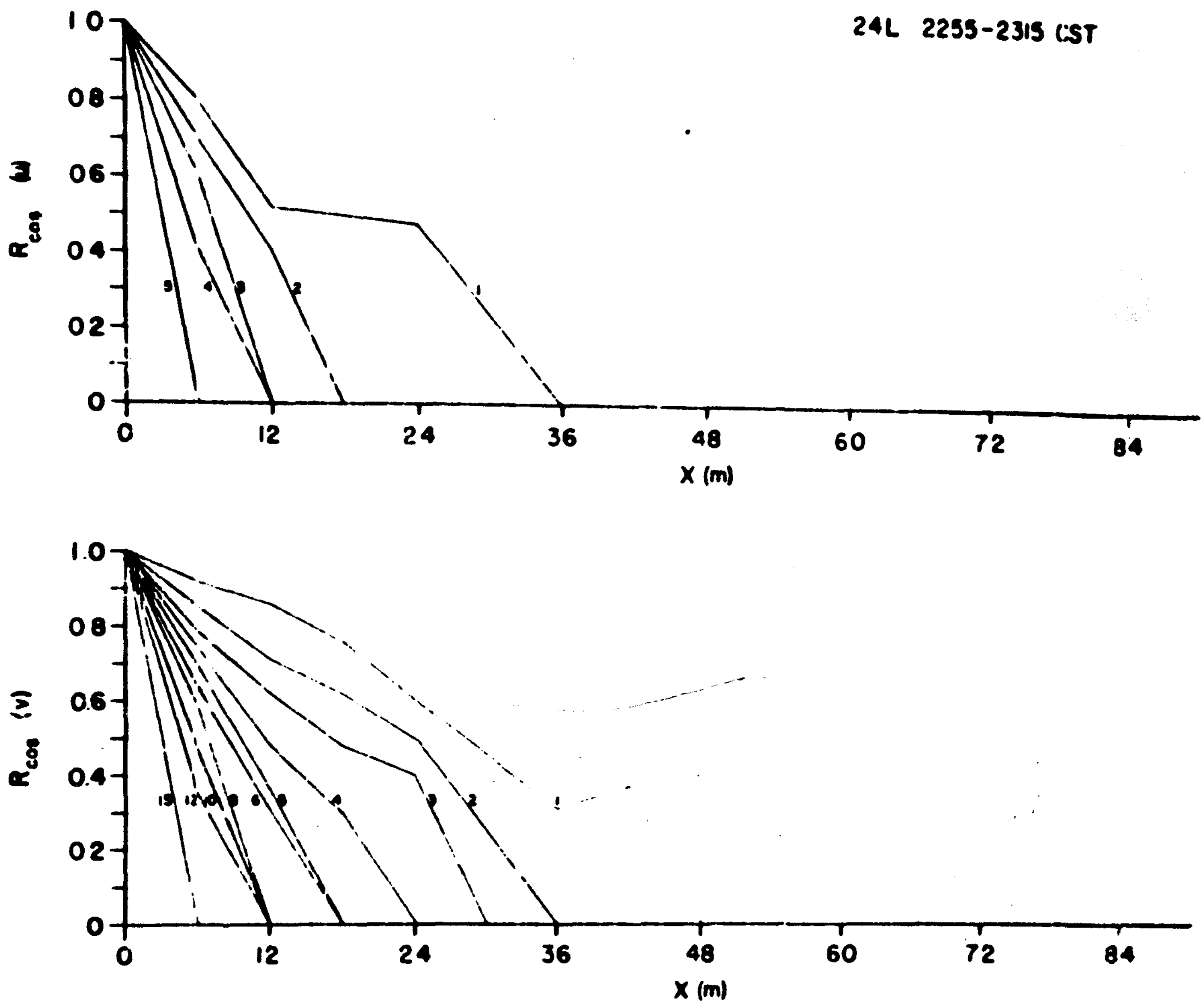

Fig. 26. Scale diagrams for the u- and v-velocity components during a typical nighttime experiment; instruments spaced along the mean wind direction.

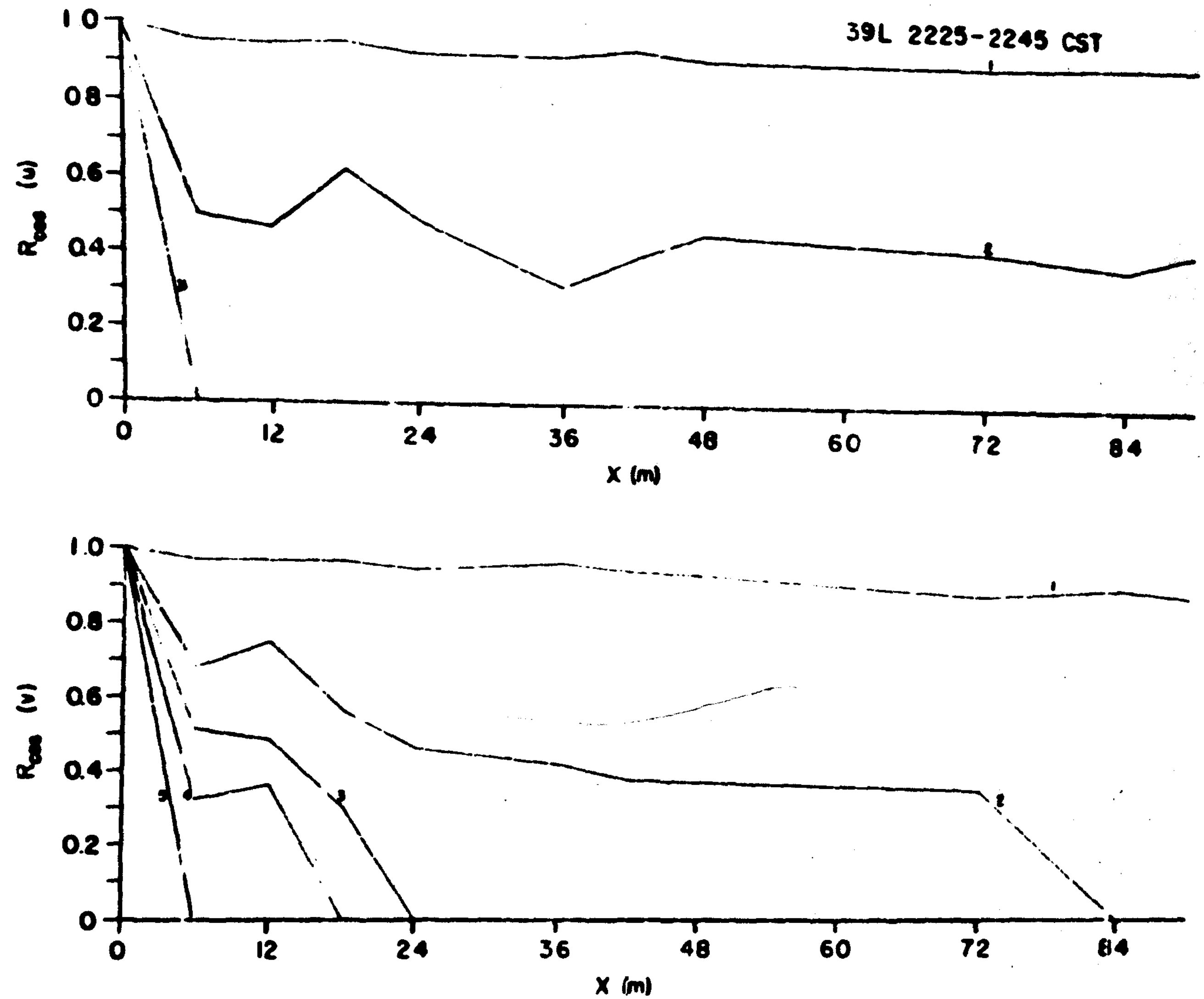

Fig. 27. Scale diagrams for the u- and v-velocity components during a nighttime experiment characterized by long-period fluctuations; longitudinal orientation.

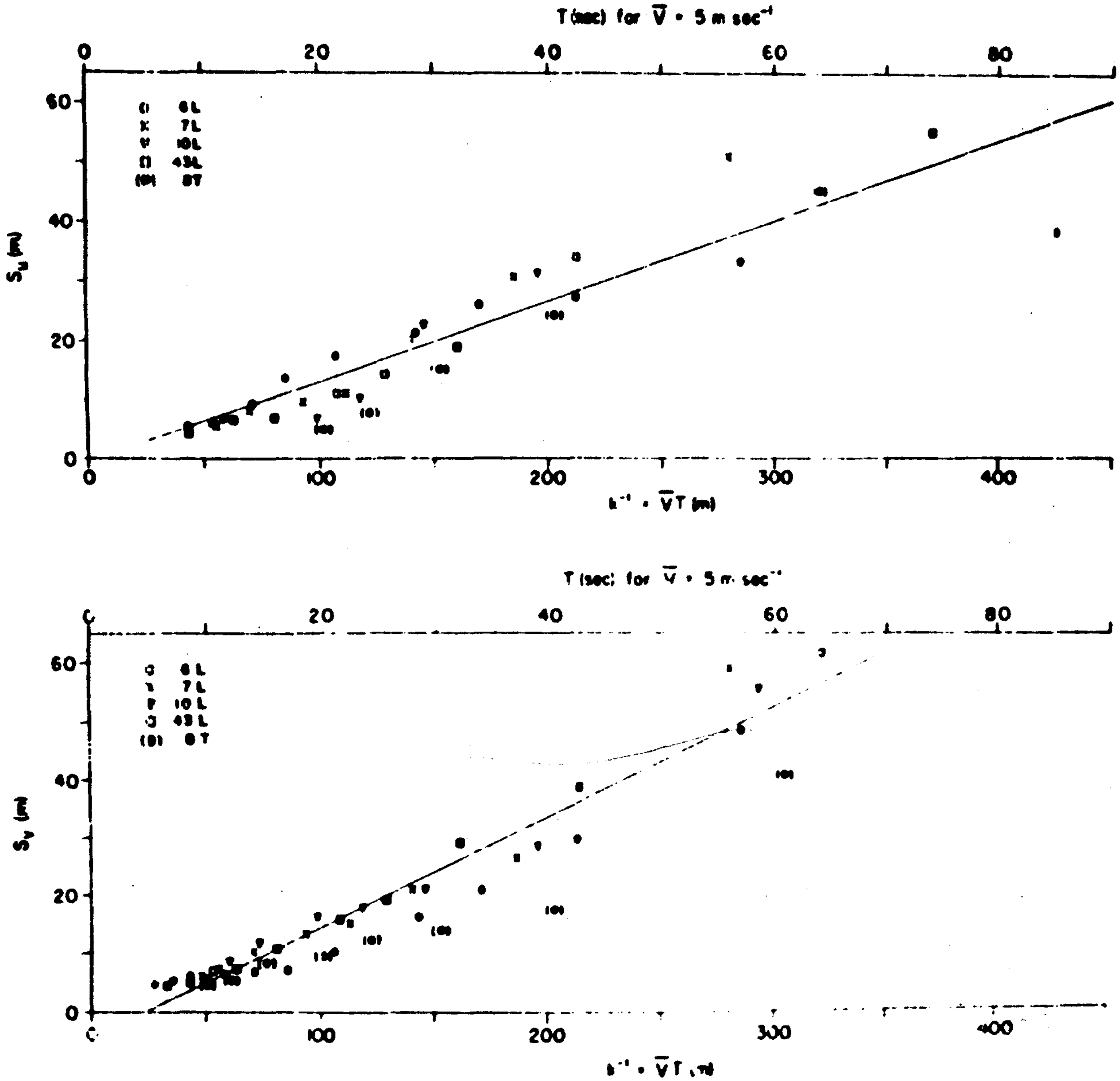

Fig. 28. Scales of turbulence for the u- and v-velocity components of daytime experiments plotted as functions of inverse wave number.

Table 4. Central frequencies and band widths of frequency intervals associated with selected values of $\underline{k}$ used in obtaining scale estimates; for convenience, data are inverted and expressed in terms of period rather than frequency.

$\underline{k}$	$T_c = 1/f_c$ (sec)	Band width (sec)
1	128	256-85
2	64	85-51
3	43	51-37
4	32	37-28
5	26	28-23
6	21	23-20
8	16	17-15
10	12.8	13.5-12.2
12	10.7	11.1-10.2
15	8.5	8.8- 8.2
20	6.4	6.6- 6.2
24	5.3	5.4- 5.2
30	4.25	4.3- 4.2
40	3.20	3.24- 3.16
59	2.18	2.19- 2.15

The scale estimates for Run No. 8, which refer to a transverse orientation, have not been included in the regression calculations; these estimates, particularly in the case of the v-component, appear to be smaller than the corresponding longitudinal scales. The linear relationship between the longitudinal scale estimates and inverse wave number implies the equivalence of space and time spectra; in other words, spatial correlations determined at fixed separation distances $\underline{x}$ along the direction of the mean wind correspond to points on the autocorrelation curve (based on measurements at a fixed point) when time and space are related by the equation

$$x = \bar{V}T \quad ,$$

where $\bar{V}$ is the mean wind speed and T is time in sec. This equivalence has been demonstrated by direct comparisons of space and time correlations obtained from the Prairie Grass fast-response data (26). The regression lines in fig. 28 show that, while the daytime longitudinal scales for the u- and v-components are closely similar, the scale estimates for the v-component tend to be slightly larger, (particularly for large inverse wave numbers). Although data for only one transverse orientation are available, these suggest that there is no great difference in the alongwind and crosswind dimensions of the u- and v-fluctuations during the daytime.

Plots of the nighttime scale estimates versus inverse wave number (see Fig. 29) tend to fall into two groups both of which show a linear relationship between the two variates. Approximately half the data tend to scatter about the regression line determined from the daytime cases; the other half tends to be situated along a regression line of significantly smaller slope. In general, the scale estimates for the transverse orientations (Run Nos. 23, 35) fit the lower regression line; Run No. 24 also fits this regression line and, in view of the mean wind direction, must be considered of doubtful orientation. The longitudinal orientations fit the upper regression line. The tentative conclusion would appear to be that, at night, the alongwind dimensions of both the u- and v-components are considerably larger than the crosswind dimensions. Panofsky et al (26) have reached the same conclusion based on a different treatment of the data. The regression lines in the figure also suggest, as in fig. 28, that the dimensions of the fluctuations in the v-component are somewhat larger than those in the u-component at all frequencies investigated. Summaries of the scale estimates for the u- and v-components adjusted to a mean wind speed of 5 m sec^{-1} and based on the regression lines in figs. 28, 29 are presented in table 5.

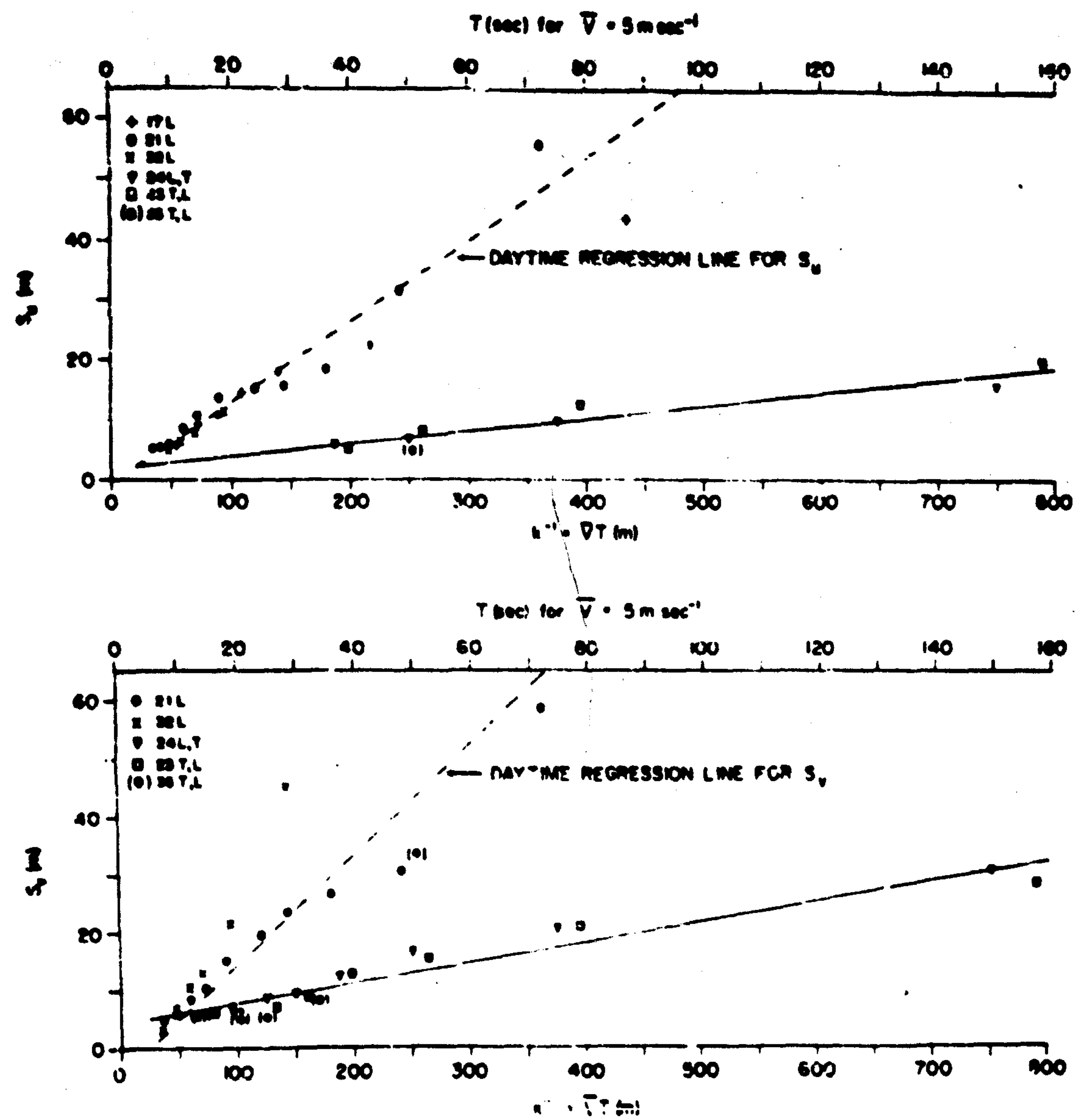

Fig. 29. Scales of turbulence for the u- and v-velocity components of nighttime experiments plotted as functions of inverse wave number.

Table 5. Estimates of the scales of turbulence for $\overline{V} = 5$ m sec^{-1} as functions of the period T (sec).

	T(sec)	90	60	30	20	15	10	5
Longitudinal orientation (daytime and nighttime[1])								
S_u (m)		60	40	20	13	10	6	< 3
S_v (m)		81	52	24	14	10	5	3
Transverse orientation (nighttime[1])								
S_u (m)		12	8	5	3	<3	<3	<3
S_v (m)		20	15	9	8	5	<3	3

[1] Nighttime spectrum of eddy sizes is not necessarily continuous within the range of period specified in the table.

The scale estimates obtained from spatial correlations refer to the average dimensions of fluctuations measured over half cycles and thus correspond to half wave lengths. It is apparent from the data in table 5 and from the regression lines in figs. 28, 29 that the wave lengths thus indicated by the longitudinal scale estimates are about three times smaller than the simple wave lengths obtained from the expression $x = \overline{V}\, T$. This is approximately the same relationship found between the Eulerian and Lagrangian scales of turbulence (26). Since the validity of the expression $x = \overline{V}\, T$ depends upon the persistence of the turbulence in the direction of the mean wind, it is suggested that the factor of 3 noted above is essentially due to important variations in azimuth wind direction that continuously alter the effective orientation of the fixed instrument array during the 20-min sampling periods.

IV. DIFFUSION MEASUREMENTS AT ROUND HILL DURING 1957

A. Introduction

Most available diffusion measurements comprise average or time-mean concentrations measured at fixed points over sampling periods of 3 to 10 min. Three-minute samples were widely used in the well-known Porton experiments (1) and 10-min sampling has been employed for the diffusion measurments made at Project Prairie Grass and for the earlier work at Round Hill. Satisfactory understanding of dispersal processes and maximum utilisation of these data require detailed knowledge of the probable variation in concentration and other diffusion parameters as a function of sampling time. For certain practical applications, and for use in formulating dispersal theories as well, it is essential to know the instantaneous distribution of concentration within the plume from a continuous point source. Recent studies of small-scale dispersal have shown that the standard deviation of asimuth wind direction and the Stability Ratio are useful meteorological indicators of diffusion (14) over sampling periods of 10 min duration; the utility of these predictors in estimating short-period dispersal is of considerable interest.

Previous investigations of the "instantaneous" field of concentration have been based largely on interpretations of photographs of visible smoke plumes (7; 16). This technique is subject to certain limitations inherent in the determination of visual range and does not provide information on the distribution of concentration within the plume. Direct measurement of effluent concentrations over short sampling periods requires detailed and comprehensive experimental procedures utilizing a tracer technique of wide flexibility. During the fall of 1957, a series of diffusion experiments of this type was conducted at the Round Hill Field Station. Suitable modifications in the sulfur-dioxide sampling network were made to permit sampling over periods as short as 0.5 min without appreciable loss in precision.

B. Description of experimental techniques

The sampling array consists of three overlapping, independently-operated, networks at travel distances of 50, 100 and 200 m. During the experiments, time-mean concentrations for sampling intervals of 0.5, 3, and 10 min were obtained at each travel distance. A schematic diagram of the field installation is shown in fig. 30. The 10-min network comprised individual stations located at a height of 1.5 m and spaced at 3-deg intervals along 180 deg of arc; limited vertical sampling was also carried out at 15-deg angular separations at heights of: 0.5, 1.0, 2.5 m (50 m); 0.5, 2.5 m (100 and 200 m). Sampling stations for the 3-min and 0.5-min networks were at a height of 1.5 m and spaced at 1.5 deg intervals along arcs of 150 and 120 deg, respectively. A section of the 100-m arc with midget impingers in position is shown in fig. 32.

The sulfur-dioxide generator used throughout Project Prairie Grass supplied the tracer.[1] The installation of the generating equipment at the

---

[1] See fig. 3. Details of source operation are described in a Geophysical Research paper to be distributed by the Air Force Cambridge Research Center.

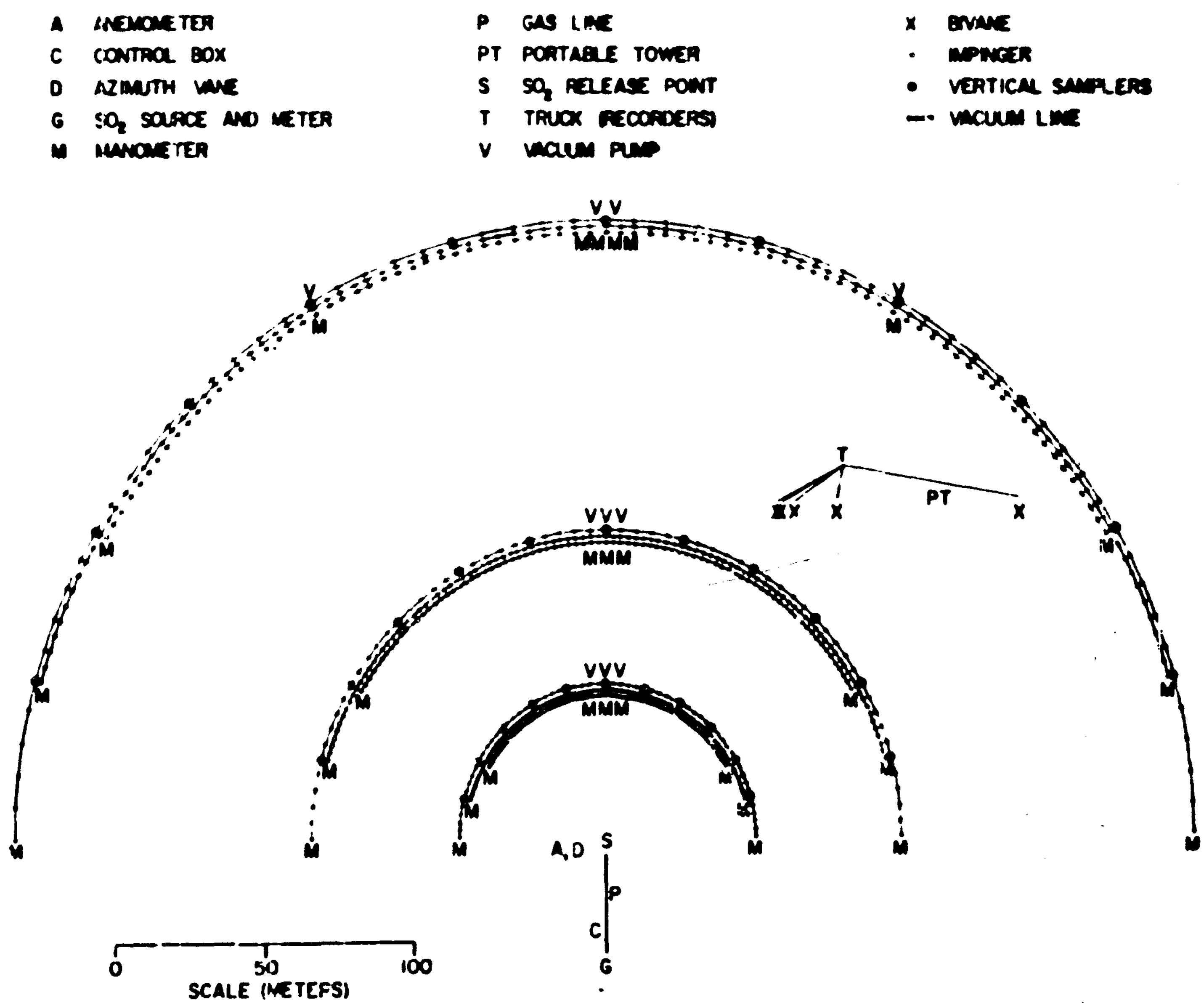

Fig. 30. Schematic diagram of field installation used for 1957 experiments at Round Hill.

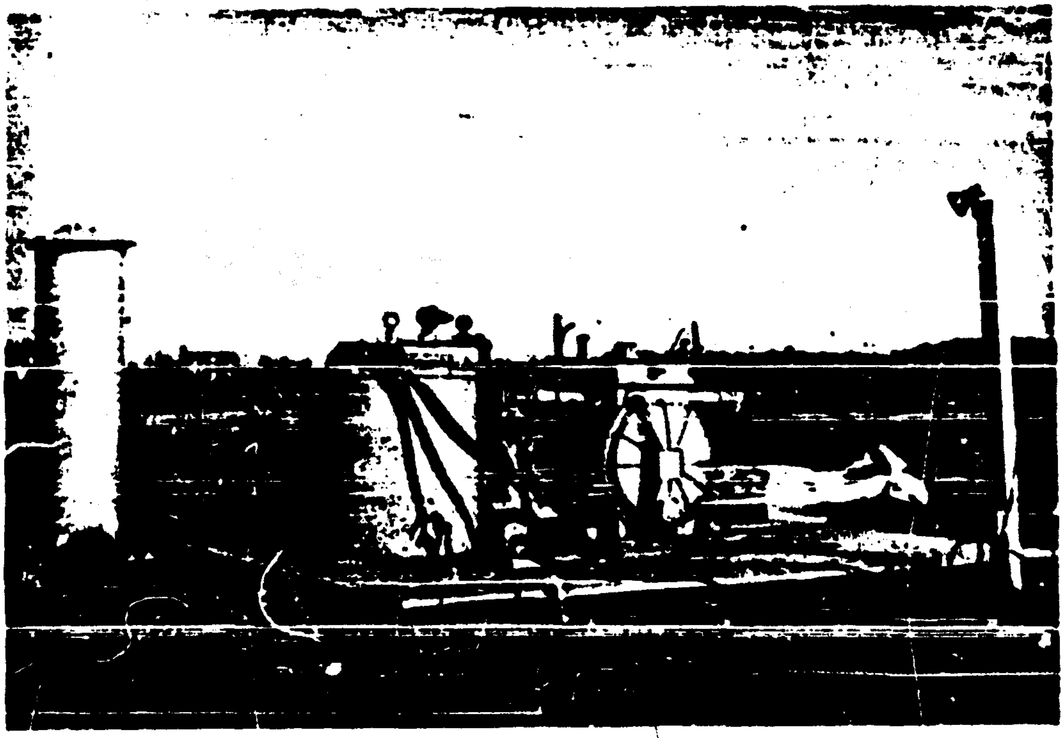

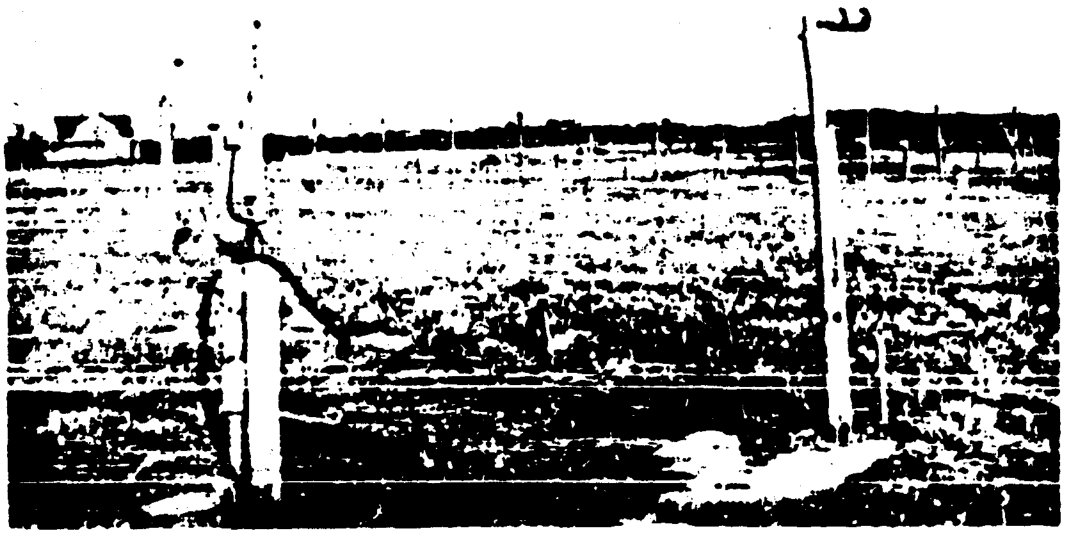

Fig. 31. Photographs of sulfur-dioxide generator (above) and release-point for the tracer (below). Generator comprises inverted tank of liquid sulfur dioxide sheltered by galvanized-iron cylinder, water bath containing vaporization chamber, and large gas meter. Plastic pipe connected to outlet of gas meter conducts tracer to release-point shown in lower photograph which is at height of 1.5 m. Cup anemometer and azimuth wind direction vane are shown at the left.

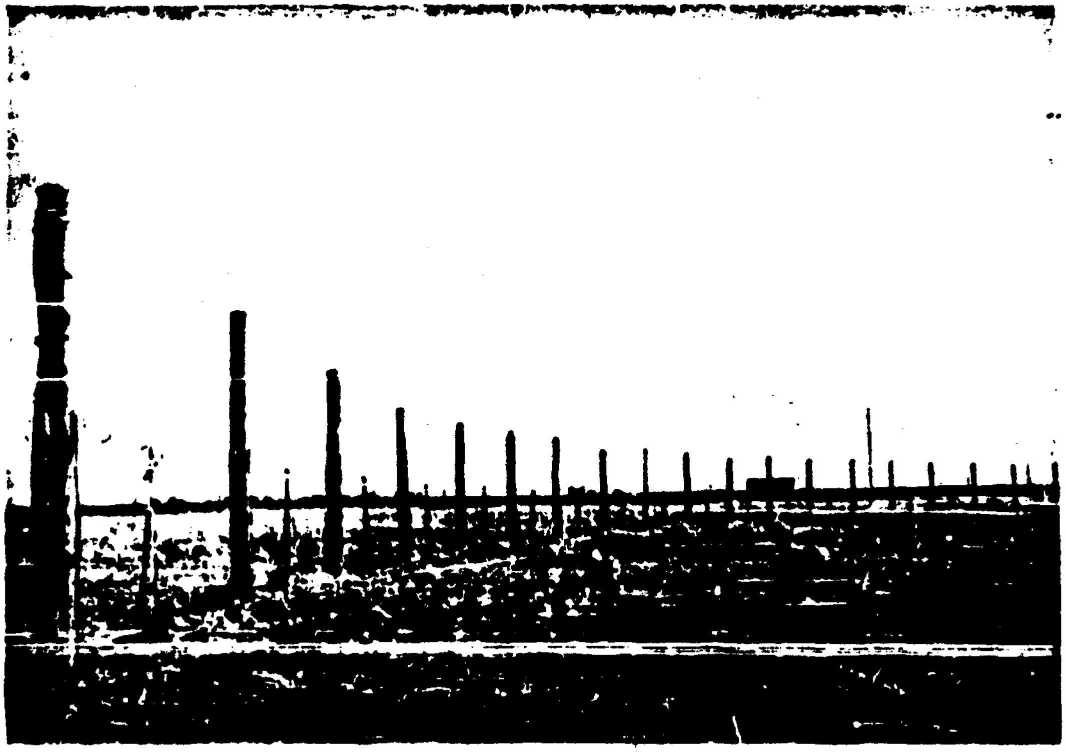

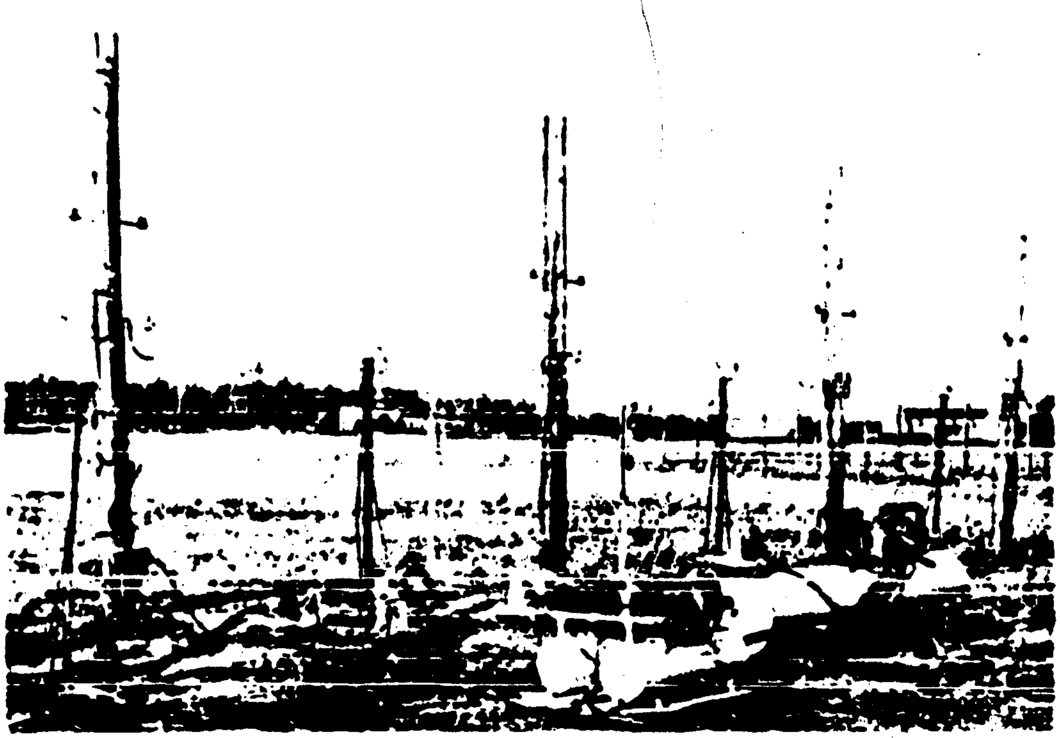

Fig. 32. Photograph of a section of the 100-m arc (above) showing cedar posts of the 10-min network and steel fence posts utilized in the 0.5- and 3-min networks. The lower photograph shows the vacuum pumps, tanks, and regulators for operating the three sampling networks at 50 m; vertical samples are obtained at heights of 0.5, 1.0, 1.5, and 2.0 m on cedar post shown at extreme left.

field site is shown in the upper photograph of fig. 31. After passing through the meter the gas was conducted underground through 2-in. plastic pipe to the release point (lower photograph of fig. 31) where it was emitted horizontally into the atmosphere at a height of 1.5 m. A source strength of about 100 g sec^{-1} was required during conditions of thermal instability while an emission rate of half that amount was sufficient under nighttime conditions of thermal stability. Prior to the start of an experiment, the tracer was permitted to traverse the entire network; the three sampling networks were then turned on simultaneously and each operated for the appropriate length of time. Aspiration of the impingers was provided by 10 vacuum tanks. Each of the three networks at each travel distance was supplied by a single vacuum source, with exception of the 0.5-min sampling network of the 200-m arc. To obtain the desired speed of response for this network, the 120-deg section was divided into two equal parts and each section provided with its own vacuum pump. The vacuum pumps, tanks and regulators used for the three networks of the 50-m arc are shown in fig. 32. Vacuum sources were controlled from a panel located upwind from the release point (see fig. 30). Solenoid-operated valves were used on all vacuum sources of the 3-min and 0.5-min networks to ensure minimum time-delay in reaching the proper rate of aeration of the samplers. The details of one of the vacuum sources may be seen in fig. 33. During a gas release, the equipment functioned as follows: (1) The vacuum pump was turned on to evacuate the tank to a predetermined value which was maintained by the regulator at the right. This vacuum was just sufficient for rapid evacuation of the line to the proper value at the start of the sampling period.

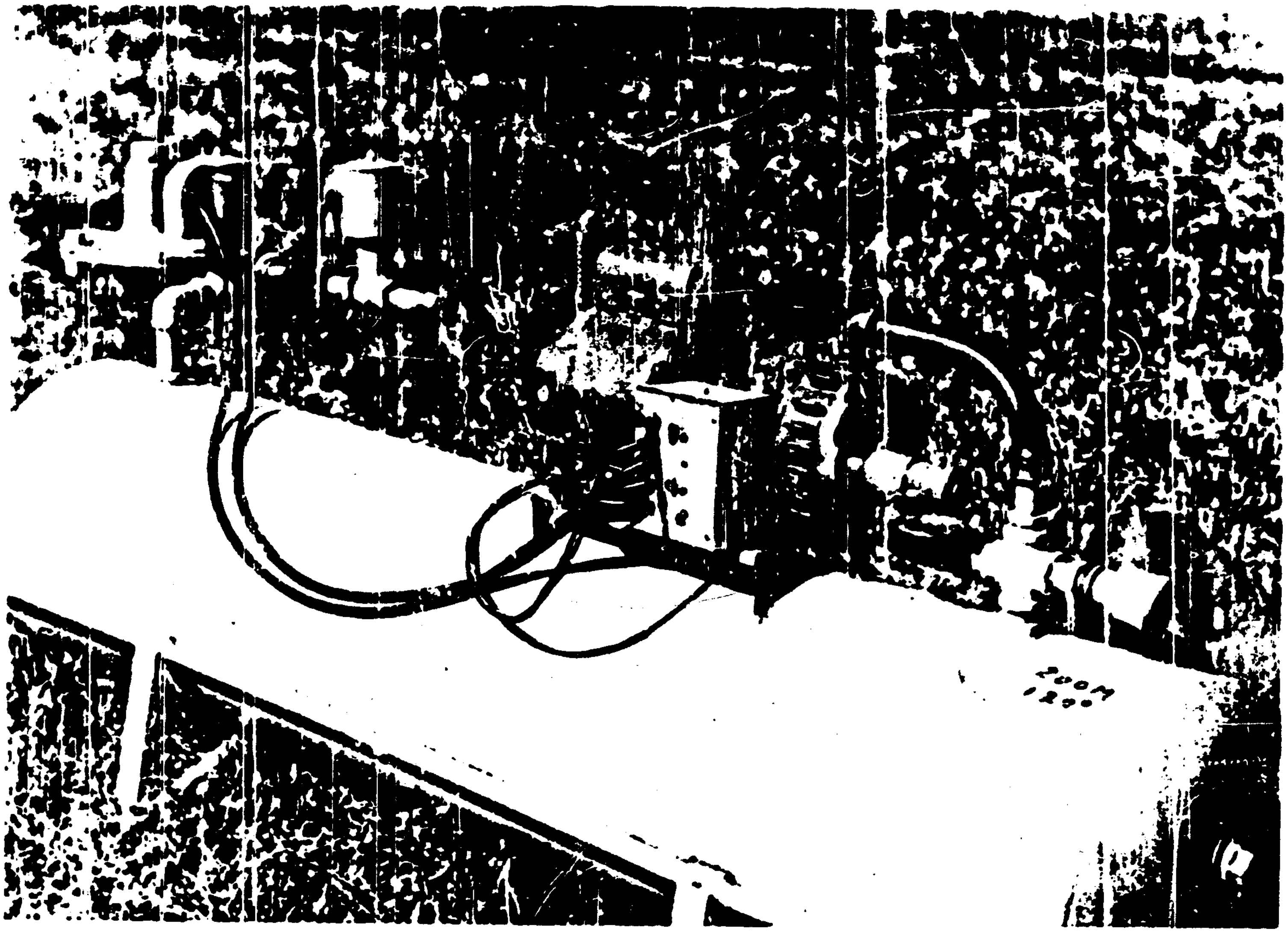

Fig. 33. Photograph of remote-controlled vacuum source showing (from left to right) vacuum regulator, solenoid-operated valves, motor for vacuum pump, relay box for operating solenoid valves, vacuum pump, gauge and regulator for initial tank vacuum.

(2) At the beginning of the sampling period, a solenoid-operated valve between the tank and the vacuum line to the impingers was opened. The vacuum regulator at the extreme left then maintained the vacuum of the system at the level required for an aeration rate of 1.5 l min^{-1} (100 mm of mercury).
(3) At the end of the sampling period, the pump was turned off, the line disconnected from the tank by the first solenoid valve and opened to the atmosphere by a second solenoid valve. Errors introduced into the concentration measurements by the above operation of the vacuum system are estimated to be less than 5 per cent.

Meteorological instrumentation included: a cup anemometer and sensitive azimuth vane located at a height of 2 m near the source; cup anemometers and ventilated thermocouples at heights of 1.5, 3, 6 and 12 m on the portable tower; and for most experiments, five bivanes equipped with heated-thermocouple anemometers oriented along a line parallel to the base line and spaced at intervals of 1, 4, 16 and 64 m. The operation of all meteorological instrumentation was controlled by a timer located within the recording truck. A 20-min observation period centered on the 10-min gas-sampling period was employed for the meteorological measurements. The location of the meteorological instrumentation at the field site is shown in fig. 30.

C. Data analysis and discussion of results

Ten field experiments were carried out during the period from 24 September to 3 December under a variety of weather conditions. Of these, four were made during the daytime and six were carried out in the evening under inversion conditions. Appendix B contains tabular summaries of the meteorological data and concentration measurements obtained during this series of experiments. Concentrations are presented in table I; source strengths and correction factors, which may be applied to the measured concentrations to compensate for the evaporational loss of impinger solution during aeration, are entered in table II; base-line wind speeds and standard deviation of azimuth wind direction σ_A for the three sampling periods are summarized in table III; profile data for wind speed and temperature are contained in table IV. The transit time across the network was usually considerably greater than 30 sec. Separate determinations at each travel distance are therefore required to establish appropriate estimates of the 0.5-min wind speed and σ_A values. Because of inherent uncertainties involved in such determinations, only rough estimates of the mean wind speed for the 0.5-min period, applicable to all travel distances, are presented. Estimates of σ_A for the 0.5-min period were obtained by dividing the maximum range in azimuth wind direction observed during 0.5-min intervals of the base-line vane record by 4.9.[1] The start of the 0.5-min sections were delayed with respect to the start of the 0.5-min sampling periods by 100/V sec, where V is the estimate of the 0.5-min wind speed in m sec^{-1}. These σ_A estimates are, therefore, most closely related to the concentration measurements made at the 100-m arc. Standard deviations of azimuth wind direction for longer sampling times were computed directly from the vane records (data abstracted at intervals of 2.5 sec).

---

[1] This approximation assumes that the vane data are normally distributed.

Horizontal concentrations profiles for four experiments are presented in fig. 34 to illustrate general features of the gas plumes. The profiles were obtained by expressing the concentrations at individual sampling stations along a given arc as percentages of the sum of all concentrations for the arc. In addition, daytime percentages for all sampling times were smoothed by a weighted 3-term moving average; nighttime data are unsmoothed. These profiles show the effect of sampling time upon plume width and upon the distribution of concentration across the plume. Fig. 34(a) shows profiles obtained at 50 m under conditions of strong midday heating. The 3-min profile tends to be bimodal but is otherwise quite similar to the 10-min distribution; in contrast, the 0.5-min profile is much narrower and more peaked than either of these. Fig. 34(b) shows profiles at 200 m obtained under slight inversion conditions. Again, except for its marked bimodal character, the 3-min profile is similar to that of the 10-min sample and the 0.5-min profile is narrower and more peaked than the other two. Fig. 34(c) shows profiles at 50 m obtained under slight inversion conditions and relatively strong gusty winds. The three profiles are rather similar, but show increasing irregularity with decreasing sampling time, as might be expected. Fig. 34(d) shows profiles at 100 m obtained under marked inversion conditions. During this experiment the profile was nearly invariant with sampling time.

The utility of the standard deviation of azimuth wind direction σ_A as a predictor of plume characteristics measured over a 10-min period has been well established in previous experiments. The data presented in figs. 35 and 36 indicate the usefulness of σ_A in estimating dispersal over shorter time

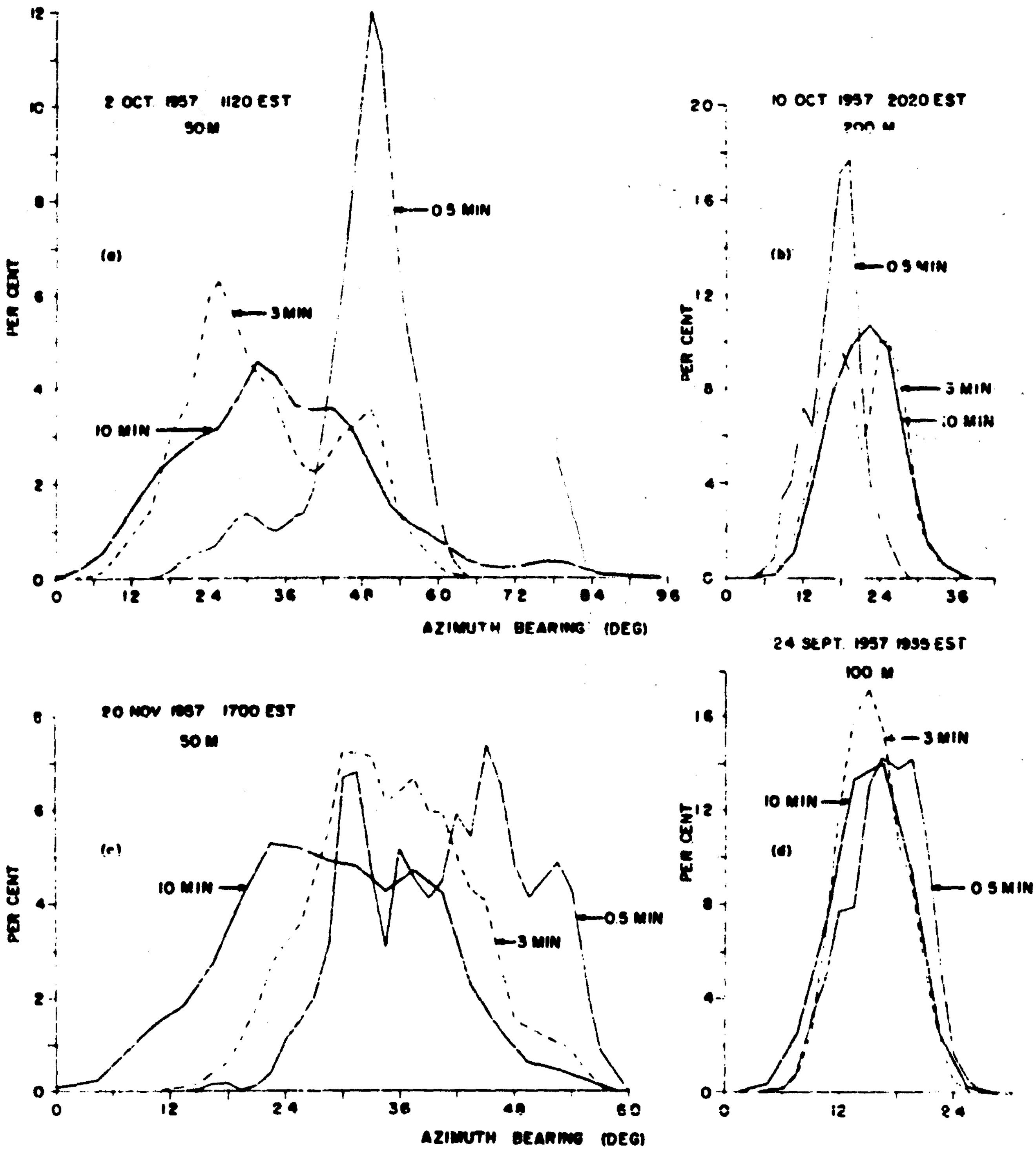

Fig. 34. Examples of horizontal concentration profiles at various travel distances for three periods of sampling.

intervals. In fig. 35 the standard deviation of cross-plume concentration at 100 m for the three sampling times has been plotted against σ_A for the same periods. In fig. 36, peak concentrations at 100 m, adjusted to a standard source strength of 1 g sec^{-1} and a mean wind speed of 5 m sec^{-1}, are plotted (for the three sampling times) against the reciprocal of σ_A. Daytime and nighttime data are indicated by open and filled symbols, respectively; least-squares regression lines have been fitted to the combined data. These two figures suggest that the relationships previously found between σ_A and plume characteristics over periods of 10-min duration still hold for periods as short as 0.5 min. The scatter of points for the 0.5 min observations may be largely due to uncertainties in establishing the proper value of σ_A. The large σ_A value for the point enclosed by parentheses in figs. 35 and 36 resulted from a single large fluctuation of very high frequency. Under such unusual circumstances, the determination of σ_A from the range shown by the vane record clearly leads to doubtful results.

Measurements of basic plume features (standard deviation of lateral concentration, peak concentration, and integrated-crosswind concentration) for individual diffusion experiments are summarized in table 6. The adjusted concentrations are based in part upon rough estimates of the mean wind speed during the shorter (3-min and 0.5-min) sampling periods obtained from conventional cup anemometers. Use of these estimates tends to eliminate some of the actual variation in the concentrations; in the extreme, observed variations in the 0.5-min peak concentrations may be reduced by about 20 per cent by this factor.

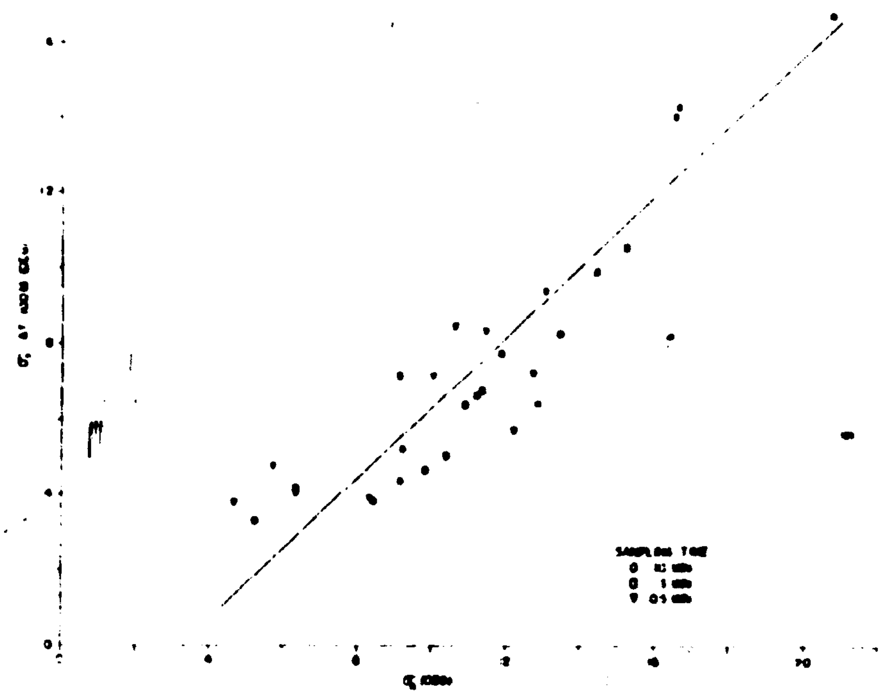

Fig. 35. Standard deviation of concentration along lateral coordinate σ_y at 100 m versus standard deviation of asimuth wind direction. Open symbols denote daytime observation; closed symbols refer to nighttime observations.

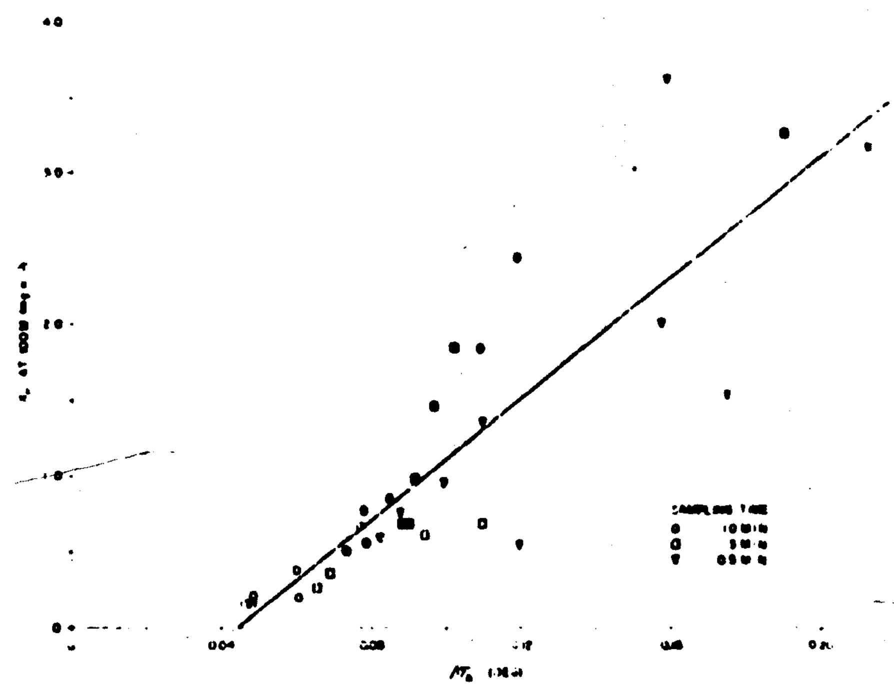

Fig. 36. Peak concentration at 100 m versus inverse standard deviation of asimuth wind direction. Concentrations are adjusted to source strength of 1 g sec^{-1} and mean wind speed of 5 m sec^{-1}. Open symbols denote daytime observations and closed symbols refer to nighttime observations.

Table 6. Plume characteristics for three periods of sampling.[1]

(a) Cross-plume standard deviation of concentration σ_y (deg)

Travel distance	50 m			100 m			200 m		
Sampling time (min)	10	3	0.5	10	3	0.5	10	3	0.5
Run No.									
1	5.7	5.2	4.6	3.8	3.4	3.8	2.7	2.4	2.3
2	14.9	11.7	8.1	14.0	10.6	4.0	13.1	10.4	5.1
3	8.1	7.0	5.4	6.4	6.4	4.3	5.0	5.5	4.0
4	15.1	10.2	10.7	14.3	7.1	8.3	12.5	7.4	8.7
5	7.3	6.2	4.7	5.2	4.7	4.2	3.1	2.6	3.0
6	9.2	6.2	6.5	7.7	5.1	4.1	6.7	3.7	4.0
7	10.4	8.1	8.7	8.3	6.7	5.7	6.4	6.0	3.9
8	9.2	8.2	8.8	7.3	6.8	7.2	5.9	5.4	5.5
9	11.6	10.9	9.7	9.4	8.5	4.8	8.1	7.1	4.7
10	17.3	10.6	6.3	16.7	9.9	5.6	17.5	6.5	2.4

(b) Peak concentration χ_p (mg m^{-3}) adjusted to a source strength of 1 g sec^{-1} and a mean wind speed of 5 m sec^{-1}

Travel distance	50 m			100 m			200 m		
Sampling time (min)	10	3	0.5	10	3	0.5	10	3	0.5
Run No.									
1	4.02	5.68	8.38	2.44	3.28	3.18	1.00	1.12	0.33
2	1.13	1.21	1.87	0.19	0.26	0.54	0.05	0.06	0.17
3	2.72	4.04	2.93	0.77	0.98	1.35	0.23	0.21	0.33
4	1.36	2.75	3.22	0.38	0.69	0.74	0.10	0.17	0.22
5	3.21	4.56	4.99	1.84	2.10	3.64	0.89	0.60	0.20
6	2.52	4.67	4.41	0.85	1.46	2.02	0.27	0.48	0.23
7	1.44	1.88	1.65	0.50	0.68	0.59	0.27	0.17	0.04
8	1.59	2.78	1.90	0.56	0.68	0.95	0.16	0.18	0.24
9	2.02	2.19	3.43	0.67	0.61	1.54	0.19	0.20	0.44
10	0.93	1.96	1.96	0.22	0.36	0.16	0.03	0.08	0.16

---

[1] Adjusted concentrations in parts (b), (c), of the table refer to source strengths and wind speed estimates found in tables II, III of Appendix B.

Table 6. (cont.)

(c) Integrated-crosswind concentration CIC (mg m^{-2}) adjusted to a source strength of 1 g sec^{-1} and a mean wind speed of 5 m sec^{-1}

Travel distance	50 m			100 m			200 m		
Sampling time (min)	10	3	0.5	10	3	0.5	10	3	0.5
Run No.									
1	45.38	53.97	59.01	17.30	19.02	22.03	4.74	4.33	1.39
2	24.80	19.08	15.52	5.07	4.70	2.98	1.13	1.14	1.26
3	32.10	37.50	27.72	8.57	9.56	9.59	2.17	2.09	1.87
4	30.81	35.82	57.98	7.61	8.22	9.42	1.72	1.79	2.49
5	41.13	43.49	34.33	18.25	18.61	26.50	4.83	2.89	1.09
6	36.90	40.08	48.27	10.50	11.99	13.78	2.56	2.82	1.55
7	27.17	25.92	24.99	6.99	6.69	3.81	1.69	1.50	0.33
8	25.73	28.66	21.05	6.69	7.57	7.02	1.72	1.88	1.48
9	40.24	37.54	45.02	10.87	10.28	13.43	2.53	2.39	3.06
10	27.05	26.77	21.42	5.56	5.05	1.34	0.87	0.78	0.68

Table 7. Effect of sampling time on plume parameters at three travel distances. Values for 3-min and 0.5-min sampling times are normalized with respect to the 10-min values.

(a) Cross-plume standard deviation of concentration σ_y.

	σ_y (3 min) / σ_y (10 min)				σ_y (0.5 min) / σ_y (10 min)			
Run No.	50m	100m	200m	Mean	50m	100m	200m	Mean
1	0.92	0.87	0.88	0.89	0.80	0.99	0.84	0.88
2	0.78	0.75	0.79	0.77	0.54	0.28	0.39	0.40
3	0.87	1.00	1.10	0.97	0.67	0.67	0.80	0.71
4	0.67	0.50	0.59	0.59	0.71	0.58	0.70	0.66
5	0.85	0.90	0.83	0.86	0.64	0.80	0.97	0.60
6	0.67	0.66	0.56	0.63	0.71	0.53	0.61	0.62
7	0.78	0.81	0.93	0.84	0.84	0.69	0.60	0.71
8	0.89	0.93	0.92	0.91	0.95	0.99	0.93	0.96
9	0.94	0.90	0.88	0.91	0.83	0.51	0.58	0.64
10	0.61	0.59	0.37	0.52	0.36	0.34	0.14	0.28

(b) Peak concentration χ_p. Concentrations for each sampling time adjusted to a source strength of 1 g sec^{-1} and a mean wind speed of 5 m sec^{-1}.

	χ_p (3 min) / χ_p (10 min)				χ_p (0.5 min) / χ_p (10 min)			
Run No.	50m	100m	200m	Mean	50m	100m	200m	Mean
1	1.41	1.34	1.12	1.29	2.08	1.30	0.33	1.24
2	1.07	1.36	1.34	1.25	1.65	2.81	3.60	2.69
3	1.49	1.27	0.91	1.22	1.08	1.75	1.43	1.42
4	2.02	1.79	1.74	1.85	2.37	1.93	2.26	2.19
5	1.42	1.14	0.68	1.08	1.55	1.98	0.23	1.25
6	1.85	1.73	1.79	1.79	1.75	2.39	0.85	1.66
7	1.31	1.34	0.97	1.21	1.28	1.17	0.26	0.90
8	1.75	1.22	1.17	1.38	1.19	1.71	1.53	1.48
9	1.08	0.91	1.06	1.02	1.70	2.30	2.32	2.11
10	2.10	1.64	2.39	2.04	2.10	0.73	4.97	2.60

Table 7. (Cont.)

(c) Integrated-crosswind concentration CIC. Concentrations for each sampling time adjusted to a source strength of 1 g sec^{-1} and a mean wind speed of g m sec^{-1}.

	CIC (3 min) / CIC (10 min)				CIC (0.5 min) / CIC (10 min)			
Run No.	50m	100m	200m	Mean	50m	100m	200m	Mean
1	1.19	1.10	0.91	1.07	1.30	1.27	0.29	0.95
2	0.77	0.93	1.01	0.90	0.63	0.59	1.12	0.78
3	1.17	1.12	0.96	1.08	0.86	1.12	0.86	0.95
4	1.16	1.08	1.04	1.09	1.88	1.24	1.45	1.52
5	1.06	1.02	0.60	0.89	0.83	1.45	0.23	0.84
6	1.09	1.14	1.10	1.11	1.31	1.31	0.61	1.08
7	0.95	0.96	0.89	0.93	0.92	0.54	0.19	0.55
8	1.11	1.13	1.09	1.11	0.82	1.05	0.86	0.91
9	0.93	0.95	0.94	0.94	1.12	1.24	1.21	1.19
10	0.99	0.91	0.90	0.93	0.79	0.24	0.78	0.60

Table 8. Summary of observed variations in plume parameters with period of sampling [illegible] daytime and nighttime experiments; entries are based on rati[illegible] table 7.

Ratio	Daytime		Nighttime	
	Range	Mean	Range	Mean
χ_p (3 min) / χ_p (10 min)	0.91-2.39	1.54 (1.27)	0.68-1.85	1.33 (1.04)
σ_y (3 min) / σ_y (10 min)	0.37-0.94	0.70 (0.81)	0.56-1.10	0.85 (0.96)
CIC (3 min) / CIC (10 min)	0.77-1.16	0.97	0.60-1.19	1.03
χ_p (0.5 min) / χ_p (10 min)	0.73-4.97	2.40 (1.64)	0.23-2.39	1.32 (1.26)
σ_y (0.5 min) / σ_y (10 min)	0.14-0.83	0.50 (0.63)	0.53-0.99	0.78 (0.80)
CIC (0.5 min) / CIC (10 min)	0.24-1.88	1.02	0.19-1.45	0.88

Variations in characteristic plume parameters with sampling time are indicated in table 7 which presents ratios of χ_p, σ_y, and CIC measured over 3- and 0.5-min periods to their respective 10-min values. The data in table 8 show the extremes and arithmetic means of these ratios for both daytime and nighttime experiments. Table entries enclosed by parentheses are based on average ratios of σ_A (0.5-min and 3-min) to σ_A (10-min) obtained from the complete azimuth vane record[1]. According to the data in the table, peak concentrations measured over periods of 0.5 and 3 min are on the average about 2.4 and 1.5 times larger, respectively, than the 10-min values for the daytime experiments. At night, both the 0.5- and 3-min peak concentrations exceed the 10-min peak concentration by a factor of 1.3. In the daytime experiments, the 0.5-min and 3-min σ_y values are on the average about 0.5 and 0.7, respectively, of the 10-min σ_y. At night, both the 0.5- and 3-min σ_y values are about 0.8 of the 10-min σ_y. As might be expected, the indicated average variation in CIC with sampling time is almost negligible. These results may be compared with Sutton's (29) estimate of 0.57 for the ratio of the instantaneous plume width at 100 m to the 3-min time-mean width, in conditions of near-neutral stability; and, Gosline's (28) measurements near the base of a tall stack which show maximum concentrations for sampling intervals of a few seconds that are 3 to 4 times larger than similar concentrations for 1- to 3-min sampling intervals.

---

[1] The sequence of 240 observations for each 10-min period was subdivided into consecutive sub-sections of 10, 20, 30, 40, 60, and 120 points. Standard deviations for each sub-section were then averaged to obtain representative values. See table III of Appendix B.

Some of the experimental results are rather surprising. Three of the nighttime experiments (Run Nos. 1, 5, and 6 in table 6) show 0.5-min peak concentrations at 200 m that are considerably lower than the 10-min peak concentrations; in each case the 0.5-min plume widths (as evidenced by the σ_y values) are less than the 10-min widths. Assuming that the concentration measurements are approximately correct, the most likely explanation for these anomalies is that there are occasional large short-period variations in the height of the plume axis and/or the vertical distribution of concentration. For some purposes it is desirable to remove inhomogeneities of this type from the data; this may be accomplished by normalizing the 0.5- and 3-min CIC values at each travel distance with respect to the 10-min CIC. Ratios of average peak concentration for the various sampling intervals are then given by the relative heights of the maximum ordinates of the lateral concentration profiles (see fig. 34). If the data are adjusted in this manner, the average ratios of the 0.5- and 3-min peak concentrations to the 10-min values are 2.69 and 1.58, respectively, for the daytime experiments. For the nighttime data, similar ratios have values of 1.48 and 1.28. These results do not appear to differ significantly from those previously obtained from un-normalized data.

Although the results obtained during the diffusion experiments indicate that the standard deviation of azimuth wind direction σ_A is a useful predictor of diffusion parameters over the 0.5- to 10-min range of sampling interval, it is difficult to establish statistically significant relationships between diffusion measurements for the 3- and 0.5-min periods and σ_A values for the same intervals. Linear correlations between these variates are below the level of significance[1] unless the σ_A are averages obtained from the entire length of azimuth vane record (see table III in Appendix B). Part of the difficulty is explained by the small sample size and by the impossiblity of obtaining satisfactory short-period estimates of σ_A and mean wind speed from available meteorological information. However, it appears likely that direct relationships between σ_A and observed plume characteristics must eventually break down as the length of the sampling interval approaches some lower limit, say 1 sec. Whatever the exact nature of the physics of the dispersal process, the primary features of the plume at any given instant represent an integration of turbulent structure over time and space. A wind-direction vane with a small characteristic time is responsive, over short time intervals, to a fine structure of turbulence that may bear little relationship to the structural elements that determine the geometry of the plume at a given instant.

It is possible, however, to establish statistically significant relationships between the 10-min σ_A values and ratios of the type presented in table 7. Estimates of the ratios of σ_y and χ_P for the 0.5- and 3-min intervals to their respective 10-min values at all three travel distances are entered in table 9. The estimates are based on least-square regression lines obtained from the logarithms of the variates; the procedure is identical with that used for the Prairie Grass data shown in figs. 9 to 14. Correlation coefficients and standard errors of estimate appear in table 10. Concentrations used in the

---

[1]For 8 degrees of freedom, the 95-per cent level of significance requires a correlation of about 0.70.

Table 9. Estimates of the ratios of σ_y and χ_p for 0.5- and 3-min sampling periods to their respective 10-min values as functions of σ_A for 10-min periods. Entries based on regression analysis of the logarithms of the variates. Mean values obtained by averaging observed ratios at the three travel distances before computing regression equations.

σ_y (3 min) / σ_y (10 min)

σ_A (deg)	50m	100m	200m	Mean
8	0.95	1.00	1.06	1.00
10	0.88	0.89	0.91	0.89
12	0.82	0.81	0.80	0.81
15	0.75	0.72	0.69	0.72
20	0.68	0.62	0.56	0.62

σ_y (0.5 min) / σ_y (10 min)

σ_A (deg)	50m	100m	200m	Mean
8	0.92	1.06	1.32	1.08
10	0.81	0.82	0.92	0.85
12	0.72	0.66	0.68	0.70
15	0.63	0.51	0.47	0.55
20	0.53	0.36	0.30	0.40

χ_p (3 min) / χ_p (10 min)

σ_A (deg)	50m	100m	200m	Mean
8	1.16	1.03	0.94	1.04
10	1.28	1.15	1.09	1.18
12	1.40	1.25	1.24	1.30
15	1.55	1.39	1.45	1.47
20	1.78	1.60	1.76	1.73

χ_p (0.5 min) / χ_p (10 min)

σ_A (deg)	50m	100m	200m	Mean
8	1.33	1.04	0.78	0.98
10	1.46	1.36	1.14	1.32
12	1.57	1.69	1.55	1.63
15	1.72	2.21	2.27	2.11
20	1.93	3.13	3.71	2.93

analysis were adjusted so that the 0.5-min and 3-min CIC values at each travel distance were equal to the 10-min CIC. This tends to smooth the individual observations by minimizing inhomogeneities of the type discussed on page 55.

Rough estimates of the average 0.5- and 3-min standard peak concentration to be expected at the three travel distances are entered in table 11 for selected values of σ_A. These estimates were obtained by applying the mean ratios shown in table 9 to the concentrations indicated in fig. 9 for appropriate values of σ_A. The results generally apply for a range of thermal stratification from near-neutral to extreme instability; the data do not permit estimates

Table 10. Correlations r between the logarithm of the standard deviation of azimuth wind direction σ_A and the logarithm of the indicated ratios. Standard errors of estimate S_y are to be applied to ratios presented in table 9 and are expressed as factors by which estimates should be multiplied to give limits within which approximately two-thirds of the cases are found. Sample size is 10.

	σ_y (3 min) / σ_y (10 min)				σ_y (0.5 min) / σ_y (10 min)			
	50m	100m	200m	Mean	50m	100m	200m	Mean
r	-0.67	-0.62	-0.58	-0.64	-0.59	-0.76	-0.77	-0.78
S_y	1.11	1.18	1.28	1.17	1.24	1.29	1.41	1.24
	0.90	0.85	0.78	0.85	0.81	0.77	0.71	0.80

	χ_p (3 min) / χ_p (10 min)				χ_p (0.5 min) / χ_p (10 min)			
	50m	100m	200m	Mean	50m	100m	200m	Mean
r	0.66	0.63	0.61	0.68	0.39	0.76	0.84	0.77
S_y	1.15	1.16	1.26	1.17	1.28	1.31	1.33	1.27
	0.87	0.86	0.79	0.86	0.78	0.77	0.75	0.79

for stable thermal stratification. The extreme range in peak concentration that might be encountered during the shorter sampling periods is indicated by the entries in table 8. A table of σ_y estimates may be constructed by the same procedure, using the results shown in fig. 13. More reliable estimates require additional measurements.

Vertical concentration measurements obtained during the 1957 diffusion experiments are summarized in table 12. For convenience, all measurements have been normalized with respect to the concentration at a height of 1.5 m. Vertical profiles located near the edges of the plume were omitted from the calculations. The results at 50 m show maximum concentrations at a height of 0.5 m for all the experiments. With the exception of Run Nos. 1, 5, and 6, made during light winds and moderately stable thermal stratification, the tracer is uniformly mixed within the layer from ground level to a height of 1.5 m after it has travelled 100 m from the source. In the presence of light winds and stable stratification, approximate uniformity is attained within this layer by the time the tracer reaches 200m.

Table 11. Estimates of peak concentration (at height of 1.5 m) for three periods of sampling as function of σ_A. Ten-minute concentrations are based on Prairie Grass data of fig. 9. Estimates for other sampling intervals were obtained by applying mean ratios presented in table 9. Concentrations are adjusted to source strength of 1 g sec^{-1} and a mean wind speed of 5 m sec^{-1}.

	Concentration (mg m^{-3})								
Travel distance	50 m			100 m			200 m		
Sampling time (min)	10	3	0.5	10	3	0.5	10	3	0.5
σ_A (deg)									
8	4.51	4.51	4.51	1.56	1.56	1.56	0.47	0.47	0.47
10	3.56	4.20	4.70	1.12	1.32	1.48	0.32	0.37	0.42
12	2.29	2.98	3.73	0.60	0.78	0.98	0.15	0.19	0.24
15	1.85	2.72	3.90	0.44	0.64	0.92	0.10	0.14	0.20
20	1.41	2.44	4.13	0.29	0.50	0.85	0.06	0.10	0.16

Table 12. Relative concentration at various sampling heights expressed as percentage of concentration at height of 1.5 m.

Travel distance	50m	100m	200m	50m	100m	200m
Height (m)		Run No. 1			Run No. 2	
2.5	0.63	0.61	0.78	0.75	0.99	0.93
1.5	1.00	1.00	1.00	1.00	1.00	1.00
1.0	1 26			0.97		
0.5	1.42	1.31	1.10	1.07	1.04	1.08
		Run No. 3			Run No. 4	
2.5	0.84	0.96	0.91	0.76	0.91	0.97
1.5	1.00	1.00	1.00	1.00	1.00	1.00
1.0	1.03			1.16		
0.5	1.04	1.06	1.06	1.17	1.09	0.97
		Run No. 5			Run No. 6	
2.5	0.42	0.50	0.76	0.61	0.80	0.93
1.5	1.00	1.00	1.00	1.00	1.00	1.00
1.0	1.63			1.19		
0.5	2.59	1.30	1.15	1.24	1.20	1.02
		Run No. 7			Run No. 8	
2.5	0.72	0.94	1.04	0.76	0.92	0.90
1.5	1.00	1.00	1.00	1.00	1.00	1.00
1.0	1.13			1.14		
0.5	1.22	1.01	1.01	1.29	0.97	0.94
		Run No. 9			Run No. 10	
2.5	0.79	0.81	0.92	0.71	0.88	0.96
1.5	1.00	1.00	1.00	1.00	1.00	1.00
1.0	1.10			1.13		
0.5	1.17	1.10	1.03	1.22	1.01	0.95

V. DEVELOPMENTS IN METEOROLOGICAL INSTRUMENTATION

A. Lightweight cup anemometers

The conventional three-cup anemometers used in the field experiments at Round Hill during 1954-1955 and at O'Neill, Nebraska during Project Prairie Grass have starting and stopping speeds of the order of 1 m sec^{-1}. Measurements based on the records of these instruments are consequently not representative for mean wind speeds below about 2 m sec^{-1}. In order to obtain satisfactory measurements at low wind speeds, low-inertia cup anemometers of the photocell-type (27) have been developed. Details of the construction of the anemometers are shown in fig. 37. The cups are spun from aluminum sheets measuring 0.038 cm in thickness and cadmium plated as a protection against weathering. The support arms are made from 0.159 cm aluminum tubing and fastened to the cups by small (00-90) brass screws. The cups are 3.35 cm in diameter and the distance from the cup center to the vertical shaft is 4.5 cm. The vertical shaft, made from 0.23 cm hardened-steel drill rod, is supported at the top and bottom by miniature ball bearings manufactured by Miniature Precision Bearings, Inc. Jewel bearings may also be used. The beam from the light source, a grain of wheat bulb manufactured by the General Electric Co., is interrupted by a single-slot chopper (metal disk attached to the lower part of the vertical shaft). The slot in the chopper permits the light beam to fall on a Clairex photocell (type CL-3) once during each rotation of the cup wheel. Output of the photocell (photo diode) is amplified and shaped into a square wave that drives a binary scaler; the scaler provides a means for halving the number of cup revolutions counted by the

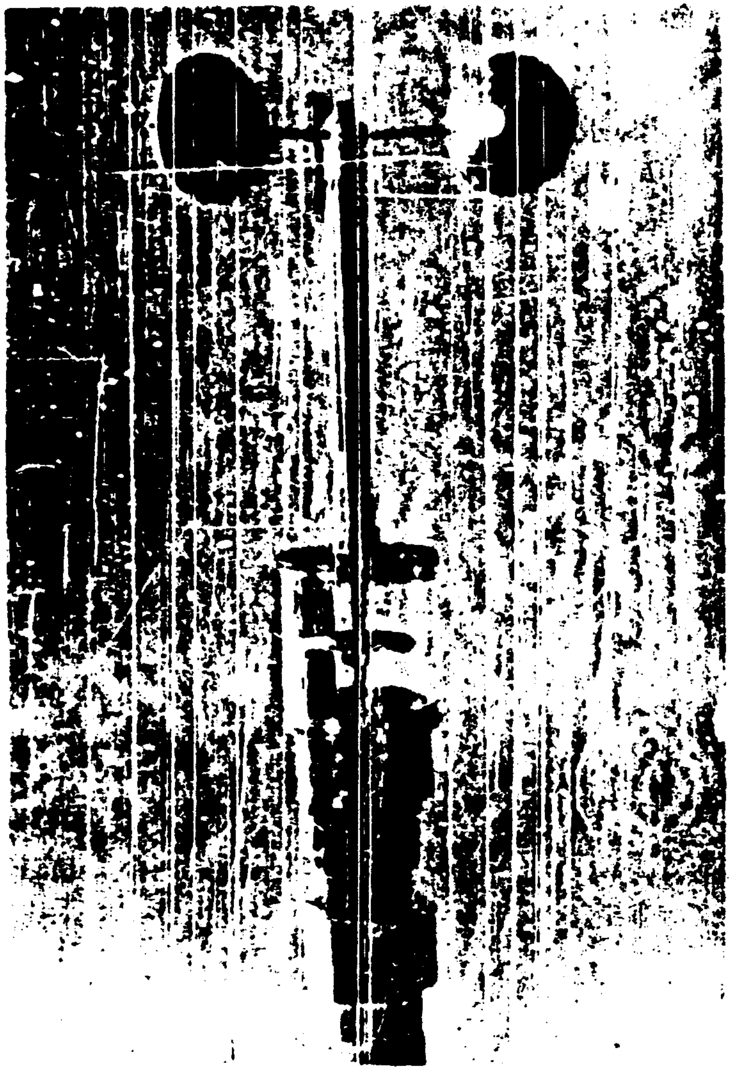

Fig. 37. Closeup of lightweight anemometer showing cadmium-plated aluminum cups (above) and (below) light source, photocell, and chopper for interrupting light beam.

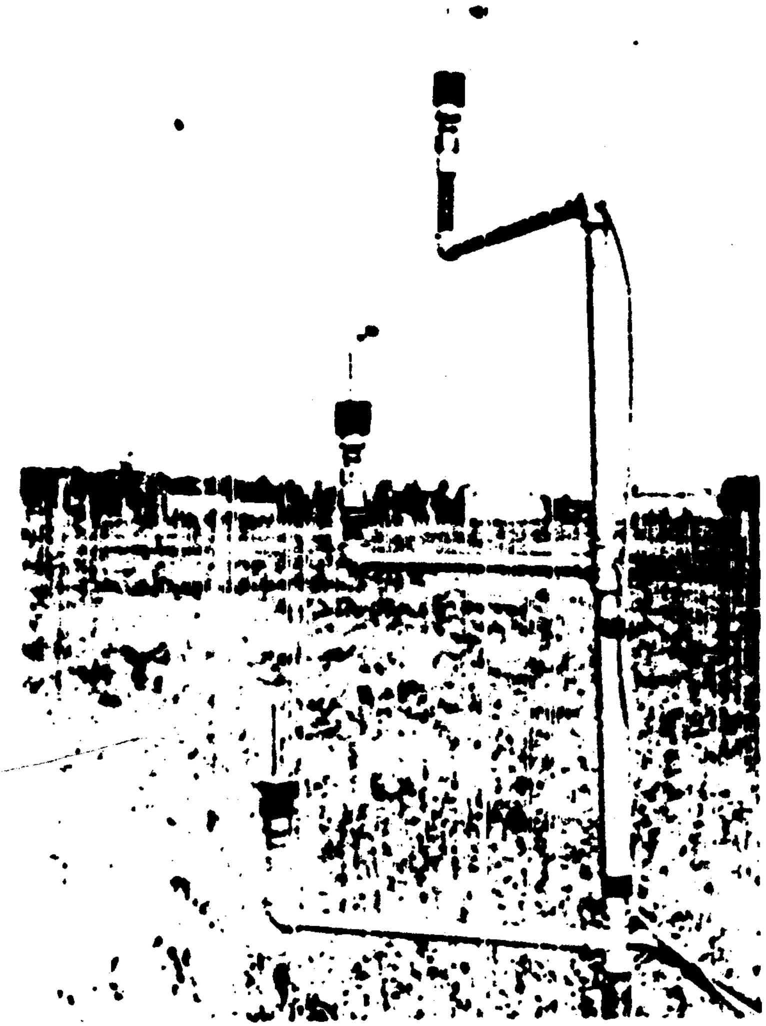

Fig. 38. Field installation of lightweight cup anemometers mounted at heights of 0.5, 1.0, and 1.5 m.

photo cell. The output of the scaler is amplified and serves to operate both a mechanical counter and the pen of an Esterline-Angus operations recorder. Field installation of three anemometers is shown in fig. 38; in this application, the instruments complement vertical profile information obtained from the conventional three-cup anemometers installed on the portable tower.

The instruments have been tested in the project wind tunnel to determine calibration characteristics and their response to rapid fluctuations in air speed. Based on the results for a range of tunnel speeds from 1 to 11 m sec^{-1}, the calibration is approximately given by the linear relationship

$$\bar{V} = 0.36 + 0.82\ N \quad ,$$

where $\bar{V}$ is the wind speed in m sec^{-1} and N is the number of revolutions of the cup wheel per second. Investigations of the deceleration and acceleration characteristics of the anemometers were conducted with the instruments placed in the air stream at the rear of the tunnel. In the deceleration tests, the instruments were allowed to reach equilibrium with respect to various tunnel air speeds and were then suddenly isolated from the air stream by means of a large cardboard box placed over the cups. In acceleration tests, the box was first placed over the cups and then quickly removed to expose the cups to pre-determined tunnel air speeds. Results of acceleration tests indicate that it requires less than 0.5 sec for the cups to reach 63 per cent of the impressed wind speeds within the range from 2 to 10 m sec^{-1}. Similar characteristic times for deceleration varied from about 1 sec, for an initial wind speed of 10 m sec^{-1}, to about 8 sec for an initial wind speed of 2 m sec^{-1}.

Due to the many uncertainties involved in the test procedure, these results provide only rough estimates of the actual response characteristics of the instruments to sudden changes in wind velocity.

B. Automatic data handling and processing system

One of the most formidable problems in empirical investigations of meteorological phenomena is that of data reduction. Fast-response instrumentation, in particular, produces a tremendous number of individual observations within a very short time. Success in obtaining measurements of the requisite type and in the quantity required for further investigations of the structure of turbulence depends in large measure upon the availability of automatic data handling and processing techniques; otherwise, the time and labor involved in the reduction of the data very seriously limits the scope of any experimental program that might be contemplated. Abstraction of the Prairie Grass fast-response observations from the original chart traces involved elaborate automatic equipment and required approximately 8 months for completion. Presentation of the original data in a more usable form would have eliminated the major part of this effort. For these reasons, considerable attention has been focused on the development of a system for the automatic collection and presentation of fast-response measurements; the system has purposely been made sufficiently versatile so that information from other instruments, particularly slow-response types, may also be accomodated. The data processing system performs four major functions: encoding of analog information (shaft rotation, temperature, voltage, etc.)

from sensing elements in the form of binary numbers; storage of these numbers in a relay memory until they can be placed on perforated paper tape; decoding of the perforated paper tape; and, presentation of the data either in the form of sequences printed on an IBM typewriter or as entries on punch cards. Photographs of various components of the system are shown in fig. 39 and a block diagram of the various steps involved in the data processing is presented in fig. 40.

There are a number of suitable analog to binary converters available. Two types have been tested as possible substitutes for the Giannini microtorque potentiometers used in the present bivanes: a Bendix (Eclipse-Pioneer) converter (Type OS-1-A1); and, a perforated circular disk of our own design for use with multiple light sources and photocells. In each case, shaft rotation is represented by integral binary numbers between 2^0 and 2^8; this permits a minimum resolution of 1.4 deg for a 360-deg shaft rotation. In the case of the bivane, azimuth and elevation angle are sampled simultaneously once every second and the information stored in separate relay memories. The number of sensing-element outputs that may be sampled simultaneously is limited only by the number of memory units available; each unit consists of 10 single-pole, double-throw relays and is connected with a single analog to binary converter. If the data are sampled at longer intervals (1 min, for example) one relay memory can be used for more than one analog converter. The programming disk performs the following functions: determines the sampling sequence of observations and the rate of sampling of the outputs of the analog

(a)

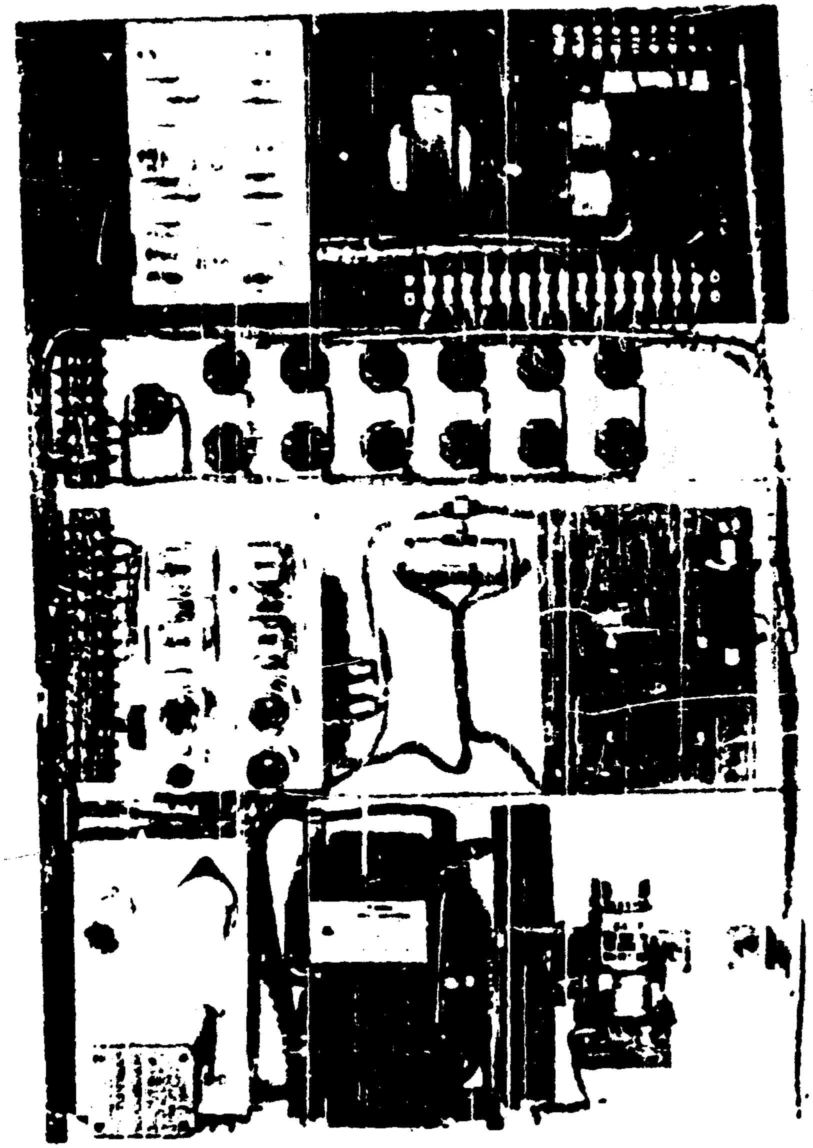

(b)

Fig. 39. Front view of data read-out panel (a) showing tape reader, relay memory I, and control switches. Rear view of data read-out panel (b) showing: distributor and power supply for tape reader; relay memory I; control relays and photocell amplifiers for programming disk; synchronous motor for driving programming disk; high voltage power supply for photocell amplifiers and 6 v d.c. power supply. Cable at lower right leads to binary to decimal converter and relay memory II.

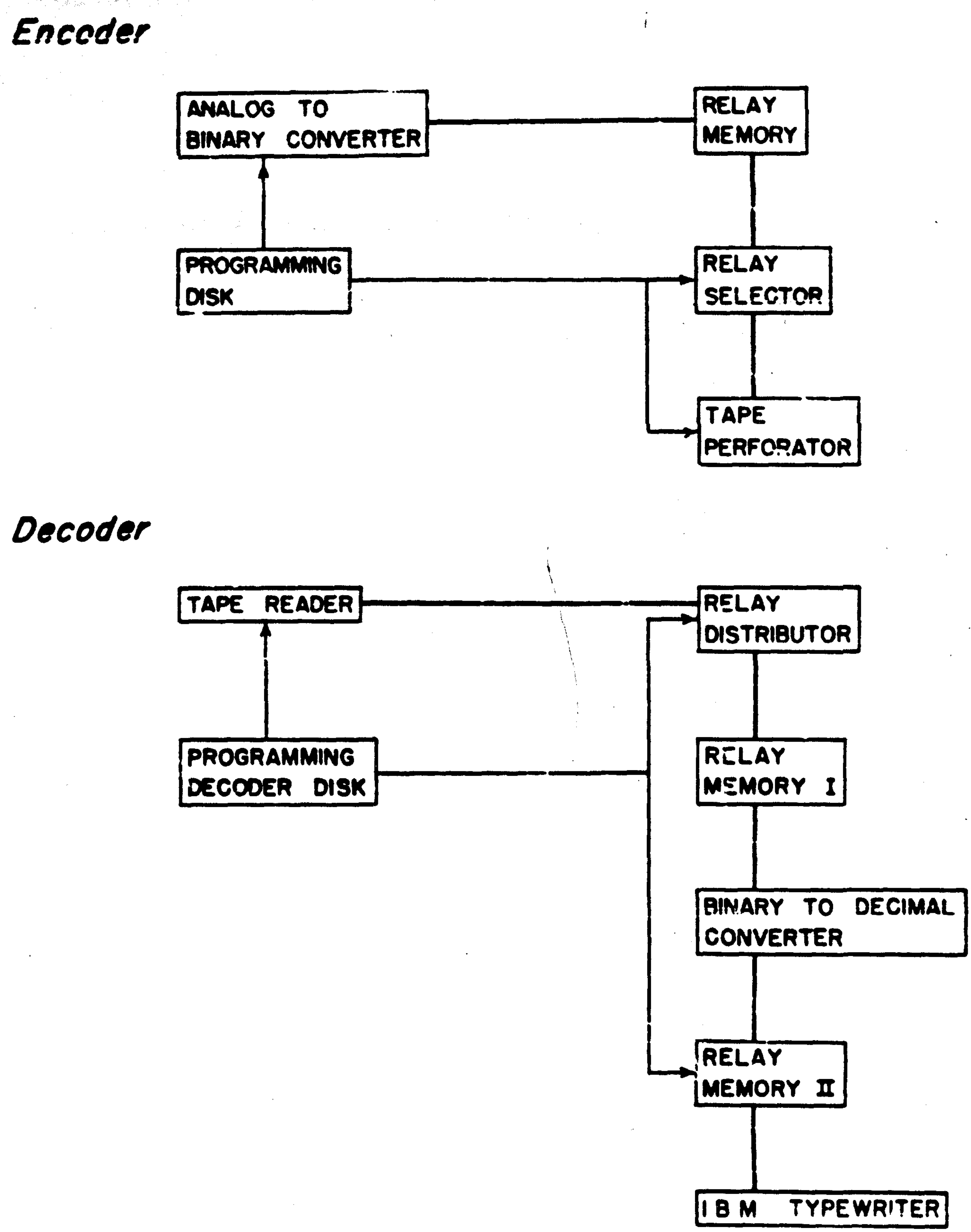

Fig. 40. Block diagrams showing principal components involved in encoding and decoding procedures of data processing system.

to binary converters; selects data from the relay memories and reads them into the tape perforator along with an identification code; activates the perforator magnets which control the tape advance; clears the relay memories for storage of other data. The present tape perforator will accept 8 bits of information per second; if additional capacity is required, the number of perforators may be increased or a faster tape perforator of more recent design might be substituted.

The decoding operation is controlled by a programming disk similar, but less complicated, than the one used in coding the input data. A Multiplex transmitter (model No. 1A) is used to read the perforated tape; the information is channeled into the proper section of the relay memory I by a relay distributor. The binary to decimal converter decodes the binary numbers stored in relay memory I and the resulting bits of information are stored in relay memory II until they can be printed out on an electric typewriter and/or entered on punch cards.

Assembly of the components of the data handling system has been completed only to the extent indicated in fig. 39. The binary to decimal converter, comprised of a series of telephone-type relays which decode the binary numbers and hold them in appropriate relay memories until they can be printed by an electric typewriter, is only partially completed.

REFERENCES

1. Sutton, O. G., 1947 a: The problem of diffusion in the lower atmosphere. Quart. J. r. met. Soc., 73, 257-281.

2. ____________, 1947 b: The theoretical distribution of airborne pollution from factory chimneys. Quart. J. r. met. Soc., 73, 426-436.

3. Deacon, E. L., 1949: Vertical diffusion in the lowest layers of the atmosphere. Quart. J. r. met. Soc., 75, 89-103.

4. Calder, K. L., 1952: Some recent British work on the problem of diffusion in the lower atmosphere. Proc. U. S. Tech. Conf. Air Poll., New York, Mc Graw-Hill, 787-792.

5. Stewart, N. G., H. J. Gale, and R. N. Crooks, 1954: The atmospheric diffusion of gases discharged from the chimney of the Harwell Pile (BEPO). Atom. En. Res. Estab. Rep. HP/R 1452. Harwell, 40 pp.

6. Barad, M. L., and D. A. Haugen, 1958: An evaluation of Sutton's hypothesis for diffusion from a continuous point source. (Paper presented at New York Meeting of Am. meteor. Soc., 28 Jan. 1958.)

7. Hilst, G. R., 1957: The dispersion of stack gases in stable atmospheres. (To be published in J. Air Poll, Cont. Assoc.)

8. Hewson, E. W., H. E. Cramer, G. C. Gill, and F. A. Record, 1951: Research on turbulence and diffusion of particulate matter in the lower layers of the atmosphere. Final rep. under Contract No. AF 28(099)-7, Mass. Inst. of Tech., 80 pp.

9. Cramer, H. E., G. C. Gill, and F. A. Record, 1954: Research on atmospheric turbulence and associated diffusion of aerosols and gases near the earth's surface. Final Rep. under Contract No. AF 19(604)-145, Mass. Inst. of Tech., 49 pp.

10. Cramer, H. E., and F. A. Record, 1953: The variation with height of the vertical flux of heat and momentum. J. Meteor., 10, 219-226.

11. Cramer, H. E., and F. A. Record, 1955: Power spectra of the eddy-velocity components. J. Meteor., 12, 146-151.

12. Record, F. A., and H. E. Cramer, 1957: Preliminary Analysis of Project Prairie Grass diffusion measurements. (Paper to be published in J. Air Poll. Cont. Assoc.)

13. Cramer, H. E., and F. A. Record, 1957: Field studies of atmospheric diffusion and the structure of turbulence. Amer. Ind. Hyg. Assoc. Quart., 18, 126-131.

14. Cramer, H. E., 1957: A practical method for estimating the dispersal of atmospheric contaminants. Proc. First. Nat. Conf. on App. Meteor., C. 33-55.

15. Hay, J. S. and F. Pasquill, 1957: Diffusion experiments from a fixed source at a height of a few hundred feet in the atmosphere. J. Fluid Mech., 2, 299-310.

16. Davidson, B. and J. Halitsky, 1957: A method of estimating the field of instantaneous ground concentration from tower bivane data. (Paper to be published in J. Air Poll. Cont. Assoc.)

17. Lettau, H. H. and B. Davidson, 1957: Exploring the atmosphere's first mile. London., Pergamon Press, 2 vols, 578 pp.

18. Hastings, C. E., 1949: A new type instrument for measuring air velocity. AIEE Misc. Paper No. 49-23, 7 pp.

19. Hastings, C. E. and C. R. Weiske, 1951: A compensated thermal anemometer and flowmeter. AIEE Misc. Paper No. 51-149, 11 pp.

20. Dryden, H. L., G. B. Schubauer, W. C. Mock, Jr., and H. K. Skramstad, 1937: Measurements of the intensity and scale of wind-tunnel turbulence and their relation to the critical Reynold's number of spheres. N. A. C. A. rep. No. 581, 32 pp.

21. Tukey, J. W., 1949: The sampling theory of power spectrum estimates. Symposium on applications of autocorrelation analysis to physical problems at Woods Hole, O. N. R., Washington, D. C., 47-67.

22. Mac Cready, P. B., 1953: Structure of atmospheric turbulence. J. Meteor., 10, 434-449.

23. Panofsky, H. A., and R. J. Deland, 1957: Structure of turbulence at O'Neill, Nebraska and its relation to the structure at Brookhaven National Laboratory, Upton, Long Island. Contract No. AF 19(604)-1027, AFCRC-TR-58-201.

24. Suomi, V. E., 1957: Energy budget studies at the earth's surface and development of the sonic anemometer for spectrum analysis. Contract No. AF 19(122)-461, AFCRC-TR-56-274.

25. Howcroft, J. G., and J. R. Smith, 1956: A selective analysis of the scale of atmospheric turbulence. J. Meteor., 13, 75-81.

26. Panofsky, H. A., V. R. K. Rao, and H. E. Cramer, 1958: An observational study of the relation between space and time spectra. (To be published in Quart. J. r. met. Soc.)

27. Kassander, A. R., Jr., R. M. Stewart, Jr., and H. Falk, 1954: A simple low-inertia anemometer of the three-cup type. Sci. Rep. No. 3 under Contract AF 19(122)-440, Iowa State College, Ames, Iowa.

28. Gosline, C. A., 1952: Dispersion from short stacks. Chem. Eng. Progr., 48, 165-172.

29. Sutton, O. G., 1953: Micrometeorology. McGraw-Hill, New York, p. [illegible].

ACKNOWLEDGMENTS

The authors wish to acknowledge the helpful suggestions and other important contributions made by the project supervisor, Professor H. G. Houghton. The research described in this report would not have been possible without the splendid cooperation and vital contributions of the following members of the Round Hill staff: Helene Banvie, George Fontes, Harry V. Geary, John E. Luby, and James H. Peers. Mr. Gerald C. Gill, now at the University of Michigan, participated in the research program during 1954 and the first half of 1955.

APPENDIX A

SUMMARY OF DIFFUSION MEASUREMENTS AND METEOROLOGICAL OBSERVATIONS OBTAINED AT ROUND HILL DURING 1954 - 1955

Table I. Ten-minute average concentrations of sulfur-dioxide gas and frequency distributions of azimuth wind direction.

Explanatory Notes

Concentrations refer to measurements at height of 2 m along three semicircular arcs at travel distances of 50, 100, and 200 m from a continuous point source of sulfur-dioxide gas located 30 cm above ground level. Individual sampling stations were spaced at intervals of 3 deg and are identified in the table by post numbers of the sampling network, post no. 1 being located along the base line of the array directly north-northeast of the release point for the gas.

Frequency distributions of azimuth wind direction are based on records from a wind vane located at a height of 2 m near the source for mean wind speeds in excess of 2 m sec^{-1}; otherwise, the distributions were obtained from bivane data. Entries are in terms of percentage frequency of occurrence within 3-deg class intervals referred to the post numbers of the sampling network.

Although no data are available on the vertical distribution of concentrations, it is apparent from the measurements that the axis of the time-mean gas plume was on occasion lower than the height of the samplers. This phenomenon is of particular significance at short travel distances in the presence of stable thermal stratification and light winds. On the basis of indirect evidence, the following concentration data are considered non-representative of axial plume concentration. At 50 m: Run Nos. 6, 7, 9, 10, and 13; at 100 m: Run Nos. 9, 10, 13; at 200 m: Run Nos. 9, 10 are possibly non-representative.

SULFUR-DIOXIDE CONCENTRATIONS AND ASSOCIATED FREQUENCY DISTRIBUTION OF AZIMUTH WIND DIRECTION

DATE 13 August 1954 - Run #1 TIME 0915-0925 E.S.T.

Post number	Wind Direction (per cent)	Concentration ($mg\ m^{-3}$) Arc 50m	100m	200m
1				
2				
3				
4				
5				
6				
7				
8				
9				0.010
10	0.42			0.015
11				0.005
12				
13				0.015
14	0.42	0.035		0.005
15	0.42	0.040		0.015
16	0.42	0.040		0.015
17	0.83	0.075	0.015	0.015
18	0.42	0.145	0.040	0.015
19	1.24	0.140	0.040	0.010
20	0.83	0.305	0.055	0.010
21	1.24	0.315	0.095	0.025
22		0.185	0.040	0.025
23	1.66	0.185	0.065	0.005
24	0.83	0.355	0.065	0.025
25	1.66	0.440	0.085	0.035
26	0.42	0.360	0.095	0.040
27	0.83	0.300	0.065	0.040
28	0.83	0.265	0.065	0.035
29	1.24	0.215	0.045	0.035
30	0.83	0.195	0.070	0.020
31	1.24	0.165	0.030	0.030
32	2.49	0.215	0.035	0.015
33	0.42	0.235	0.045	0.025
34	2.90	0.255	0.055	0.035
35	2.90	0.385	0.075	0.040
36	2.07	0.370	0.090	0.035
37	1.24	0.435	0.100	0.045
38	2.90	0.375	0.075	0.040
39	1.24	0.400	0.060	0.040
40	2.07	0.395	0.075	0.050
41	4.98	0.425	0.085	0.030
42	4.56	0.480	0.100	0.035
43	4.98	0.985	0.150	0.030
44	7.06	0.830	0.165	0.015
45	6.23	0.940	0.220	0.030
46	2.90	0.940	0.160	0.035
47	5.40	1.13	0.050	0.020
48	10.79	1.04	0.055	0.015
49	4.15	0.755	0.035	0.005
50	2.49	0.595	0.020	0.005
51	2.90	0.370	0.065	0.005
52	2.07	0.240		
53	0.42	0.065		
54	1.66	0.015		
55				
56				
57	0.42			
58	2.07			
59				
60				
61	0.42			
>61	1.49			

SULFUR-DIOXIDE CONCENTRATIONS AND ASSOCIATED FREQUENCY DISTRIBUTION OF AZIMUTH WIND DIRECTION

DATE 7 October 1954 - Run #2 TIME 1400-1410 E.S.T.

Post number	Wind Direction (per cent)	Concentration ($mg\ m^{-3}$) Arc 50m	100m	200m
1				
2				
3				
4				
5				
6				
7				
8				
9				
10				
11				
12				
13				
14				
15				
16				
17				
18				
19				
20				
21				
22				
23				
24				
25				
26				
27				
28				
29				
30				
31				
32	0.42			
33	0.42	0.040		
34	0.42	0.130		
35	0.42	0.160	0.025	
36	0.83	0.365	0.130	0.015
37	1.66	0.435	0.165	0.020
38	0.83	0.935	0.225	0.050
39	1.66	1.82	0.365	0.060
40	4.56	3.23	0.605	0.140
41	5.81	4.93	1.14	0.280
42	7.47	6.15	1.92	0.320
43	7.88	7.05	2.06	0.460
44	9.13	6.76	1.95	0.430
45	6.22	6.24	1.45	0.320
46	4.15	4.41	1.58	0.335
47	7.05	3.65	1.25	0.280
48	5.40	4.29	0.980	0.270
49	4.56	3.97	0.725	0.155
50	6.64	3.16	0.695	0.135
51	2.49	2.08	0.685	0.115
52	4.15	2.97	0.685	0.145
53	3.73	1.80	0.585	0.090
54	4.56	1.56	0.285	0.060
55	2.49	1.29	0.255	0.015
56	0.83	0.580	0.200	
57	1.66	0.605	0.130	
58	1.24	0.985	0.055	
59	1.24	1.09	0.015	
60	0.83	0.770	0.005	
61	0.83	0.335	0.005	
62	0.42			

SULFUR-DIOXIDE CONCENTRATIONS AND ASSOCIATED FREQUENCY DISTRIBUTION OF AZIMUTH WIND DIRECTION

DATE 21 October 1954 - Run #3 TIME 0910-0920 E.S.T.

Post number	Wind Direction (per cent)	Concentration ($mg\ m^{-3}$) Arc 50m	100m	200m
1				
2				
3				
4				
5				
6				
7				
8				
9				
10				
11				
12				
13				
14				
15				
16				
17				
18				
19				
20				
21				
22				
23				
24				
25				
26				
27		0.050		
28				
29		0.075		
30		0.075		0.050
31	1.66	0.420		0.030
32	1.24	1.45		
33	1.24	2.22		
34	1.66	5.45	0.140	0.055
35	4.56	11.2	0.770	
36	4.15	19.0	1.59	0.085
37	8.71	20.6	3.43	0.055
38	9.55	21.5	5.50	0.300
39	9.55	27.2	7.16	0.850
40	5.81	27.0	7.15	1.92
41	11.62	24.9	6.80	2.29
42	9.55	28.3	8.92	2.29
43	7.88	28.7	9.89	2.16
44	7.88	25.3	8.08	2.24
45	4.98	22.9	6.02	1.80
46	3.73	13.8	3.59	0.970
47	3.32	7.30	1.72	0.340
48	2.49	4.18	0.650	0.055
49	0.42	1.18	0.240	
50		0.220	0.050	0.240
51		0.040	0.020	0.090
52		0.040		0.005
53				0.015
54		0.015		0.010
55		0.075	0.140	0.005
56		0.025	0.160	
57			0.120	0.015
58				0.060
59				0.115
60			0.100	0.110
61				0.160

SULFUR-DIOXIDE CONCENTRATIONS AND ASSOCIATED FREQUENCY DISTRIBUTION OF AZIMUTH WIND DIRECTION

DATE 28 October 1954 - Run #4 TIME 1040-1050 E.S.T.

Post number	Wind Direction (per cent)	Concentration ($mg\ m^{-3}$) Arc 50m	100m	200m
1				
2				
3				
4				
5				
6				
7				
8				
9				
10				
11	0.42			
12				
13		0.120		
14		0.540	0.035	
15		0.720	0.050	
16		1.46	0.070	
17	1.24	1.84	0.110	
18	0.42	1.13	0.260	
19	1.24	1.02	0.390	
20	0.42	1.42	0.460	0.040
21	1.66	1.86	0.630	0.075
22	0.42	3.51	1.24	0.100
23	2.49	5.32	1.13	0.150
24	5.81	6.63	0.920	0.150
25	4.98	5.88	1.30	0.150
26	4.15	5.00	1.09	0.210
27	4.98	5.28	0.920	0.250
28	4.98	5.47	1.03	0.110
29	2.90	4.81	0.760	0.100
30	4.15	3.93	0.720	0.150
31	5.40	3.61	1.38	0.100
32	2.07	4.00	1.05	0.140
33	2.90	5.19	1.33	0.220
34	7.06	4.36	1.03	0.210
35	2.07	2.56	0.890	0.140
36	2.07	2.36	0.980	0.170
37	0.83	2.82	0.800	0.190
38	2.90	3.12	0.750	0.160
39	2.49	2.69	0.570	0.100
40	1.66	2.98	0.570	0.080
41	3.73	3.08	0.620	0.045
42	2.49	2.28	0.640	0.030
43	1.24	2.39	0.720	0.050
44	2.07	2.55	0.870	0.040
45	0.83	2.08	0.790	0.050
46	2.49	2.53	0.770	0.030
47	2.49	2.39	0.800	
48	2.90	2.16	0.480	
49	1.66	1.74	0.130	
50	0.42	1.74	0.025	
51	1.66	1.49	0.015	
52	0.42	1.45		
53	0.42	0.970		
54	2.07	0.970		
55	0.83	0.790		
56	1.24	0.390		
57	0.83	0.270		
58	1.24	0.100		
59	0.42	0.065		
60	0.42			
61				
62	[illegible]			

SULFUR-DIOXIDE CONCENTRATIONS AND ASSOCIATED FREQUENCY DISTRIBUTION OF AZIMUTH WIND DIRECTION

DATE 9 November 1954 - Run #5 TIME 1010-1020 E.S.T.

Post number	Wind Direction (per cent)	Concentration ($mg\ m^{-3}$) Arc 50m	100m	200m
1				
2				
3				
4				
5				
6				
7				
8				
9				
10				
11				
12				
13				
14				
15				
16				
17				
18				
19				
20				
21				
22				
23				
24				
25				
26				
27				
28				
29				
30				
31				

Post number	Wind Direction (per cent)	Concentration ($mg\ m^{-3}$) Arc 50m	100m	200m
32				
33				
34				
35		0.015		
36		0.055		
37		0.110	0.080	
38	1.28	0.370	0.115	0.005
39	2.56	1.04	0.480	0.135
40	0.85	2.23	0.460	0.190
41	1.28	2.29	1.03	0.230
42	2.14	2.01	1.09	0.300
43	2.99	1.93	0.860	0.260
44	4.70	2.15	0.570	[illegible]
45	3.85	2.98	[illegible]	[illegible]
46	6.84	3.73	[illegible]	[illegible]
47	6.41	6.86	1.56	0.250
48	9.83	10.3	3.22	0.480
49	5.13	12.6	3.75	0.730
50	6.41	13.0	2.97	0.700
51	10.68	12.4	3.05	0.730
52	8.97	11.6	3.54	0.950
53	6.84	12.2	3.15	0.770
54	8.12	8.86	2.91	0.640
55	2.14	6.30	2.20	0.410
56	5.56	4.45	1.41	0.070
57	2.56	2.75	0.340	
58	0.43	1.27	0.030	
59	0.43	0.590	0.020	
60		0.230	0.025	
61		0.065	0.005	

Film just no [illegible]

SULFUR-DIOXIDE CONCENTRATIONS AND ASSOCIATED FREQUENCY DISTRIBUTION OF AZIMUTH WIND DIRECTION

DATE 1 December 1954 - Run #6 TIME 1045-1055 E.S.T.

Post number	Wind Direction (per cent)	Concentration ($mg\ m^{-3}$) Arc 50m	100m	200m
1				
2				
3				
4				
5				
6				
7				
8				
9				
10				
11				
12				
13				
14				
15				
16				
17				
18				
19				
20				
21				
22				
23				
24		0.130		
25	0.42	0.850	0.015	
26	1.46	2.44	0.070	
27	3.77	2.97	0.350	0.005
28	2.51	2.87	1.04	0.150
29	3.77	3.90	1.94	0.290
30	4.60	4.16	1.75	0.410
31	4.60	4.77	1.08	0.260
32	1.25	3.58	1.00	0.350
33	2.93	3.22	1.07	0.380
34	1.67	3.82	1.02	0.280
35	1.26	5.13	1.01	0.290
36	2.52	5.81	0.540	0.230
37	5.23	5.09	1.29	0.270
38	6.28	4.42	1.77	0.310
39	7.53	7.04	2.16	0.370
40	8.16	8.97	2.41	0.570
41	6.90	9.21	3.02	0.920
42	12.77	8.70	3.01	0.660
43	8.78	7.04	2.62	0.430
44	3.14	7.37	2.18	0.320
45	2.09	8.35	1.32	0.360
46	1.67	5.70	1.16	0.085
47	1.46	3.33	0.470	0.085
48	2.30	2.11	0.300	0.085
49	1.46	1.76	0.420	0.035
50	1.05	1.47	0.320	
51	0.42	0.940	0.140	0.090
52		0.720	0.085	0.020
53		0.750	0.005	0.040
54		0.300		0.060
55		0.110		0.050
56		0.070		
57		0.055		
58		0.020		
59				
60				
61				

SULFUR-DIOXIDE CONCENTRATIONS AND ASSOCIATED FREQUENCY DISTRIBUTION OF AZIMUTH WIND DIRECTION

DATE 2 March 1955 - Run #7 TIME 1145-1155 E.S.T.

Post number	Wind Direction (per cent)	Concentration ($mg\ m^{-3}$) Arc 50m	100m	200m
1		0.125	0.030	
2		0.105	0.100	0.005
3		0.320	0.075	
4		1.52	0.195	0.015
5	1.60	2.90	0.660	0.095
6	5.75	6.21	1.72	0.340
7	4.79	11.2	3.47	0.810
8	14.38	13.3	4.55	1.20
9	10.54	14.1	5.12	1.35
10	13.74	13.7	4.90	1.24
11	12.46	11.7	4.01	1.07
12	14.38	8.93	2.71	0.770
13	6.39	[illegible].05	1.48	0.350
14	8.31	3.61	0.990	0.130
15	4.15	2.31	0.370	0.030
16	3.19	0.870	0.160	0.005
17	0.32	0.155	0.005	
18		0.025		
19			0.010	
20		0.010	0.010	
21		0.010		
22		0.010		
23		0.010		
24				
25				
26				
27				
28				
29				
30				
31				

Post number	Wind Direction (per cent)	Concentration ($mg\ m^{-3}$) Arc 50m	100m	200m
32				
33				
34				
35				
36				
37				
38				
39				
40				
41				
42				
43				
44				
45				
46				
47				
48				
49				
50				
51				
52				
53				
54				
55				
56				
57				
58				
59				
60				
61				

SULFUR-DIOXIDE CONCENTRATIONS AND ASSOCIATED FREQUENCY DISTRIBUTION OF AZIMUTH WIND DIRECTION

DATE 3 March 1955 - Run #8 TIME 1035-1045 E.S.T.

Post number	Wind Direction (per cent)	Concentration ($mg\ m^{-3}$) Arc 50m	100m	200m
1				
2				
3				
4				
5				
6				
7				
8				
9				
10				
11				
12				
13				
14				
15				
16				
17				
18				
19				
20				
21				
22				
23				
24				
25		0.290	0.380	0.135
26	0.42	1.54	0.960	0.330
27		2.36	1.16	0.310
28	0.84	2.62	1.40	0.630
29	2.09	3.68	2.07	0.690
30	1.67	5.26	2.02	0.500
31	7.11	5.02	1.18	0.320
32	3.35	6.34	0.780	0.145
33	7.95	5.44	1.07	0.125
34	4.18	4.37	0.870	0.165
35	1.26	2.68	0.740	0.165
36	3.35	4.67	1.02	0.165
37	0.84	5.08	0.980	0.250
38	2.09	3.71	1.07	0.210
39	1.67	3.85	1.02	0.300
40	2.09	5.67	0.880	0.280
41	4.60	6.86	1.60	0.270
42	5.02	8.86	2.64	0.460
43	7.11	9.82	2.51	0.520
44	7.11	8.07	2.99	0.470
45	6.70	9.05	2.72	0.290
46	10.04	8.03	2.30	0.290
47	5.02	11.1	1.96	0.175
48	3.77	9.42	2.14	0.210
49	2.09	9.42	2.48	0.380
50	3.77	11.0	2.07	0.600
51	1.67	8.12	2.00	0.410
52	0.42	7.02	1.12	0.290
53	2.93	5.54	0.760	0.145
54	0.42	2.69	0.870	0.310
55	0.42	1.51	0.680	0.050
56		0.450	0.105	
57		0.105		
58		0.125		
59		0.100		
60		0.040		
61		0.045		

SULFUR-DIOXIDE CONCENTRATIONS AND ASSOCIATED FREQUENCY DISTRIBUTION OF AZIMUTH WIND DIRECTION

DATE 7 March 1955 - Run #9 TIME 1140-1150 E.S.T.

Post number	Wind Direction (per cent)	Concentration ($mg\ m^{-3}$) Arc 50m	100m	200m
1	0.42	0.145	0.050	
2		0.480	0.070	
3	0.42	1.85	0.145	0.010
4	0.84	2.59	0.820	0.060
5	2.53	4.77	1.44	0.340
6	5.91	6.65	2.40	0.640
7	4.64	10.1	3.34	0.970
8	13.08	14.4	4.96	1.24
9	12.66	16.5	5.97	1.56
10	11.39	16.4	5.03	1.30
11	12.66	13.3	4.45	0.960
12	10.12	8.82	2.92	0.680
13	6.33	6.97	2.07	0.460
14	5.91	4.67	1.23	0.410
15	2.95	2.83	0.520	0.370
16	1.27	2.02	0.750	0.270
17	1.69	1.74	0.850	0.040
18	2.11	1.16	0.260	
19	1.27	0.390	0.070	
20	1.69	0.070		
21	1.69	0.015		
22	0.42			
23				
24				
25				
26				
27				
28				
29				
30				
31				
32				
33				
34				
35				
36				
37				
38				
39				
40				
41				
42				
43				
44				
45				
46				
47				
48				
49				
50				
51				
52				
53				
54				
55				
56				
57				
58				
59				
60				
61				

ULFUR-DIOXIDE CONCENTRATIONS AND ASSOCIATED FREQUENCY DISTRIBUTION OF AZIMUTH WIND DIRECTION

ATE 23 March 1955 - Run #10 TIME 1125-1135 E.S.T.

Post number	Wind Direction (per cent)	Concentration ($mg\ m^{-3}$) Arc 50m	100m	200m
1				
2				
3				
4				
5				
6				
7				
8	0.42			
9	0.84	0.065		
10	0.42	0.120		
11	0.42	0.420	0.020	
12	0.42	0.850	0.065	
13	2.51	1.92	0.165	
14	2.93	2.44	0.380	
15	4.18	3.61	0.780	0.030
16	7.95	5.39	1.09	0.200
17	5.86	7.32	1.98	0.370
18	7.95	8.75	2.57	0.560
19	8.79	8.71	2.34	0.630
20	7.53	8.13	2.17	0.490
21	5.85	6.90	2.14	0.540
22	6.27	6.49	2.18	0.450
23	6.69	5.01	1.71	0.300
24	3.35	4.66	1.27	0.180
25	6.69	4.74	1.26	0.310
26	3.35	3.78	1.37	0.250
27	3.77	3.28	0.790	0.230
28	2.51	3.16	0.880	0.220
29	1.67	2.51	1.19	0.350
30	2.09	2.91	0.990	0.260
31	2.09	2.19	0.900	0.160

Post number	Wind Direction (per cent)	Concentration ($mg\ m^{-3}$) Arc 50m	100m	200m
32	1.26	1.19	0.370	0.060
33	2.51	0.760	0.085	0.030
34	0.42	0.420	0.085	
35	0.42	0.330	0.035	
36		0.250		
37		0.115		
38	0.84	0.035		
39		0.030		
40				
41				
42				
43				
44				
45				
46				
47				
48				
49				
50				
51				
52				
53				
54				
55				
56				
57				
58				
59				
60				
61				

SULFUR-DIOXIDE CONCENTRATIONS AND ASSOCIATED FREQUENCY DISTRIBUTION OF AZIMUTH WIND DIRECTION

DATE 23 March 1955 - Run #11 TIME 1545-1555 E.S.T.

Post number	Wind Direction (per cent)	Concentration ($mg\ m^{-3}$) Arc 50m	100m	200m
1				
2				
3				
4				
5				
6				
7				
8				
9				
10				
11		0.065		
12		0.280		
13		0.290		
14		0.500	0.145	
15	2.08	1.16	0.270	
16	2.50	2.36	0.820	0.065
17	1.25	3.09	0.850	0.135
18	2.92	3.98	1.07	0.210
19	5.42	5.63	1.45	0.340
20	5.83	7.15	1.67	0.460
21	7.08	8.08	2.30	0.460
22	13.34	8.15	3.21	0.530
23	11.67	8.15	2.30	0.650
24	8.75	7.70	2.41	0.700
25	5.83	6.82	2.55	0.750
26	6.25	7.00	2.23	0.560
27	5.42	6.30	1.65	0.340
28	4.58	5.29	1.49	0.220
29	4.58	4.35	0.990	0.165
30	5.83	3.53	0.740	0.080
31	1.25	2.76	0.560	0.025

Post number	Wind Direction (per cent)	Concentration ($mg\ m^{-3}$) Arc 50m	100m	200m
32	1.67	1.23	0.260	
33	0.83	0.830	0.025	
34	1.67	0.350		
35	0.83	0.100		
36	0.42			
37				
38				
39				
40				
41				
42				
43				
44				
45				
46				
47				
48				
49				
50				
51				
52				
53				
54				
55				
56				
57				
58				
59				
60				
61				

SULFUR-DIOXIDE CONCENTRATIONS AND ASSOCIATED FREQUENCY DISTRIBUTION OF AZIMUTH WIND DIRECTION

DATE 25 March 1955 - Run #12 TIME 1050-1100 E.S.T.

Post number	Wind Direction (per cent)	Concentration ($mg\ m^{-3}$) Arc 50m	100m	200m
1				
2				
3				
4				
5				
6				
7		0.035		
8	0.63	0.160		
9	2.30	0.440		
10	4.17	0.940	0.085	
11	6.89	4.19	0.400	0.050
12	4.80	5.67	1.73	0.330
13	2.30	6.25	1.92	0.400
14	3.13	5.71	1.04	0.125
15	4.17	4.65	0.900	0.085
16	2.50	3.78	0.950	0.130
17	3.76	6.37	1.44	0.200
18	4.17	8.68	1.94	0.340
19	4.17	11.2	2.60	0.480
20	3.76	10.3	3.29	0.490
21	6.89	11.0	2.83	0.430
22	3.34	10.4	2.14	0.350
23	3.76	7.50	1.26	0.240
24	4.59	6.44	1.36	0.300
25	3.75	7.12	1.50	0.290
26	3.34	6.41	1.60	0.340
27	6.47	6.19	1.80	0.410
28	6.47	5.38	2.38	0.360
29	3.76	5.24	1.45	0.230
30	2.09	4.41	0.800	0.180
31	2.30	3.15	0.450	0.160
32	1.46	2.60	0.540	0.030
33	1.25	2.25	0.420	
34	0.63	1.00	0.410	
35	0.63	0.840	0.290	
36	0.84	0.930	0.015	
37	0.63	0.590		
38	1.04	0.530		
39		0.910		
40		0.115		
41		0.015		
42				
43				
44				
45				
46				
47				
48				
49				
50				
51				
52				
53				
54				
55				
56				
57				
58				
59				
60				
61				

SULFUR-DIOXIDE CONCENTRATIONS AND ASSOCIATED FREQUENCY DISTRIBUTION OF AZIMUTH WIND DIRECTION

DATE 28 March 1955 - Run #13 TIME 1505-1515 E.S.T.

Post number	Wind Direction (per cent)	Concentration ($mg\ m^{-3}$) Arc 50m	100m	200m	Post number	Wind Direction (per cent)	Concentration ($mg\ m^{-3}$) Arc 50m	100m	200m
1					32	3.73	3.49	0.800	0.290
2					33	3.93	3.30	0.810	0.220
3					34	3.93	2.82	0.750	0.165
4					35	2.28	2.65	0.600	0.085
5					36	4.56	1.75	0.470	0.055
6					37	1.24	1.15	0.210	
7					38	1.24	0.840	0.110	
8					39	1.45	0.430	0.035	
9					40	0.21	0.300		
10	0.21				41		0.145		
11					42	0.21	0.030		
12	0.21				43		0.025		
13					44				
14					45				
15	0.41				46				
16	0.41	0.030			47				
17		0.110			48				
18	1.45	0.350	0.025		49				
19	0.62	0.600	0.055		50				
20	2.07	1.31	0.140		51				
21	4.14	2.31	0.340		52				
22	5.59	3.34	0.340	0.055	53				
23	7.25	4.65	1.12	0.205	54				
24	9.52	4.79	1.57	0.370	55				
25	6.83	6.35	1.88	0.610	56				
26	9.73	7.35	2.48	0.700	57				
27	7.04	8.16	2.53	0.490	58				
28	7.66	7.53	1.95	0.400	59				
29	4.56	6.84	1.65	0.370	60				
30	6.00	5.68	1.41	0.310	61				
31	3.52	4.28	0.990	0.330					

SULFUR-DIOXIDE CONCENTRATIONS AND ASSOCIATED FREQUENCY DISTRIBUTION OF AZIMUTH WIND DIRECTION

DATE 29 March 1955 - Run #14   TIME 1120-1130 E.S.T.

Post number	Wind Direction (per cent)	Concentration ($mg\ m^{-3}$) Arc 50m	100m	200m
1				
2				
3				
4				
5	0.62			
6	0.41			
7	0.62	0.085		
8	0.41	0.170		
9	1.04	0.300		
10	0.83	0.340	0.015	
11	0.83	0.480	0.055	0.030
12	1.04	1.26	0.085	0.040
13	1.04	1.35	0.205	0.070
14	1.45	1.94	0.390	0.060
15	1.87	3.07	0.690	0.115
16	2.07	3.91	1.15	0.200
17	2.07	5.56	1.16	0.100
18	4.56	4.86	1.10	0.100
19	1.87	3.35	1.15	0.090
20	3.11	3.55	1.11	0.135
21	1.66	5.50	0.970	0.220
22	3.74	6.84	1.62	0.240
23	6.64	10.3	1.81	0.330
24	6.02	12.1	2.64	0.410
25	3.53	10.0	2.56	0.650
26	6.64	7.97	3.25	0.960
27	5.19	7.77	3.04	0.900
28	8.30	6.52	2.16	0.620
29	4.15	7.59	2.02	0.440
30	4.98	7.40	1.69	0.490
31	1.87	5.57	1.63	0.460
32	4.15	5.10	1.26	0.250
33	1.45	3.75	0.730	0.050
34	5.39	2.18	0.390	0.030
35	2.70	1.50	0.490	0.030
36	3.32	1.92	0.180	0.010
37	0.83	1.52	0.110	
38	1.66	1.21	0.015	
39	1.04	0.640		
40	0.41	0.375		
41		0.140		
42		0.170		
43	0.62			
44	0.21			
45	0.21			
46	0.41			
47				
48	0.83			
49	0.21			
50				
51				
52				
53				
54				
55				
56				
57				
58				
59				
60				
61				

SULFUR-DIOXIDE CONCENTRATIONS AND ASSOCIATED FREQUENCY DISTRIBUTION OF AZIMUTH WIND DIRECTION

DATE 30 March 1955 - Run #15 TIME 1030-1040 EST E.S.T.

Post number	Wind Direction (per cent)	Concentration (mg m^{-3}) Arc 50m	100m	200m
1				
2				
3				
4				
5				
6				
7				
8				
9				
10				
11				
12				
13				
14				
15				
16				
17				
18	0.21	0.025		
19	0.41	0.140		
20		0.145		
21	0.83	0.550		
22	0.21	1.34	0.030	
23	1.25	1.60	0.145	
24	1.87	2.65	0.350	
25	0.83	3.69	0.430	
26	1.87	2.44	0.600	0.035
27	1.25	1.97	0.710	0.070
28	2.08	1.87	0.330	0.125
29	1.45	[illegible]	0.330	0.035
30	0.41	2.11	0.230	0.045
31	4.25	3.62	0.480	0.115
32	3.53	2.71	1.09	0.075
33	1.04	3.56	0.390	0.020
34	1.66	3.24	0.240	0.040
35	2.49	3.41	0.740	0.040
36	3.11	5.08	1.04	0.075
37	2.49	7.07	1.23	0.105
38	2.49	7.43	1.68	0.130
39	3.73	7.42	1.81	0.360
40	3.94	5.88	1.71	0.410
41	2.90	3.50	1.80	0.330
42	2.08	3.18	1.75	0.300
43	3.53	4.49	1.16	0.185
44	3.94	4.62	1.19	0.200
45	4.15	4.03	1.30	0.195
46	7.05	5.30	1.12	0.350
47	5.81	6.14	2.04	0.510
48	6.43	6.26	2.55	0.690
49	4.56	8.59	2.41	0.630
50	4.98	12.6	2.46	0.620
51	7.05	8.93	2.68	0.690
52	3.94	5.44	1.88	0.530
53	1.04	3.03	1.07	0.290
54	0.83	1.97	0.660	0.250
55		2.05	0.770	0.160
56		2.13	0.540	0.135
57		1.65	0.530	0.135
58	0.41	0.470	0.360	0.070
59		0.150	0.290	
60		0.035	0.030	
61				

...LFUR-DIOXIDE CONCENTRATIONS AND ASSOCIATED FREQUENCY DISTRIBUTION OF AZIMUTH ... DIRECTION

...TE 31 March 1955 - Run #16 TIME 2040-2050 E.S.T.

Post number	Wind Direction (per cent)	Concentration ($mg\ m^{-3}$) Arc 50m	100m	200m
1				
2				
3				
4				
5				
6				
7				
8				
9	0.21			
10				
11	0.21	0.010		
12		0.010		
13	0.21	0.030		
14		0.025		
15		0.055		
16		0.020	0.005	
17		0.075	0.020	
18		0.045	0.010	
19	0.41	0.050		
20	0.21	0.420	0.020	
21	1.25	1.52	0.030	
22	3.11	2.49	0.220	0.005
23	4.98	4.27	0.430	0.020
24	8.92	6.66	0.780	0.060
25	4.98	12.0	1.99	0.185
26	10.16	15.2	5.40	0.590
27	13.90	16.4	6.59	1.50
28	15.14	16.4	6.90	2.23
29	6.43	18.6	7.44	2.55
30	5.60	19.0	5.74	2.13
31	4.77	15.9	3.80	1.28
32	5.19	11.1	2.69	0.610
33	3.94	6.20	2.11	0.185
34	2.07	3.32	1.26	0.065
35	2.70	2.53	0.490	0.040
36	1.25	2.50	0.095	0.005
37	1.66	1.46	0.045	
38	1.45	0.450	0.025	
39	0.41	0.025	0.010	
40	0.21	0.035	0.010	
41	0.21			
42	0.21			
43				
44	0.21			
45				
46				
47				
48				
49				
50				
51				
52				
53				
54				
55				
56				
57				
58				
59				
60				
61				

SULFUR-DIOXIDE CONCENTRATIONS AND ASSOCIATED FREQUENCY DISTRIBUTION OF AZIMUTH WIND DIRECTION

DATE 31 March 1955 - Run #17 TIME 2215-2225 E.S.T.

Post number	Wind Direction (per cent)	Concentration ($mg\ m^{-3}$) Arc 50m	100m	200m	Post number	Wind Direction (per cent)	Concentration ($mg\ m^{-3}$) Arc 50m	100m	200m
1					32	0.21	1.45		
2					33		0.095		
3					34	0.21	0.010		
4					35	0.21	0.035		
5					36				
6					37				
7					38				
8					39				
9					40				
10					41				
11					42				
12					43				
13					44				
14	0.21				45				
15	0.41				46				
16	0.21				47				
17	1.24				48				
18	1.87	0.215			49				
19	0.62	2.63			50				
20	3.73	6.16	0.055		51				
21	6.22	11.7	0.450		52				
22	11.00	26.0	4.91	0.045	53				
23	10.17	49.8	12.6	0.860	54				
24	9.75	53.3	31.1	7.03	55				
25	11.41	59.9	32.4	14.1	56				
26	15.97	55.4	24.2	9.50	57				
27	11.83	44.9	15.1	3.18	58				
28	12.56	20.1	4.51	0.670	59				
29	0.83	5.50	0.550	0.030	60				
30	0.62	4.13	0.105		61				
31	0.62	3.38							

[illegible] CONCENTRATIONS AND ASSOCIATED FREQUENCY DISTRIBUTION OF AZIMUTH [illegible] DIRECTION

13 June 1955 - Run #18 TIME 2035-2045 E.S.T.

Post number	Wind Direction (per cent)	Concentration ($mg\ m^{-3}$) Arc 50m	100m	200m
1				
2				
3	0.41			
4	0.62			
5	1.04			
6	1.04	0.500		
7	1.85	2.61	0.035	
8	3.10	5.98	0.300	0.035
9	4.14	11.1	1.14	0.190
10	7.66	19.7	3.92	0.500
11	5.38	37.1	8.88	1.75
12	12.42	38.2	14.8	3.34
13	7.87	33.3	13.7	3.67
14	9.94	28.5	9.27	2.59
15	6.83	23.3	8.27	1.99
16	[illegible]	[illegible]	6.51	1.27
17	6.62	16.4	3.95	0.540
18	7.66	11.2	1.76	0.150
19	5.18	5.86	0.170	0.030
20	1.86	2.26	0.030	
21	2.90	0.250		
22	1.66	0.100		
23	1.04			
24	1.04			
25	0.21			
26	0.41			
27	0.21			
28				
29				
30				
31				

Post number	Wind Direction (per cent)	Concentration ($mg\ m^{-3}$) Arc 50m	100m	200m
32				
33				
34				
35				
36				
37				
38				
39				
40				
41				
42				
43				
44				
45				
46				
47				
48				
49				
50				
51				
52				
53				
54				
55				
56				
57				
58				
59				
60				
61				

SULFUR-DIOXIDE CONCENTRATIONS AND ASSOCIATED FREQUENCY DISTRIBUTION OF AZIMUTH WIND DIRECTION

DATE 13 June 1955 - Run #19 TIME 2240-2250 E.S.T.

Post number	Wind Direction (per cent)	Concentration ($mg\ m^{-3}$) Arc 50m	100m	200m
1				
2				
3				
4				
5				
6				
7				
8	0.21			
9	0.21	0.030		
10	0.21	0.030		
11	0.41	0.125		
12	0.41	0.320	0.010	
13	0.21	1.31	0.010	
14	2.28	1.94	0.095	
15	2.90	3.06	0.280	
16	4.14	5.53	0.390	
17	3.73	9.55	1.64	0.025
18	6.21	17.7	3.51	0.560
19	7.25	24.0	5.28	1.20
20	7.45	26.8	7.27	2.10
21	7.04	34.7	11.0	3.33
22	6.62	34.7	12.4	4.33
23	9.52	26.7	10.6	3.28
24	7.45	20.9	7.93	1.67
25	8.07	16.0	4.13	0.880
26	8.07	13.7	2.38	0.390
27	6.00	8.35	0.660	0.180
28	4.97	3.93	0.230	0.040
29	2.69	1.57	0.030	0.020
30	1.66	0.460		
31	1.04	0.460		
32	1.04	0.090		
33	0.21			
34				
35				
36				
37				
38				
39				
40				
41				
42				
43				
44				
45				
46				
47				
48				
49				
50				
51				
52				
53				
54				
55				
56				
57				
58				
59				
60				
61				

SULFUR-DIOXIDE CONCENTRATIONS AND ASSOCIATED FREQUENCY DISTRIBUTION OF AZIMUTH WIND DIRECTION

DATE 15 June 1955 - Run #20 TIME 2050-2100 E.S.T.

Post number	Wind Direction (per cent)	Concentration ($mg\ m^{-3}$) Arc 50m	100m	200m
1				
2				
3				
4				
5				
6	1.66	0.310		
7	3.83	2.09	0.040	0.015
8	6.82	8.88	1.53	0.610
9	10.48	34.4	10.5	8.75
10	12.98	77.3	39.1	25.1
11	15.81	131	67.7	21.8
12	12.98	116	43.6	12.3
13	12.14	58.0	29.2	3.46
14	9.15	41.1	21.5	2.24
15	5.99	51.3	14.6	2.09
16	3.99	53.0	10.2	0.450
17	1.83	33.5	6.79	0.035
18	1.00	17.4	2.38	
19	1.00	4.15	0.870	
20	0.17	1.82	0.060	
21		0.250		
22	0.17	0.025		
23				
24				
25				
26				
27				
28				
29				
30				
31				

Post number	Wind Direction (per cent)	Concentration ($mg\ m^{-3}$) Arc 50m	100m	200m
32				
33				
34				
35				
36				
37				
38				
39				
40				
41				
42				
43				
44				
45				
46				
47				
48				
49				
50				
51				
52				
53				
54				
55				
56				
57				
58				
59				
60				
61				

SULFUR-DIOXIDE CONCENTRATIONS AND ASSOCIATED FREQUENCY DISTRIBUTION OF AZIMUTH WIND DIRECTION

DATE 19 October 1955- Run #21 TIME 2245-2255 E.S.T.

Post number	Wind Direction (per cent)	Concentration ($mg\ m^{-3}$) Arc 50m	100m	200m
1				
2				
3				
4				
5				
6				
7				
8				
9				
10				
11				
12				
13				
14				
15				
16	0.17			
17	0.83	0.075		
18	0.33	0.960		
19	0.83	3.57	0.020	
20	1.00	14.0	0.120	
21	1.83	19.3	1.35	0.015
22	5.49	21.8	5.41	0.340
23	14.97	37.6	17.8	1.84
24	11.65	39.4	28.1	6.62
25	20.30	41.1	30.3	11.0
26	11.65	39.8	26.1	9.21
27	10.48	31.9	18.2	4.86
28	9.98	20.3	7.96	2.84
29	5.32	14.4	2.44	0.470
30	1.83	5.64	0.320	0.025
31	2.00	0.620	0.025	

Post number	Wind Direction (per cent)	Concentration ($mg\ m^{-3}$) Arc 50m	100m	200m
32	0.50	0.120		
33	0.17			
34	0.33			
35	0.17			
36	0.17			
37				
38				
39				
40				
41				
42				
43				
44				
45				
46				
47				
48				
49				
50				
51				
52				
53				
54				
55				
56				
57				
58				
59				
60				
61				

SULFUR-DIOXIDE CONCENTRATIONS AND ASSOCIATED FREQUENCY DISTRIBUTION OF AZIMUTH WIND DIRECTION

DATE 20 October 1955 - Run #22 TIME 0050-0100 E.S.T.

Post number	Wind Direction (per cent)	Concentration ($mg\ m^{-3}$) Arc 50m	100m	200m
1				
2				
3				
4				
5				
6				
7				
8				
9				
10				
11				
12				
13				
14				
15				
16				
17		0.015		
18		0.400	0.015	
19	0.16	2.76	0.065	
20	1.93	14.4	1.92	0.070
21	5.00	30.1	9.20	1.03
22	13.39	40.1	21.8	6.33
23	20.32	41.1	34.2	12.3
24	20.97	41.8	35.7	15.7
25	16.93	37.4	27.3	10.4
26	8.23	23.4	7.95	1.43
27	7.10	10.2	0.780	0.090
28	3.23	1.45	0.085	0.015
29	1.45	0.100	0.010	
30	0.32	0.030		
31	0.97	0.030		

Post number	Wind Direction (per cent)	Concentration ($mg\ m^{-3}$) Arc 50m	100m	200m
32				
33				
34				
35				
36				
37				
38				
39				
40				
41				
42				
43				
44				
45				
46				
47				
48				
49				
50				
51				
52				
53				
54				
55				
56				
57				
58				
59				
60				
61				

SULFUR-DIOXIDE CONCENTRATIONS AND ASSOCIATED FREQUENCY DISTRIBUTION OF AZIMUTH WIND DIRECTION

DATE 25 October 1955 - Run #23 TIME 2235-2245 E.S.T.

Post number	Wind Direction (per cent)	Concentration ($mg\ m^{-3}$) Arc 50m	100m	200m
1				
2				
3				
4				
5				
6				
7				
8		0.050		
9		0.530	0.015	
10	0.17	3.53	0.100	
11	0.33	10.4	0.830	
12	0.50	13.8	3.77	0.055
13	1.33	22.8	8.89	0.330
14	4.31	33.5	13.5	2.01
15	6.80	45.3	17.7	6.52
16	6.80	38.2	19.9	7.37
17	12.27	35.7	14.4	4.20
18	13.76	32.8	15.2	5.02
19	16.25	32.2	18.6	5.24
20	13.43	27.0	17.8	4.76
21	14.43	22.8	10.9	4.19
22	6.14	28.7	13.0	4.20
23	1.82	20.9	10.9	3.41
24	1.16	13.0	2.71	0.940
25	0.50	4.44	0.540	0.035
26		0.560	0.110	
27		0.095	0.010	
28		0.020		
29				
30				
31				
32				
33				
34				
35				
36				
37				
38				
39				
40				
41				
42				
43				
44				
45				
46				
47				
48				
49				
50				
51				
52				
53				
54				
55				
56				
57				
58				
59				
60				
61				

SULFUR-DIOXIDE CONCENTRATIONS AND ASSOCIATED FREQUENCY DISTRIBUTION OF AZIMUTH WIND DIRECTION

DATE 27 October 1955 - Run #24 TIME 2035-2045 E.S.T.

Post number	Wind Direction (per cent)	Concentration ($mg\ m^{-3}$) Arc 50m	100m	200m
1				
2				
3				
4				
5				
6				
7				
8				
9				
10				
11				
12				
13				
14				
15				
16				
17				
18				
19				
20				
21				
22				
23				
24		0.025		
25		0.260		
26	0.83	0.710		
27	1.00	2.83	0.095	
28	4.33	5.10	0.760	
29	3.83	9.76	5.84	0.660
30	4.50	13.7	11.3	4.13
31	15.17	25.5	11.1	7.52
32	20.17	25.8	19.1	13.0
33	22.67	25.9	22.9	17.8
34	17.50	17.4	25.1	13.4
35	8.17	4.24	5.51	0.170
36	1.50	0.180	0.260	
37	0.33	0.010	0.005	
38				
39				
40				
41				
42				
43				
44				
45				
46				
47				
48				
49				
50				
51				
52				
53				
54				
55				
56				
57				
58				
59				
60				
61				

SULFUR-DIOXIDE CONCENTRATIONS AND ASSOCIATED FREQUENCY DISTRIBUTION OF AZIMUTH WIND DIRECTION

DATE 27 October 1955 - Run #25 TIME 2145-2155 E.S.T.

Post number	Wind Direction (per cent)	Concentration ($mg\ m^{-3}$) Arc 50m	100m	200m
1				
2				
3				
4				
5				
6				
7				
8				
9				
10				
11				
12				
13				
14				
15				
16				
17				
18				
19				
20				
21				
22				
23				
24				
25				
26				
27				
28				
29		0.030	0.020	
30	0.17	0.400	0.010	
31	2.32	7.77	0.060	0.020

Post number	Wind Direction (per cent)	Concentration ($mg\ m^{-3}$) Arc 50m	100m	200m
32	1.99	17.4	2.30	0.015
33	6.62	24.7	10.2	0.150
34	7.78	23.6	12.8	2.68
35	18.87	23.6	10.7	4.66
36	17.88	27.0	24.3	6.99
37	13.41	19.5	20.3	10.1
38	10.10	12.5	13.1	12.3
39	9.93	11.0	8.33	11.3
40	3.48	11.2	6.60	11.1
41	4.30	12.4	6.25	7.82
42	2.98	8.14	6.89	6.99
43	0.17	5.73	10.0	7.70
44		6.37	8.99	6.63
45		6.49	6.38	5.64
46		6.53	7.62	0.350
47		5.03	6.55	0.015
48		3.44	4.48	
49		1.38	0.640	
50		1.96	0.035	
51		0.160		
52		0.030		
53				
54				
55				
56				
57				
58				
59				
60				
61				

SULFUR-DIOXIDE CONCENTRATIONS AND ASSOCIATED FREQUENCY DISTRIBUTION OF AZIMUTH WIND DIRECTION

DATE 31 October 1955 - Run #26 TIME 2105-2115 E.S.T.

Post number	Wind Direction (per cent)	Concentration ($mg\ m^{-3}$) Arc 50m	100m	200m
1				
2				
3				
4				
5				
6				
7				
8				
9				
10				
11				
12				
13				
14				
15				
16				
17				
18				
19	0.21			
20	0.21			
21	0.41			
22	0.41			
23	0.62	0.245	0.005	
24	0.41	0.610	0.010	
25	2.29	1.85	0.050	
26	2.91	4.99	0.045	
27	8.11	8.34	1.66	0.085
28	7.28	12.6	2.94	0.380
29	8.73	19.9	4.99	1.13
30	7.90	20.6	6.24	1.67
31	10.60	19.5	7.25	2.39
32	13.31	17.5	8.20	2.62
33	8.73	18.1	8.02	2.07
34	7.28	20.0	7.49	2.29
35	8.73	17.9	5.31	1.21
36	3.74	13.3	2.69	0.230
37	3.33	8.57	0.790	0.025
38	1.66	3.71	0.170	
39	2.08	0.970	0.010	
40	0.21	0.160	0.005	
41	0.21	0.020		
42	0.21			
43	0.21			
44	0.21			
45				
46				
47				
48				
49				
50				
51				
52				
53				
54				
55				
56				
57				
58				
59				
60				
61				

SULFUR-DIOXIDE CONCENTRATIONS AND ASSOCIATED FREQUENCY DISTRIBUTION OF AZIMUTH WIND DIRECTION

DATE 31 October 1955 - Run #27 TIME 2250-2300 E.S.T.

Post number	Wind Direction (per cent)	Concentration ($mg\ m^{-3}$) Arc 50m	100m	200m	Post number	Wind Direction (per cent)	Concentration ($mg\ m^{-3}$) Arc 50m	100m	200m
1					32	2.07	1.04	0.200	0.015
2					33	3.11	2.52	0.520	0.015
3					34	3.11	5.36	0.730	0.180
4					35	7.26	7.84	1.20	0.690
5					36	9.13	11.2	2.96	0.260
6					37	11.62	16.9	3.24	1.14
7					38	7.88	17.5	4.06	1.22
8					39	9.13	13.3	4.86	1.16
9					40	10.15	11.5	3.75	1.00
10					41	7.47	10.6	3.65	0.900
11					42	4.56	9.81	2.81	0.660
12					43	3.32	9.49	2.59	0.500
13					44	4.36	9.98	1.94	0.540
14					45	3.11	8.72	0.830	0.260
15					46	2.49	4.25	0.340	0.160
16					47	1.04	3.69	0.610	0.010
17					48	1.04	2.78	0.390	
18					49	1.66	1.24	0.470	
19					50	0.62	0.690	0.270	
20					51	0.21	0.640	0.015	
21					52	0.42	0.320	0.015	
22	0.42				53		0.105		
23	0.21				54		0.010		
24	0.62				55				
25	0.21	0.045			56				
26	0.42	0.450			57				
27	0.83	0.460			58				
28	0.42	0.4[illegible]			59				
29	1.24	0.[illegible]30	0.065		60				
30	1.04	0.300	0.150		61				
31	0.83	0.690	0.115	0.015					

SULFUR-DIOXIDE CONCENTRATIONS AND ASSOCIATED FREQUENCY DISTRIBUTION OF AZIMUTH WIND DIRECTION

DATE 8 November 1955 - Run #28 TIME 2130-2140 E.S.T.

Post number	Wind Direction (per cent)	Concentration ($mg\ m^{-3}$) Arc 50m	100m	200m
1				
2				
3				
4				
5				
6				
7				
8				
9				
10				
11	0.17			
12	0.83	0.110		
13	1.33	4.83	0.030	
14	2.99	15.2	3.52	
15	6.99	40.8	11.7	0.300
16	10.48	47.4	27.8	9.37
17	11.31	51.3	41.4	22.0
18	14.31	34.7	22.2	10.2
19	10.47	26.8	8.39	2.39
20	11.15	16.8	3.80	1.13
21	6.49	25.9	8.97	2.49
22	4.33	19.5	11.8	4.65
23	2.83	17.5	7.55	3.46
24	2.33	8.24	5.00	0.940
25	2.33	3.11	0.660	0.210
26	2.33	1.20	0.020	
27	0.83	0.060		
28	0.17			
29	0.33			
30				
31				

Post number	Wind Direction (per cent)	Concentration ($mg\ m^{-3}$) Arc 50m	100m	200m
32				
33				
34				
35				
36				
37				
38				
39				
40				
41				
42				
43				
44				
45				
46				
47				
48				
49				
50				
51				
52				
53				
54				
55				
56				
57				
58				
59				
60				
61				

SULFUR-DIOXIDE CONCENTRATIONS AND ASSOCIATED FREQUENCY DISTRIBUTION OF AZIMUTH WIND DIRECTION

DATE 8 November 1955 - Run #29 TIME 2310-2320 E.S.T.

Post number	Wind Direction (per cent)	Concentration ($mg\ m^{-3}$) Arc 50m	100m	200m
1				
2				
3				
4				
5				
6				
7				
8				
9				
10				
11				
12				
13	0.17			
14	0.17	0.015		
15	0.33	0.160	0.020	
16	0.50	2.20	0.040	0.015
17	0.83	7.97	0.160	0.030
18	1.50	15.3	0.360	0.020
19	3.16	29.6	5.22	0.330
20	6.31	47.8	13.7	1.86
21	8.80	60.8	22.2	5.39
22	17.77	68.5	36.4	12.4
23	18.60	63.8	34.6	16.4
24	19.10	42.1	18.2	8.67
25	9.30	17.7	8.15	2.84
26	8.14	6.55	1.74	0.340
27	4.32	3.33	0.380	0.035
28	0.66	0.710	0.070	
29	0.17	0.[illegible]5		
30	0.17			
31				

Post number	Wind Direction (per cent)	Concentration ($mg\ m^{-3}$) Arc 50m	100m	200m
32				
33				
34				
35				
36				
37				
38				
39				
40				
41				
42				
43				
44				
45				
46				
47				
48				
49				
50				
51				
52				
53				
54				
55				
56				
57				
58				
59				
60				
61				

Table II. Summary of source strengths Q for the 1954-1955 diffusion experiments and correction factors by which concentration data presented in table 1 should be multiplied to compensate for evaporational loss of impinger solution during aeration.

Run No.	Date	Time(EST)	Q(g sec^{-1})	Arc radius (m) 50	100	200
1	8-13-54	0915-0925	1.00	0.93	0.93	0.92
2	10- 7-54	1400-1410	4.43	0.91	0.94	0.93
3	10-21-54	0910-0920	11.4[illegible]	0.90	0.91	0.92
4	10-28-54	1040-1050	6.67	0.91	0.87	0.86
5	11- 9-54	1010-1020	8.82	0.95	0.94	0.96
6	12- 1-54	1045-1055	7.24	0.96	0.91	0.92
7	3- 2-55	1145-1155	9.16	0.95	0.94	0.96
8	3- 3-55	1035-1045	9.31	0.96	0.94	0.93
9	3- 7-55	1140-1150	9.84	0.98	0.99	0.97
10	3-23-55	1125-1135	10.04	0.96	0.97	0.97
11	3-23-55	1545-1555	9.96	0.98	0.97	0.98
12	3-25-55	1050-1100	9.92	0.97	0.97	0.97
13	3-28-55	1505-1515	9.98	0.99	0.96	0.97
14	3-29-55	1120-1130	9.96	0.97	0.97	0.97
15	3-30-55	1030-1040	9.95	0.97	0.97	0.97
16	3-31-55	2040-2050	9.96	0.95	0.95	0.95
17	3-31-55	2215-2225	9.88	0.96	0.96	0.96
18	6-13-55	2035-2045	8.[illegible]	0.98	0.98	0.98
19	6-13-55	2240-2250	8.58	0.97	0.97	0.96
20	6-15-55	2050-2100	8.48	0.98	0.98	0.97
21	10-19-55	2245-2255	6.23	0.95	0.94	0.94
22	10-20-55	0050-0100	6.42	0.97	0.97	0.96
23	10-25-55	2235-2245	6.60	0.98	0.98	0.99
24	10-27-55	2035-2045	5.72	0.96	0.96	0.97
25	10-27-55	2145-2155	5.77	0.96	0.97	0.97
26	10-31-55	2105-2115	6.87	0.98	0.98	0.98
27	10-31-55	2250-2300	6.65	0.98	0.96	0.97
28	11- 8-55	2130-2140	7.94	0.96	0.95	0.95
29	11- 8-55	2310-2320	7.96	0.96	0.96	0.97

Table III. Summary of meteorological observations for 1954-1955 field experiments at Round Hill. Explanation of symbols: $\bar{V}_z$, $\bar{T}_z$ are the mean wind speed in m sec^{-1} and the mean air temperature in deg C, respectively (subscripts refer to the height of the measurements in m); σ_E, σ_A are standard deviations of elevation and azimuth angle, respectively, in deg; M signifies missing data.

Run No.	$\bar{V}_2$*	σ_E	σ_A**	Vertical profiles of mean wind speed and air temperature							
				$\bar{V}_{1.5}$	$\bar{V}_3$	$\bar{V}_6$	$\bar{V}_{12}$	$\bar{T}_{1.5}$	$\bar{T}_3$	$\bar{T}_6$	$\bar{T}_{12}$
1	2.17	11.2	30.4	M	M	M	M	M	M	M	M
2	4.04	6.1	17.6	M	M	M	M	M	M	M	M
3	2.84	5.3	12.5	M	M	M	M	M	M	M	M
4	2.62	10.8	31.5	M	M	M	M	M	M	M	M
5	5.25	4.6	13.9	M	M	M	M	M	M	M	M
6	4.21	4.9	15.5	3.73	4.34	4.70	5.00	4.00	3.73	3.59	3.38
7	8.76	4.0	8.4	7.94	9.21	10.32	M	6.00	5.69	5.43	5.18
8	3.86	5.7	19.8	3.53	4.04	4.39	4.59	2.20	1.91	1.58	1.44
9	7.46	M	11.0	6.77	7.79	8.65	9.46	0.40	0.10	-0.15	-0.41
10	7.12	M	16.6	6.77	7.84	8.65	9.56	5.10	4.91	4.78	4.61
11	7.76	M	13.0	7.08	8.24	8.95	9.71	6.00	6.01	6.02	5.99
12	4.30	5.1	18.6	3.99	4.49	4.85	5.20	5.90	5.48	5.27	4.80
13	9.20	M	15.3	9.31	10.73	11.69	12.65	4.00	3.92	3.89	3.81
14	4.38	5.1	22.0	4.39	4.90	5.25	5.61	3.80	3.32	3.04	2.70
15	4.46	5.2	25.9	4.44	4.90	5.35	5.71	12.75	12.30	12.01	11.76
16	4.56	7.4	12.8	4.70	5.35	5.91	6.47	6.80	7.07	7.23	7.36
17	2.40	6.7	9.5	2.26	2.92	3.23	3.48	6.80	7.30	7.61	7.85
18	2.94	5.5	10.8	2.62	M	3.63	4.09	15.00	15.17	15.26	15.32
19	2.71	5.9	11.8	2.47	M	3.43	3.78	17.00	17.14	17.22	17.29
20	1.87	4.0	8.5	1.76	2.11	2.52	2.97	17.00	17.23	17.40	17.54
21	1.49	4.2	7.7	1.48	1.76	2.21	2.65	13.20	13.31	13.39	13.45
22	1.79	2.8	5.9	1.64	2.13	2.65	3.13	9.70	10.09	10.33	10.55
23	1.74	3.1	7.5	1.84	1.94	2.42	2.70	3.90	4.18	4.41	4.60
24	1.98	1.8	5.1	1.93	2.10	2.69	3.43	5.70	6.57	6.91	7.32
25	1.63	1.7	6.8	1.55	1.89	2.47	2.91	4.50	6.39	7.03	7.43
26	2.79	5.5	10.6	2.70	2.94	3.33	3.75	11.00	11.17	11.26	11.32
27	3.32	5.8	13.8	3.51	3.85	4.26	4.52	11.50	11.59	11.60	11.59
28	1.79	2.9	8.9	1.85	2.05	2.55	2.76	5.10	5.53	5.76	5.90
29	1.78	3.2	6.8	1.72	2.06	2.62	3.11	2.60	3.02	3.29	3.44

*Averages of values from cup anemometer near source and from vertical profile data.

**Averages of data from bivanes and vane near source except for wind speeds below 2 m sec^{-1} when only bivane data were used.

APPENDIX B

SUMMARY OF DIFFUSION MEASUREMENTS AND METEOROLOGICAL OBSERVATIONS OBTAINED AT ROUND HILL DURING 1957

Table I. Sulfur-dioxide concentrations for three periods of sampling and 10-min frequency distributions of azimuth wind direction.

Explanatory Notes

Concentration data comprise average values, determined at a height of 1.5 m, for sampling periods of 10, 3, and 0.5 min at travel distances of 50, 100, and 200 m from a continuous point source of sulfur-dioxide gas. The sampling network consisted of three independently-operated, overlapping arrays located along semicircular arcs. The 10-min array extended over 180 deg of arc and individual stations were spaced at 3-deg intervals; the 3-min array extended over 150 deg of arc and individual stations were spaced at intervals of 1.5 deg; the 0.5-min array used a 1.5-deg separation and extended over an arc of 120 deg. Entries in the table refer to consecutive post numbers of the sampling network, post No. 1 being directly north-northeast of the release point for the tracer. Post Nos. 1 to 6 and 106 to 111 utilized a 3-deg separation interval; the separation between all other consecutive post numbers is 1.5 deg. Vertical sampling was also carried out within the 10-min array at intervals of 15-deg along each semicircular arc. Concentration data are available at these locations for the following additional heights: (50-m arc) 0.5, 1.0, 2.5 m; (100- and 200-m arcs) 0.5, 2.5 m.

The 10-min frequency distributions of azimuth wind direction are based on the records of a vane located at a height of 2 m near the source. Entries represent percentage frequency of occurrence within 3-deg class intervals centered on posts of the sampling network.

In the conduct of the diffusion experiments, the tracer was released horizontally at a height of 1.5 m and permitted to traverse the entire array before the individual samplers were set in operation. The three networks were turned on simultaneously and operation of each network terminated after the appropriate sampling time had elapsed. The emission of the tracer was discontinued after the end of the 10-min sampling period.

SULFUR-DIOXIDE CONCENTRATIONS AND ASSOCIATED FREQUENCY DISTRIBUTION OF AZIMUTH WIND DIRECTION - Run #1

DATE 24 September 1957 TIME 1935 E.S.T. PERIOD OF SAMPLING 10 min

Post number	Wind direction (per cent)	Concentration ($mg\ m^{-3}$) Arc 50m	100m	200m
38	0.42			
40				
42				
44				
46				
48	0.42			
50	1.67			
52		0.630		
54	2.91	5.45		
56	3.75	29.2	0.672	
58	3.33	138	8.12	
60	9.58	282	50.5	1.80
62	14.17	457	141	20.7
64	12.92	471	270	74.8
66	25.42	450	285	117
68	8.33	437	190	54.9
70	6.25	257	53.9	5.96
72	5.00	85.0	6.15	0.231
74	2.91	24.5	0.752	
76	0.83	1.68	0.106	
78	1.25			
80	0.42			
82	0.42			

Post number	Wind direction (per cent)	Concentration ($mg\ m^{-3}$) Arc 50m	100m	200m

Post Number	Height (m)	Concentration ($mg\ m^{-3}$) Arc 50m	100m	200m
56	2.5	19.6	1.93	
	1.0	40.9		
	0.5	49.3	0.182	
66	2.5	265	174	91.2
	1.0	510		
	0.5	520	374	129
76	2.5	2.45	0.031	
	1.0	2.19		
	0.5	1.66	4.15	
	2.5			
	1.0			
	0.5			
	2.5			
	1.0			
	0.5			
	2.5			
	1.0			
	0.5			
	2.5			
	1.0			
	0.5			

SULFUR-DIOXIDE CONCENTRATIONS

DATE 24 September 1957 TIME 1935 C.S.T. PERIOD OF SAMPLING 3 MINUTES

Post No.	Concentration ($mg\ m^{-3}$) Arc 50m	100m	200m	Post No.	Concentration ($mg\ m^{-3}$) Arc 50m	100m	200m
15				52			
16				53			
17				54	0.603		
18				55	2.93		
19				56	9.80		
20				57	28.0	0.280	
21				58	83.0	1.31	
22				59	160	3.67	0.357
23				60	272	16.9	0.343
24				61	377	57.0	1.00
25				62	533	151	7.97
26				63	580	269	27.3
27				64	620	357	78.0
28				65	663	383	131
29				66	643	343	123
30				67	650	240	75.7
31				68	540	200	35.7
32				69	390	120	15.9
33				70	298	53.0	5.33
34				71	198	13.4	1.23
35				72	125	3.83	0.383
36				73	66.3		
37				74	27.4		
38				75	5.43		
39				76	3.10		
40				77	0.560		
41				78			
42				79			
43				80			
44				81			
45				82			
46				83			
47				84			
48				85			
49				86			
50				87			
51				88			

SULFUR-DIOXIDE CONCENTRATIONS

DATE 24 September 1957 TIME 1935 C.S.T. PERIOD OF SAMPLING 0.5 minutes

Post No.	Concentration ($mg\ m^{-3}$) Arc 50m	100m	200m
15			
16			
17			
18			
19			
20			
21			
22			
23			
24			
25			
26			
27			
28			
29			
30			
31			
32			
33			
34			
35			
36			
37			
38			
39			
40			
41			
42			
43			
44			
45			
46			
47			
48			
49			
50			
51			

Post No.	Concentration ($mg\ m^{-3}$) Arc 50m	100m	200m
52			
53			
54			
55			
56	4.54		
57	14.3		
58	47.2	5.20	
59	92.2	7.60	
60	173	22.2	
61	348	89.2	
62	490	142	
63	618	224	
64	808	228	2.14
65	822	376	8.20
66	846	412	20.0
67	1088	398	33.2
68	788	410	38.4
69	610	316	35.2
70	506	161	20.0
71	258	50.0	4.68
72	121	18.4	
73	23.2	1.36	
74	2.22		
75	3.54		
76			
77			
78			
79			
80			
81			
82			
83			
84			
85			
86			
87			
88			

SULFUR-DIOXIDE CONCENTRATIONS AND ASSOCIATED FREQUENCY DISTRIBUTION OF AZIMUTH WIND DIRECTION - Run #2

DATE 2 October 1957 TIME 1120 E.S.T. PERIOD OF SAMPLING 10 min

Post number	Wind direction (per cent)	Concentration ($mg\ m^{-3}$) Arc 50m	100m	200m
24	0.42	0.092		
26		2.54		
28	0.42	4.59	0.117	
30	1.66	14.2	0.655	
32	2.49	29.9	2.38	0.252
34	2.07	52.2	7.68	0.851
36	1.66	68.1	10.8	1.78
38	4.98	76.9	16.6	2.73
40	4.56	85.1	19.9	3.79
42	6.64	93.1	21.4	4.85
44	4.56	89.8	22.8	5.44
46	5.81	162	21.9	4.89
48	7.88	115	23.0	5.75
50	5.39	103	22.5	5.50
52	6.22	97.7	22.1	5.74
54	8.71	110	20.5	5.68
56	9.54	94.9	18.6	4.69
58	6.22	65.8	19.9	3.59
60	2.49	40.9	12.1	1.92
62	2.07	30.5	9.50	2.28
64	2.91	30.7	7.53	1.66
66	4.15	18.1	4.53	1.07
68	3.32	9.51	1.89	1.26
70	1.25	6.73	1.87	0.841
72	1.25	3.95	1.73	0.491
74	0.83	7.51	2.49	0.302
76	1.25	10.6	2.10	0.079
78	0.42	[illegible]	[illegible]	
80	0.83	4.39	0.134	
82		1.90	[illegible]	

Post number	Wind direction (per cent)	Concentration ($mg\ m^{-3}$) Arc 50m	100m	200m
84		1.41		
86		0.077		

Post number	Height (m)	Concentration ($mg\ m^{-3}$) Arc 50m	100m	200m
26	2.5	2.54		
	1.0	1.74		
	0.5	1.49		
36	2.5	52.8	11.6	1.52
	1.0	71.5		
	0.5	73.7	10.6	1.70
46	2.5	81.6	19.7	4.77
	1.0	105		
	0.5	110	23.3	4.52
56	2.5	79.0	19.0	4.04
	1.0	98.6		
	0.5	110	19.9	4.66
66	2.5	17.4	4.73	1.09
	1.0	20.1		
	0.5	22.3	5.43	1.56
76	2.5	7.15	1.93	0.077
	1.0	10.5		
	0.5	12.5	1.89	0.036
86	2.5	0.093		
	1.0	[illegible]		
	0.5	0.059		

SULFUR-DIOXIDE CONCENTRATIONS

DATE 2 October 1957 TIME 1120 [illegible].S.T. PERIOD OF SAMPLING 3 Minutes

Post No.	Concentration (mg m^{-3}) Arc 50m	100m	200m	Post No.	Concentration (mg m^{-3}) Arc 50m	100m	200m
15				52	47.7	22.2	6.80
16				53	52.7	23.[illegible]	7.40
17				54	61.7	24.1	7.60
18				55	66.7	22.0	7.40
19				56	72.3	21.7	7.40
20				57	71.3	19.1	6.13
21				58	86.0	18.1	3.83
22				59	69.7	16.2	3.05
23				60	42.0	12.1	1.68
24				61	28.5	7.30	0.750
25				62	21.5	4.63	0.257
26				63	16.9	1.91	0.243
27				64	10.7	1.41	
28	0.467	0.363		65	5.83	0.620	
29	0.643	0.660		66	2.20	0.187	
30	2.87	1.38		67	0.693		
31	6.80	1.31	0.257	68			
32	13.3	1.24	0.517	69			
33	21.3	2.08	0.880	70			
34	24.1	2.64	1.45	71			
35	32.5	3.97	1.78	72			
36	45.3	6.10	1.75	73			
37	71.0	7.90	2.91	74			
38	78.7	13.1	3.31	75			
39	76.7	16.5	3.93	76			
40	105	14.9	3.77	77			
41	139	21.7	3.05	78			
42	146	25.7	3.80	79			
43	126	27.0	4.07	80			
44	116	24.9	5.03	81			
45	102	25.6	5.73	82			
46	93.7	29.5	6.00	83			
47	95.0	31.1	6.00	84			
48	84.7	29.5	6.27	85			
49	69.7	24.6	5.20	86			
50	53.0	20.1	6.53	[illegible]			
51	52.3	18.5	6.50	[illegible]			

SULFUR-DIOXIDE CONCENTRATIONS

DATE 2 October 1957 TIME 1120 C.S.T. PERIOD OF SAMPLING 0.5 Minutes

Post No.	Concentration (mg m^{-3}) Arc 50m	100m	200m
15			
16			
17			
18			
19			
20			
21			
22			
23			
24			
25			
26			
27			
28			
29			
30			
31			
32			
33			
34			
35			
36			
37	1.30		
38	6.06		
39	7.86		
40	8.46		
41	10.7		
42	10.1		
43	16.9		
44	22.1		
45	21.2		
46	22.8		
47	15.9		
48	16.9		1.28
49	[illegible]	[illegible]	1.22
50	22.1	3.30	0.980
51	22.8	3.72	2.38

Post No.	Concentration (mg m^{-3}) Arc 50m	100m	200m
52	23.8	8.04	5.66
53	56.4	8.04	13.6
54	68.4	10.2	19.2
55	111	18.4	19.2
56	124	34.5	16.0
57	176	57.5	15.6
58	210	62.1	10.6
59	196	47.7	5.36
60	135	34.1	5.36
61	101	15.3	9.80
62	79.0	7.54	1.64
63	70.2	1.82	1.54
64	44.6	2.50	0.920
65	19.8		0.960
66	11.8		2.36
67	1.66		
68			
69			
70			
71			
72			
73			
74			
75			
76			
77			
78			
79			
80			
81			
82			
83			
84			
85			
86			
87			
88			

SULFUR-DIOXIDE CONCENTRATIONS AND ASSOCIATED FREQUENCY DISTRIBUTION OF AZIMUTH WIND DIRECTION - Run #3

DATE 10 October 1957 TIME [illegible] E.S.T. PERIOD OF SAMPLING 10 min

Post number	Wind direction (per cent)	Concentration (mg m^{-3}) Arc 50m	100m	200m
46	0.42			
48		0.031		
50	1.25	0.486		
52	0.83	0.616		
54	1.25	4.32		
56	2.50	11.9	0.203	
58	3.33	21.1	1.34	0.038
60	2.50	44.8	4.51	0.266
62	7.50	82.1	21.9	2.08
64	5.42	121	36.6	8.30
66	9.17	154	56.6	16.3
68	5.00	238	69.8	20.4
70	10.00	262	73.9	22.3
72	10.83	205	59.1	20.1
74	9.17	136	44.8	10.3
76	5.42	110	25.4	3.24
78	7.50	86.5	13.3	0.355
80	6.25	39.3	3.84	0.102
82	4.58	16.8	0.509	
84	2.92	6.01	0.179	
86	2.08	2.87	0.061	
88	1.66	0.706		
90		0.072		
92	0.42	0.047		
94		0.031		

Post number	Wind direction (per cent)	Concentration (mg m^{-3}) Arc 50m	100m	200m

Post Number	Height (m)	Concentration (mg m^{-3}) Arc 50m	100m	200m
56	2.5	11.7	0.218	
	1.0	10.7		
	0.5	9.10	0.211	
66	2.5	10[illegible]	50.1	14.9
	1.0	189		
	0.5	211	62.4	16.3
76	2.5	80.9	25.9	M
	1.0	125		
	0.5	140	25.6	3.65
86	2.5	2.71	M	
	1.0	2.41		
	0.5	2.19	0.115	
	2.5			
	1.0			
	0.5			
	2.5			
	1.0			
	0.5			
	2.5			
	1.0			
	0.5			

[illegible] CONCENTRATIONS

DATE 10 October 1957 TIME 2022 [illegible].S.T. PERIOD OF SAMPLING 3 [illegible]

Post No.	Concentration ($mg\ m^{-3}$) Arc 50m	100m	200m	Post No.	Concentration ($mg\ m^{-3}$) Arc 50m	100m	200m
15				52			
16				53			
17				54			
18				55			
19				56	0.493		
20				57	4.33	0.557	
21				58	5.10	0.383	0.103
22				59	12.2	3.60	0.457
23				60	22.6	4.07	0.643
24				61	39.0	15.3	1.34
25				62	60.3	24.1	3.07
26				63	77.7	27.2	6.07
27				64	81.3	24.6	9.23
28				65	115	33.3	16.2
29				66	159	43.7	18.4
30				67	200	51.0	18.1
31				68	235	72.0	16.0
32				69	324	83.7	9.83
33				70	360	87.3	[illegible]
34				71	350	77.7	18.8
35				72	299	67.7	[illegible]
36				73	229	60.3	15.9
37				74	157	53.0	11.9
38				75	118	40.0	5.10
39				76	99.0	29.2	[illegible]
40				77	102	23.6	1.37
41				78	99.0	16.4	0.307
42				79	69.0	11.3	[illegible]
43				80	41.7	3.10	
44				81	38.7	0.163	
45				82	24.3		
46				83	9.23		
47				84	[illegible]		
48				85	[illegible]		
49				86	[illegible]		
50				[illegible]	[illegible]		
51				[illegible]	[illegible]		

SULFUR-DIOXIDE CONCENTRATIONS

DATE 10 October 1957 TIME 2020 E.S.T. PERIOD OF SAMPLING 0.5 Minutes

Post No.	Concentration (mg m^{-3}) Arc 50m	100m	200m
15			
16			
17			
18			
19			
20			
21			
22			
23			
24			
25			
26			
27			
28			
29			
30			
31			
32			
33			
34			
35			
36			
37			
38			
39			
40			
41			
42			
43			
44			
45			
46			
47			
48			
49			
50			
51			

Post No.	Concentration (mg m^{-3}) Arc 50m	100m	200m
52			
53			
54			
55			
56	2.70		
57	15.8		
58	26.2		
59	42.4	1.10	0.560
60	87.4	5.18	1.30
61	112	27.0	5.46
62	185	42.4	7.16
63	216	39.8	11.4
64	173	48.8	9.96
65	197	69.2	16.2
66	200	80.4	21.6
67	218	92.2	27.0
68	173	107	27.8
69	246	114	14.6
70	232	105	6.32
71	115	52.2	4.10
72	56.4	14.9	2.50
73	13.0	5.70	1.18
74	13.2	0.800	
75	4.20		
76	0.720		
77			
78			
79			
80			
81			
82			
83			
84			
85			
86			
87			
88			

SULPHUR-DIOXIDE CONCENTRATIONS AND ASSOCIATED FREQUENCY DISTRIBUTION OF AZIMUTH WIND DIRECTION - Run [illegible]4

DATE 4 November 1957 TIME 1200 C.S.T. PERIOD OF SAMPLING 10 min

Post number	Wind direction (per cent)	Concentration ($mg\ m^{-3}$) Arc 50m	100m	200m
26				
28			0.171	
30		1.16	0.684	
32	0.83	5.28	2.07	0.076
34	1.67	6.99	3.17	0.220
36	3.33	25.4	8.09	1.77
38	5.00	51.1	18.2	4.65
40	6.67	100	32.8	6.75
42	7.92	126	43.3	12.0
44	5.42	162	46.1	14.2
46	5.83	187	54.2	12.8
48	8.75	191	52.2	11.3
50	9.58	171	42.5	10.4
52	4.17	116	30.3	8.20
54	5.00	101	24.5	4.96
56	8.33	96.6	20.2	5.58
58	5.42	M	22.3	4.96
60	5.00	116	22.8	4.41
62	0.42	133	21.5	3.34
64	2.08	94.5	17.6	3.05
66	1.25	94.2	14.2	2.69
68	2.92	71.3	16.5	1.93
70	2.08	51.9	6.86	0.950
72	2.50	29.4	4.25	0.610
74	2.08	9.00	3.63	0.410
76	2.08	8.14	2.30	0.197
78	0.42	8.31	1.16	
80		3.43	1.37	
82	0.83	2.94	0.344	
84	0.42	4.62	[illegible]	

Post number	Wind direction (per cent)	Concentration ($mg\ m^{-3}$) Arc 50m	100m	200m
86		5.68		
88		2.47		
90		0.110		
92		0.321		

Post number	Height (m)	Concentration ($mg\ m^{-3}$) Arc 50m	100m	200m
36	2.5	23.6	6.89	1.83
	1.0	24.1		
	0.5	28.3	9.10	M
46	2.5	138	50.1	10.9
	1.0	216		
	0.5	236	56.7	12.2
56	2.5	61.6	19.8	5.53
	1.0	108		
	0.5	125	23.8	5.58
66	2.5	64.9	15.8	2.71
	1.0	105		
	0.5	112	15.0	2.59
76	2.5	5.97	1.39	0.235
	1.0	10.0		
	0.5	11.0	2.41	0.158
86	2.5	4.09		
	1.0	5.00		
	0.5	4.56		
	2.5			
	1.0			
	0.5			

SULPHUR-DIOXIDE CONCENTRATIONS

DATE 4 November 1957 TIME 1200 E.S.T. PERIOD OF SAMPLING 3 Minutes

Post No.	Concentration (mg m^{-3}) Arc 50m	100m	200m
15			
16			
17			
18			
19			
20			
21			
22			
23			
24			
25			
26			
27			
28		0.867	
29	0.780	1.54	
30	3.10	2.74	
31	14.5	4.30	
32	17.7	7.23	0.170
33	14.6	7.87	0.193
34	15.7	7.97	0.440
35	32.7	10.7	0.697
36	57.0	17.2	1.23
37	101	22.0	2.67
38	118	31.9	7.13
39	155	47.7	10.2
40	213	61.0	14.3
41	211	74.3	17.4
42	246	87.3	26.2
43	305	96.7	26.8
44	315	96.0	24.4
45	323	99.0	22.0
46	417	112	19.6
47	427	97.3	18.0
48	413	92.7	17.4
49	397	91.7	17.2
50	367	73.3	11.5
51	263	53.3	9.53
52	183	28.6	5.83
53	160	16.8	4.40
54	118	9.23	2.50
55	65.7	5.33	1.93
56	74.0	4.50	3.13
57	60.7	2.11	3.83
58	56.0	1.24	3.63
59	38.7	0.450	2.97
60	30.7	0.303	0.327
61	28.6		0.193
62	27.8		
63	37.3		
64	37.7		
65	34.7		
66	23.4		
67	27.8		
68	15.7		
69	25.0		
70	18.8		
71	13.2		
72	4.53		
73	1.43		
74	0.450		
75	0.340		
76			
77			
78			
79			
80			
81			
82			
83			
84			
85			
86			
87			
88			

SULFUR-DIOXIDE CONCENTRATIONS

DATE 4 November 1957 TIME 1200 C.S.T. PERIOD OF SAMPLING 0.5 Minutes

Post No.	Concentration ($mg\ m^{-3}$) Arc 50m	100m	200m
15			
16			
17			
18			
19			
20			
21			
22			
23			
24			
25			
26			
27			
28		4.50	
29	13.6	9.92	
30	51.0	16.1	
31	185	27.0	
32	195	43.4	
33	139	45.6	
34	111	38.8	
35	115	34.6	
36	142	41.4	
37	234	63.8	2.46
38	346	100	6.98
39	426	116	11.2
40	482	104	6.18
41	388	115	9.78
42	396	119	9.98
43	376	121	11.8
44	380	103	16.4
45	320	76.0	18.2
46	348	76.0	18.2
47	358	56.8	23.0
48	374	46.2	33.8
49	470	32.6	41.0
50	464	20.8	24.4
51	460	22.8	23.0

Post No.	Concentration ($mg\ m^{-3}$) Arc 50m	100m	200m
52	422	17.9	18.8
53	560	10.1	17.2
54	510	11.9	7.58
55	426	7.12	6.98
56	246	10.3	15.8
57	124	3.40	21.6
58	64.0	1.16	23.4
59	41.6		20.2
60	18.9		3.52
61	6.06		3.12
62	4.84		
63	3.46		
64	2.14		
65			
66			
67			
68			
69			
70			
71			
72			
73			
74			
75			
76			
77			
78			
79			
80			
81			
82			
83			
84			
85			
86			
87			
88			

SULFUR-DIOXIDE CONCENTRATIONS AND ASSOCIATED FREQUENCY DISTRIBUTION OF AZIMUTH WIND DIRECTION Run #5

DATE 6 November 1957 TIME 1745 E.S.T. PERIOD OF SAMPLING 10 min

Post number	Wind direction (per cent)	Concentration ($mg\ m^{-3}$) Arc 50m	100m	200m
32	0.42			
34				
36				
38	0.42			
40	0.83	1.28		
42	1.24	5.56		
44	2.90	21.9	0.170	
46	3.32	41.4	6.88	
48	7.88	106	15.3	
50	9.13	190	77.5	2.11
52	9.96	317	189	20.3
54	14.52	325	273	103
56	18.25	424	283	137
58	8.30	494	256	75.5
60	6.64	427	209	30.8
62	7.88	386	70.8	2.24
64	2.90	283	19.8	0.344
66	3.32	121	2.47	
68	0.83	19.9	0.571	
70	0.42	0.737	0.239	
72	0.42	0.385	0.160	
74	0.42		0.166	

Post number	Wind direction (per cent)	Concentration ($mg\ m^{-3}$) Arc 50m	100m	200m

Post Number	Height (m)	Concentration ($mg\ m^{-3}$) Arc 50m	100m	200m
46	2.5	18.3	3.33	
	1.0	71.3		
	0.5	112	6.15	
56	2.5	141	147	104
	1.0	783		
	0.5	1225	482	158
66	2.5	59.6	1.87	
	1.0	161		
	0.5	264	1.70	
	2.5			
	1.0			
	0.5			
	2.5			
	1.0			
	0.5			
	2.5			
	1.0			
	0.5			
	2.5			
	1.0			
	0.5			

[illegible] CONCENTRATIONS

DATE 6 November 1957 TIME [illegible] E.S.T. PERIOD OF SAMPLING 3 Minutes

Post No.	Concentration (mg m^{-3}) Arc 50m	100m	200m
15			
16			
17			
18			
19			
20			
21			
22			
23			
24			
25			
26			
27			
28			
29			
30			
31			
32			
33			
34			
35			
36			
37			
38			
39			
40			
41			
42			
43	0.367		
44	1.99		
45	8.17		
46	14.3	1.15	
47	19.0	2.19	
48	23.0	8.40	
49	12.5	13.2	0.170
50	26.1	16.3	1.79
51	[illegible]	[illegible]	[illegible]

Post No.	Concentration (mg m^{-3}) Arc 50m	100m	200m
52	163	132	2.37
53	229	192	25.2
54	300	246	69.7
55	393	253	80.7
56	413	243	84.3
57	557	284	67.3
58	640	272	46.0
59	633	294	14.5
60	407	258	4.87
61	390	161	0.713
62	450	116	0.187
63	343	68.7	
64	317	26.7	
65	238	10.0	
66	203	2.28	
67	142	0.240	
68	20.6	0.177	
69	4.30	0.150	
70	0.363	0.490	
71			
72			
73			
74			
75			
76			
77			
78			
79			
80			
81			
82			
83			
84			
85			
86			
87			

SULFUR-DIOXIDE CONCENTRATIONS

DATE 6 November 1957 TIME 1745 E.S.T. PERIOD OF SAMPLING 0.5 Minutes

Post No.	Concentration (mg m^{-3}) Arc 50m	100m	200m	Post No.	Concentration (mg m^{-3}) Arc 50m	100m	200m
15				52	170	232	7.72
16				53	208	332	26.4
17				54	294	468	23.0
18				55	486	400	24.2
19				56	528	476	19.7
20				57	652	442	22.8
21				58	592	370	8.54
22				59	484	296	6.20
23				60	464	175	2.80
24				61	232	19.3	1.20
25				62	121		
26				63	39.0		
27				64	14.8		
28				65	1.08		
29				66			
30				67			
31				68			
32				69			
33				70			
34				71			
35				72			
36				73			
37				74			
38				75			
39				76			
40				77			
41				78			
42				79			
43				80			
44	5.60			81			
45	43.6			82			
46	38.0	5.90		83			
47	10.1	12.3		84			
48	8.28	42.2		85			
49	13.9	63.2		86			
50	25.[illegible]	53.0		87			
51	45.6	79.8		88			

SULFUR-DIOXIDE CONCENTRATIONS AND ASSOCIATED FREQUENCY DISTRIBUTION OF AZIMUTH WIND DIRECTION - Run #6

DATE 17 November 1957 TIME 1700 E.S.T. PERIOD OF SAMPLING 10 min

Post number	Wind direction (per cent)	Concentration ($mg\ m^{-3}$) Arc 50m	100m	200m
26	0.83			
28	2.08			
30	1.25	1.00		
32	2.92	5.27		
34	5.42	14.3		
36	3.33	17.4	0.433	
38	11.25	35.1	1.33	0.039
40	7.08	65.8	8.69	0.562
42	8.33	107	26.3	2.79
44	7.08	147	50.7	8.90
46	11.67	205	62.1	19.6
48	10.42	268	89.9	28.4
50	7.91	241	79.7	20.5
52	6.67	210	64.3	16.1
54	5.42	186	55.3	14.5
56	3.75	174	50.7	11.8
58	0.83	145	38.5	8.43
60	1.67	88.3	20.1	3.68
62	1.25	37.9	8.79	0.662
64	0.42	11.5	1.64	0.200
66		2.71	0.102	
68		0.442		
70		0.056		
72				
74				
76	0.42			

Post number	Wind direction (per cent)	Concentration ($mg\ m^{-3}$) Arc 50m	100m	200m

Post number	Height (m)	Concentration ($mg\ m^{-3}$) Arc 50m	100m	200m
36	2.5	12.5	0.280	
	1.0	17.2		
	0.5	16.4	0.351	
46	2.5	105	45.7	17.1
	1.0	268		
	0.5	330	73.1	20.0
56	2.5	102	44.0	11.7
	1.0	222		
	0.5	269	61.7	12.1
66	2.5	2.96	0.092	
	1.0	1.61		
	0.5	1.00	0.046	
	2.5			
	1.0			
	0.5			
	2.5			
	1.0			
	0.5			
	2.5			
	1.0			
	0.5			

SULFUR-DIOXIDE CONCENTRATIONS

DATE 17 November 1957 TIME 1700 C.S.T. PERIOD OF SAMPLING 3 Minutes

Post No.	Concentration (mg m^{-3}) Arc 50m	100m	200m
15			
16			
17			
18			
19			
20			
21			
22			
23			
24			
25			
26			
27			
28			
29			
30			
31			
32	1.10		
33	2.47		
34	4.90		
35	6.07		
36	9.63		
37	19.0	0.210	
38	60.0	1.04	
39	112	2.82	
40	146	8.77	0.087
41	191	19.0	0.360
42	273	37.7	1.57
43	269	53.7	3.14
44	324	92.3	10.5
45	326	131	17.2
46	387	136	36.3
47	530	156	51.3
48	493	166	54.3
49	383	166	52.3
50	306	116	37.0
51	153	75.3	19.6
52	161	66.7	14.0
53	123	54.7	11.7
54	115	32.4	7.27
55	58.0	24.4	2.14
56	37.3	13.6	1.06
57	9.07	5.00	0.343
58	4.47	2.32	
59	1.77	0.860	
60	1.37	0.407	
61	0.547		
62	0.123		
63	0.183		
64	0.320		
65			
66			
67			
68			
69			
70			
71			
72			
73			
74			
75			
76			
77			
78			
79			
80			
81			
82			
83			
84			
85			
86			
87			
88			

[illegible]

DATE 17 November 1957 TIME [illegible] G.M.T. PERIOD OF SAMPLING [illegible] Minutes

Post No.	Concentration (mg m^{-3}) Arc 50m	100m	200m
15			
16			
17			
18			
19			
20			
21			
22			
23			
24			
25			
26			
27			
28			
29			
30			
31			
32			
33			
34	2.76		
35	12.9		
36	17.7		
37	31.2		
38	34.6		
39	104	0.880	
40	192	1.74	
41	332	1.78	
42	316	1.44	
43	298	1.02	
44	318	8.56	1.20
45	272	16.4	7.16
46	362	28.4	15.5
47	432	44.0	12.3
48	402	98.2	11.5
49	460	188	21.0
50	380	196	23.6
51	[illegible]	[illegible]	[illegible]

Post No.	Concentration (mg m^{-3}) Arc 50m	100m	200m
52	226	210	13.7
53	240	194	14.5
54	252	102	14.7
55	32.4	99.4	3.02
56	13.4	54.2	
57	1.62	16.0	
58	1.18	8.40	
59		1.86	
60		1.12	
61			
62			
63			
64			
65			
66			
67			
68			
69			
70			
71			
72			
73			
74			
75			
76			
77			
78			
79			
80			
81			
82			
83			
84			
85			
86			

SULFUR-DIOXIDE CONCENTRATIONS AND ASSOCIATED FREQUENCY DISTRIBUTION OF AZIMUTH WIND DIRECTION - Run #7

DATE 20 November 1957 TIME 1700 E.S.T. PERIOD OF SAMPLING 10 min

Post number	Wind direction (per cent)	Concentration ($mg\ m^{-3}$) Arc 50m	100m	200m
24	0.83	0.572		
26	2.08	2.04		
28	2.08	5.33	0.215	
30	4.16	19.0	0.930	
32	6.25	31.3	3.25	0.056
34	6.67	39.9	8.53	0.244
36	2.92	58.6	15.1	1.63
38	9.17	89.7	20.8	4.35
40	9.58	114	25.9	7.26
42	10.42	112	39.9	9.03
44	7.08	106	35.8	13.7
46	6.67	104	35.3	12.0
48	6.67	92.3	34.8	8.38
50	7.50	102	26.1	5.41
52	5.00	91.2	15.4	3.00
54	3.75	49.1	8.05	1.33
56	3.75	29.0	4.66	0.625
58	2.08	13.9	2.21	0.239
60	0.42	10.7	0.500	
62	1.67	5.88	0.065	
64		0.599		
66				
68	0.83			
70				
72	0.42			

Post number	Wind direction (per cent)	Concentration ($mg\ m^{-3}$) Arc 50m	100m	200m

Post Number	Height (m)	Concentration ($mg\ m^{-3}$) Arc 50m	100m	200m
26	2.5	3.03		
	1.0	2.49		
	0.5	1.89		
36	2.5	45.6	14.2	1.80
	1.0	63.2		
	0.5	71.5	15.2	1.44
46	2.5	69.3	31.3	10.6
	1.0	122		
	0.5	144	38.1	11.8
56	2.5	21.0	4.62	0.695
	1.0	32.8		
	0.5	30.5	4.35	0.725
	2.5			
	1.0			
	0.5			
	2.5			
	1.0			
	0.5			
	2.5			
	1.0			
	0.5			

SULFUR-DIOXIDE CONCENTRATIONS

DATE 20 November 1957 TIME 1700 C.S.T. PERIOD OF SAMPLING 3 Minutes

Post No.	Concentration ($mg\ m^{-3}$) Arc 50m	100m	200m
15			
16			
17			
18			
19			
20			
21			
22			
23			
24			
25			
26			
27			
28			
29			
30			
31			
32			
33	0.666		
34	2.02		
35	3.25	0.460	
36	6.57	2.00	
37	12.9	2.67	0.177
38	25.1	4.33	0.977
39	38.0	6.20	1.96
40	57.0	6.83	2.26
41	67.3	15.8	2.06
42	75.7	30.2	2.92
43	95.7	35.0	5.47
44	118	37.7	8.60
45	[illegible]	32.7	11.5
46	[illegible]	39.0	11.7
47	[illegible]	46.0	[illegible]
48	[illegible]	55.3	12.2
49	[illegible]	51.7	[illegible]
50	[illegible]	[illegible]	[illegible]
51	[illegible]	[illegible]	[illegible]

Post No.	Concentration ($mg\ m^{-3}$) Arc 50m	100m	200m
52	127	23.9	4.83
53	107	20.5	4.07
54	92.0	17.2	3.33
55	87.3	13.6	2.19
56	62.0	10.1	2.26
57	33.1	7.13	1.32
58	M	4.17	0.920
59	26.9	3.10	0.447
60	M	1.94	
61	19.8	0.257	
62	10.5	0.073	
63	[illegible]		
64	1.97		
65			
66			
67			
68			
69			
70			
71			
72			
73			
74			
75			
76			
77			
78			
79			
80			
81			
82			
83			
84			
85			
86			

SULFUR-DIOXIDE CONCENTRATIONS

DATE 20 November 1957 TIME 1700 C.S.T. PERIOD OF SAMPLING 0.5 Minutes

Post No.	Concentration ($mg\ m^{-3}$) Arc 50m	100m	200m
15			
16			
17			
18			
19			
20			
21			
22			
23			
24			
25			
26			
27			
28			
29			
30			
31			
32			
33			
34			
35	0.960		
36	4.08		
37	4.26		
38			
39	2.66		
40	9.94		
41	29.0	0.620	
42	40.0	0.820	
43	53.2	1.30	
44	83.2	14.4	
45	177	12.4	
46	181	11.8	
47	125	14.2	
48	81.4	29.4	1.68
49	138	25.0	2.08
50	121	62.4	4.70
51	110	56.6	4.56
52	120	29.0	4.36
53	158	23.6	4.32
54	145	34.4	4.52
55	197	29.4	2.84
56	175	20.2	2.72
57	128	12.4	2.88
58	110	6.08	
59	M	9.04	
60	130	10.4	
61	115	1.36	
62	62.2		
63	24.6		
64	13.5		
65			
66			
67			
68			
69			
70			
71			
72			
73			
74			
75			
76			
77			
78			
79			
80			
81			
82			
83			
84			
85			
86			
87			
88			

SULFUR-DIOXIDE CONCENTRATIONS AND ASSOCIATED FREQUENCY DISTRIBUTION OF AZIMUTH WIND DIRECTION - Run #8

DATE 22 November 1957 TIME 2030 E.S.T. PERIOD OF SAMPLING 10 min

Post number	Wind direction (per cent)	Concentration ($mg\ m^{-3}$) Arc 50m	100m	200m
26	0.42			
28	1.25			
30	1.25	0.893		
32	0.83	6.91		
34	2.50	20.5	1.13	
36	3.33	29.8	5.95	0.228
38	6.25	56.1	12.3	1.17
40	7.92	66.5	22.2	3.69
42	11.25	84.3	28.1	9.86
44	5.83	101	29.8	11.7
46	8.75	134	36.7	13.3
48	9.59	128	49.7	[illegible]
50	9.17	141	47.7	11.9
52	6.25	142	34.4	7.38
54	8.75	103	20.5	2.72
56	4.58	76.9	8.14	0.936
58	4.58	37.6	1.55	0.207
60	2.08	13.2	0.410	
62	1.67	5.89	0.109	
64	0.42	0.833		
66	1.25	0.278		
68	0.42			
70	0.83			
72	0.83			

Post number	Wind direction (per cent)	Concentration ($mg\ m^{-3}$) Arc 50m	100m	200m

Post Number	Height (ft)	Concentration ($mg\ m^{-3}$) Arc 50m	100m	200m
36	2.5	27.6	5.38	0.248
	1.0	30.7		
	0.5	33.5	6.03	0.196
46	2.5	85.4	32.5	12.1
	1.0	164		
	0.5	192	37.6	12.5
56	2.5	54.9	7.65	0.844
	1.0	90.3		
	0.5	101	7.28	0.884
66	2.5	0.826		
	1.0	0.330		
	0.5	0.297		
	2.5			
	1.0			
	0.5			
	2.5			
	1.0			
	0.5			
	2.5			
	1.0			
	0.5			

SULFUR-DIOXIDE CONCENTRATIONS

DATE 22 November 1957 TIME 2030 E.S.T. PERIOD OF SAMPLING 3 Minutes

Post No.	Concentration ($mg\ m^{-3}$) Arc 50m	100m	200m
15			
16			
17			
18			
19			
20			
21			
22			
23			
24			
25			
26			
27			
28			
29	0.287		
30	0.483		
31	4.03		
32	10.9		
33	21.5	0.613	
34	44.7	2.63	
35	43.3	5.10	0.180
36	59.0	9.93	0.697
37	85.3	17.6	1.01
38	85.0	26.3	3.83
39	76.0	37.3	6.17
40	73.0	43.3	9.53
41	86.3	42.0	17.4
42	124	47.7	18.8
43	143	47.3	16.7
44	169	47.7	15.8
45	235	51.7	14.4
46	285	56.3	16.3
47	249	61.3	16.4
48	198	69.3	16.8
49	193	65.3	16.6
50	187	50.7	9.37
51	145	40.7	5.[illegible]

Post No.	Concentration ($mg\ m^{-3}$) Arc 50m	100m	200m
52	132	26.4	3.31
53	87.7	11.1	1.07
54	66.0	4.40	0.133
55	51.0	2.60	
56	33.7	3.43	
57	13.6	1.40	
58	5.97		
59	3.90		
60	7.07		
61	5.53		
62	5.93		
63	3.90		
64	1.05		
65			
66			
67			
68			
69			
70			
71			
72			
73			
74			
75			
76			
77			
78			
79			
80			
81			
82			
83			
84			
85			
86			
87			
88			

SULFUR DIOXIDE CONCENTRATIONS

DATE 22 November 1957 TIME 2030 E.S.T. PERIOD OF SAMPLING 0.5 Minutes

Post No.	Concentration ($mg\ m^{-3}$) Arc 50m	100m	200m
15			
16			
17			
18			
19			
20			
21			
22			
23			
24			
25			
26			
27			
28			
29			
30			
31			
32			
33			
34			
35		1.08	
36	4.06	6.42	
37	8.52	13.4	
38	14.7	17.2	1.86
39	32.2	21.8	6.18
40	46.2	22.8	7.76
41	80.2	27.8	11.6
42	M	26.0	23.0
43	114	23.4	11.4
44	112	26.6	11.0
45	182	31.4	11.0
46	165	53.0	9.40
47	176	82.4	10.4
48	120	91.2	11.0
49	113	74.4	8.80
50	115	44.8	2.00
51	70.2	29.2	4.94
52	69.8	22.2	3.56
53	73.0	12.8	1.20
54	75.0	15.8	
55	56.8	9.24	
56	44.6	14.3	
57	34.2	6.34	
58	22.8	1.06	
59	25.2		
60	39.2		
61	36.0		
62	34.2		
63	24.6		
64	8.44		
65			
66			
67			
68			
69			
70			
71			
72			
73			
74			
75			
76			
77			
78			
79			
80			
81			
82			
83			
84			
85			
86			
87			
88			

SULFUR-DIOXIDE CONCENTRATIONS AND ASSOCIATED FREQUENCY DISTRIBUTION OF AZIMUTH WIND DIRECTION - Run #9

DATE 26 November 1957 TIME 1120 E.S.T. PERIOD OF SAMPLING 10 min

Post number	Wind direction (per cent)	Concentration (mg m^{-3}) Arc 50m	100m	200m
10		0.181		
12		1.90		
14		10.5	0.041	
16	0.42	23.7	1.37	
18	3.33	43.4	2.80	0.057
20	2.08	57.4	6.85	0.673
22	3.75	69.3	13.4	2.05
24	5.00	106	17.7	4.45
26	4.58	136	29.3	5.21
28	7.92	148	48.2	8.14
30	10.42	153	57.7	12.7
32	11.25	174	59.2	17.4
34	8.33	177	51.1	16.6
36	7.50	155	47.7	14.3
38	7.92	129	40.4	11.2
40	7.08	98.7	38.2	5.79
42	7.08	81.7	23.9	4.67
44	3.75	70.6	12.4	3.27
46	4.17	40.4	6.73	0.480
48	2.50	14.6	2.92	
50		5.57	0.686	
52		2.32	0.127	
54	1.25	3.68		
56		2.82		
58	0.83	0.275		
60				
62	0.42			
64				
66				
68				

Post number	Wind direction (per cent)	Concentration (mg m^{-3}) Arc 50m	100m	200m
70	0.42			

Post Number	Height (m)	Concentration (mg m^{-3}) Arc 50m	100m	200m
16	2.5	21.3	1.79	
	1.0	24.4		
	0.5	23.7	0.741	
26	2.5	101	23.1	4.99
	1.0	156		
	0.5	173	30.2	5.60
36	2.5	112	41.0	12.7
	1.0	174		
	0.5	201	52.9	14.2
46	2.5	32.7	5.88	0.518
	1.0	44.5		
	0.5	44.5	7.83	0.369
56	2.5	2.73		
	1.0	2.26		
	0.5	0.686		
	2.5			
	1.0			
	0.5			
	2.5			
	1.0			
	0.5			

[illegible] CONCENTRATIONS

DATE 26 November 1957 TIME 1120 C.S.T. PERIOD OF SAMPLING 3 Minutes

Post No.	Concentration (mg m^{-3}) Arc 50m	100m	200m
15	0.077		
16	0.593		
17	2.26		
18	5.57		
19	20.3		
20	31.4		
21	66.0		
22	86.3	1.49	
23	108	2.46	
24	113	6.17	0.320
25	117	16.6	0.587
26	98.3	24.6	1.44
27	94.7	36.3	2.91
28	94.0	45.7	3.63
29	102	46.7	7.60
30	104	46.7	12.3
31	110	42.3	24.3
32	107	39.7	16.8
33	131	43.0	17.7
34	147	48.7	16.9
35	156	52.7	14.5
36	173	50.7	12.0
37	176	47.0	9.80
38	197	48.7	10.8
39	193	53.0	12.0
40	154	55.3	9.23
41	129	45.3	8.90
42	124	36.3	9.80
43	114	31.3	10.1
44	94.7	22.6	8.00
45	77.0	18.6	4.17
46	58.0	12.6	0.950
47	32.7	7.20	0.087
48	17.4	2.49	
49	8.50	0.767	
50	3.13	0.423	
51	0.347		

Post No.	Concentration (mg m^{-3}) Arc 50m	100m	200m
52	0.117		
53	0.067		
54			
55			
56			
57			
58			
59			
60			
61			
62			
63			
64			
65			
66			
67			
68			
69			
70			
71			
72			
73			
74			
75			
76			
77			
78			
79			
80			
81			
82			
83			
84			
85			
86			
87			
88			

SULFUR-DIOXIDE CONCENTRATIONS

DATE 26 November 1957 TIME 1120 P.S.T. PERIOD OF SAMPLING 0.5 Minutes

Post No.	Concentration ($mg\ m^{-3}$) Arc 50m	100m	200m
15			
16			
17			
18	0.880		
19	16.1		
20	39.2		
21	110		
22	93.8	2.06	0.640
23	122	4.56	2.10
24	[illegible]	20.0	[illegible]
25	306	79.6	5.60
26	244	108	7.54
27	165	116	12.2
28	138	121	15.6
29	159	117	33.6
30	162	124	36.2
31	242	110	32.6
32	260	80.0	29.2
33	226	48.2	19.4
34	136	53.0	16.6
35	96.8	33.6	13.4
36	127	15.0	3.22
37	129	5.84	3.40
38	101	4.72	2.50
39	52.8	4.72	1.64
40	40.0	1.20	1.18
41	36.4	0.560	0.820
42	55.4		
43	54.0		
44	80.0		
45	58.0		
46	36.2		
47	18.7		
48			
49			
50			
51			

Post No.	Concentration ($mg\ m^{-3}$) Arc 50m	100m	200m
52			
53			
54			
55			
56			
57			
58			
59			
60			
61			
62			
63			
64			
65			
66			
67			
68			
69			
70			
71			
72			
73			
74			
75			
76			
77			
78			
79			
80			
81			
82			
83			
84			
85			
86			
87			
88			

SULFUR-DIOXIDE CONCENTRATIONS AND ASSOCIATED FREQUENCY DISTRIBUTION OF AZIMUTH WIND DIRECTION – Run #10

DATE 3 December 1957 TIME 1120 C.S.T. PERIOD OF SAMPLING 10 min

Post number	Wind direction (per cent)	Concentration ($mg\ m^{-3}$) Arc 50m	100m	200m
12	0.42	0.546		
14		5.57		
16	0.42	10.6	0.013	
18	1.25	19.7	0.402	0.144
20	1.67	23.3	3.28	0.367
22	2.50	29.8	6.72	1.06
24	3.33	35.9	7.52	1.18
26	6.25	51.8	14.1	1.93
28	3.75	86.6	22.6	3.59
30	4.58	98.2	25.0	4.71
32	4.58	97.4	28.4	3.03
34	7.08	115	24.8	3.79
36	3.75	119	20.2	4.26
38	5.00	101	16.1	3.23
40	5.83	79.0	16.0	2.92
42	4.58	61.8	13.8	1.46
44	3.75	82.4	14.4	1.00
46	4.16	96.9	20.2	1.43
48	3.75	105	24.2	2.79
50	5.42	101	19.0	3.49
52	5.42	105	16.6	2.41
54	1.67	49.9	14.2	3.11
56	3.33	40.0	10.3	2.78
58	2.08	40.7	4.37	1.05
60	2.92	22.3	2.19	0.597
62	2.92	15.7	1.94	0.527
64	3.75	14.3	2.86	0.967
66	2.50	28.2	4.72	1.17
68	0.83	8.96	3.50	0.166
70	1.25	3.49	0.962	

Post number	Wind direction (per cent)	Concentration ($mg\ m^{-3}$) Arc 50m	100m	200m
72	0.42	0.200	0.018	
74	0.42	0.039		
76				
78	0.42			

Post Number	Height (m)	Concentration ($mg\ m^{-3}$) Arc 50m	100m	200m
16	2.5	7.36	0.053	
	1.0	12.9		
	0.5	13.8	0.004	
26	2.5	35.5	12.6	1.70
	1.0	55.9		
	0.5	60.8	12.0	1.97
36	2.5	91.0	19.8	3.92
	1.0	131		
	0.5	143	22.1	4.03
46	2.5	69.5	19.6	1.40
	1.0	116		
	0.5	132	18.9	1.30
56	2.5	26.4	8.87	2.32
	1.0	47.6		
	0.5	51.6	11.6	2.11
66	2.5	20.2	4.86	1.21
	1.0	28.3		
	0.5	26.8	4.51	1.17
	2.5			
	1.0			
	0.5			

[illegible]-DIOXIDE CONCENTRATIONS

DATE 3 December 196[illegible] TIME 1120 [illegible].S.T. PERIOD OF SAMPLING 3 Minutes

Post No.	Concentration (mg m^{-3}) Arc 50m	100m	200m
15			
16			
17			
18			
19			
20			
21			
22			
23			
24			
25			
26			
27			
28			
29			
30			
31			
32	2.02		
33	4.80		
34	11.7		
35	16.8		
36	20.7		
37	13.5		
38	13.9	0.110	
39	13.3	0.117	
40	14.5	0.240	
41	21.8	2.34	
42	35.7	3.50	0.070
43	51.0	5.51	0.350
44	83.0	13.3	0.930
45	112	[illegible]	0.730
46	130	[illegible]	1.27
47	[illegible]	37.[illegible]	4.52
48	133	42.3	5.77
49	212	39.3	[illegible].20
50	212	37.3	7.77
51	22[illegible]	40.7	7.57

Post No.	Concentration (mg m^{-3}) Arc 50m	100m	200m
52	279	47.0	7.23
53	193	44.0	7.20
54	151	43.7	9.47
55	139	39.0	10.6
56	130	31.6	8.70
57	132	19.4	6.07
58	118	15.4	2.83
59	105	13.3	1.80
60	73.3	7.60	1.02
61	50.3	4.27	0.683
62	53.7	9.10	0.887
63	47.3	6.70	0.967
64	48.0	9.13	1.18
65	54.3	15.1	0.967
66	92.0	15.3	0.323
67	61.7	16.9	0.090
68	31.3	11.7	
69	16.5	7.20	
70	12.6	3.23	
71	9.73	0.697	
72	1.05		
73			
74			
75			
76			
77			
78			
79			
80			
[illegible]			
[illegible]			
[illegible]			
84			
[illegible]			
[illegible]			
[illegible]			

SULFUR-DIOXIDE CONCENTRATIONS

DATE 3 December 1957 TIME 1120 E.S.T. PERIOD OF SAMPLING 0.5 Minutes

Post No.	Concentration (mg m^{-3}) Arc 50m	100m	200m
15			
16			
17			
18			
19			
20			
21			
22			
23			
24			
25			
26			
27			
28			
29			
30			
31			
32			
33			
34			
35			
36			
37			
38			
39			
40			
41	3.16		
42	13.0		
43	62.8		
44	108		
45	228		
46	256	0.750	
47	258	1.62	
48	210	2.68	
49	214	[illegible].93	
50	[illegible]	12.2	
51	[illegible]	13.2	0.400

Post No.	Concentration (mg m^{-3}) Arc 50m	100m	200m
52	204	13.6	0.480
53	206	14.0	4.92
54	157	13.0	1[illegible].8
55	103	12.6	24.8
56	55.0	8.34	21.0
57	50.6	9.34	13.1
58	81.2	24.4	6.02
59	65.2	22.2	2.18
60	21.8	7.00	
61	1.42	4.78	
62			
63			
64			
65			
66			
67			
68			
69			
70			
71			
72			
73			
74			
75			
76			
77			
78			
79			
80			
81			
82			
83			
84			
85			
86			
87			
88			

Table II. Summary of source strengths and correction factors by which concentration data presented in Table I should be multiplied to compensate for evaporational loss of impinger solution during aeration.

Run No.	Date	Time(EST)	Source strength ($g\ sec^{-1}$) 10-min	3-min	0.5-min	Correction factors 10-min	3-min	0.5-min
1	9-24-57	1935	45.1	45.1	45.1	0.90	0.92	0.83**
2	10- 2-57	1120	109.0	114.0	115.0	0.91	0.93	0.90
3	10-10-57	2020	53.4	53.4	53.4	0.93	0.95	0.95
4	11- 4-57	1200	100.0	108.0	108.0	0.92	0.92	0.91
5	11- 6-57	1745	49.2	49.2	49.2	0.97	0.99	0.98
6	11-17-57	1700	53.1	54.2	54.2	0.96	0.98	0.97
7	11-20-57	1700	56.5	56.5	56.5	0.92	0.94	0.95
8	11-22-57	2030	53.8*	71.2	71.2	0.91	0.94	0.95
9	11-26-57	1120	71.2	73.6	73.6	0.96	0.97	0.98
10	12- 3-57	1120	93.4	97.5	97.5	0.94	0.96	0.97

*During last 8 min of release period, source strength decreased from about 70 $g\ sec^{-1}$ to about 35 $g\ sec^{-1}$.

**At 200 m, correction factor is 0.93.

Table III. Mean wind speeds and standard deviations of azimuth wind direction σ_A measured at height of 2 m during diffusion experiments.

Run No.	Wind speed ($m\ sec^{-1}$) at $z = 2$ m 10-min	3-min	0.5-min	σ_A (deg) at $z = 2$ m 10-min	3-min	0.5-min*
1	2.14	2.10	2.1	8.4	5.3 (8.3)**	4.7 (7.1)**
2	5.15	5.28	6.0	16.5	15.2 (15.8)	8.4 (12.7)
3	3.00	3.16	3.4	12.9	10.9 (12.7)	9.1 (10.8)
4	3.98	3.85	3.9	16.7	9.1 (11.5)	11.4 (8.8)
5	1.65	1.76	1.9	9.2	9.8 (8.9)	6.3 (7.2)
6	2.61	2.43	2.7	11.8	10.4 (10.9)	6.4 (8.9)
7	3.66	3.66	3.8	13.5	11.2 (12.7)	12.2 (10.2)
8	3.31	3.69	4.0	12.8	11.3 (12.5)	10.1 (10.4)
9	4.39	4.42	4.9	13.1	10.6 (12.0)	5.7 (8.9)
10	4.07	4.05	4.0	20.7	14.4 (13.8)	21.2 (11.0)

*Estimates not enclosed by parentheses applicable strictly at 100 m.

**Entries in parentheses are average values based on entire length of record (10 min); see p. 55 of text.

Table IV. Summary of mean wind speeds and air temperatures measured at four heights on portable tower during the diffusion experiments; entries refer to 10-min sampling time.

Run No.		Wind speed (m sec^{-1})				Air temperature (deg C)			
	Z(m)	1.5	3.0	6.0	12.0	1.5	3.0	6.0	12.0
1		2.52	2.87	3.28	3.78	12.12	12.51	12.73	12.94
2		5.36	6.12	6.57	6.98	20.00	19.54	19.33	18.97
3		3.19	3.57	3.97	4.34	14.92	15.12	15.24	15.30
4		3.99	4.44	4.85	5.05	13.40	13.27	13.19	13.09
5		M	2.11	2.46	2.82	4.45	4.86	5.09	5.25
6		2.88	3.27	3.61	3.97	11.60	11.87	12.04	12.13
7		4.04	4.70	5.20	5.78	7.60	7.79	7.92	8.04
8		3.53	4.04	4.49	5.00	4.30	4.46	4.56	4.62
9		4.29	4.80	5.20	5.46	2.95	2.49	2.27	1.98
10		4.04	4.70	5.10	5.46	3.75	3.37	3.16	2.92